



UNIwersytet Medyczny
IM. PIASTÓW ŚLĄSKICH WE WROCLAWIU

lek. Bartłomiej Kędzierski

**MOŻLIWOŚCI ZMNIEJSZENIA DAWKI PROMIENIOWANIA
W BADANIACH TOMOGRAFII KOMPUTEROWEJ
WYKONYWANYCH PRZED PRZEZSKÓRNYM WSZCZEPIENIEM
ZASTAWKI AORTALNEJ**

ROZPRAWA DOKTORSKA

PROMOTOR: dr hab. n. med. Paweł Gać, prof. UMW

WROCLAW 2023

Praca ta nie powstałaby bez wkładu pracy, wiedzy i umiejętności zespołu zaangażowanych osób. W tym miejscu chciałbym Im podziękować.

Przede wszystkim dziękuję mojemu Promotorowi,

dr. hab. Pawłowi Gać, prof. UMW,

za inspirację, cierpliwość, wyrozumiałość i motywację na kolejnych etapach pracy, wreszcie ogromny wkład merytoryczny i organizacyjny - bez tego rozprawa ta nie mogłaby powstać.

Wszystkim Współautorom cyklu publikacji:

***prof. dr hab. n. med. Krystynie Pawlas,
prof. dr hab. n. med. Rafałowi Porębie,
dr. n. med. Krystianowi Truskiewiczowi,
lek. Barbarze Dziadkowiec-Macek,
lek. Piotrowi Mackowi,
lek. Martynie Hajac (z d. Głośna)***

dziękuję za Ich wysiłek, zaangażowanie, poświęcony czas przy przygotowaniu publikacji i wniesione w nie wartości merytoryczne.

*Przy podziękowaniach nie sposób nie wspomnieć **dra Jerzego Bitta**, który „otworzył przede mną drzwi” do świata radiologii, przychylając się do mojej prośby o rozpoczęcie wolontariatu w Zakładzie Radiologii 4. Wojskowego Szpitala Klinicznego oraz **dra n. med. Bolesława Bojarskiego**, który prowadził moją specjalizację z radiologii i diagnostyki obrazowej.*

*Osobne podziękowania skierować chcę jeszcze do **mojego Promotora oraz dr. n. med. Krystiana Truskiewicza** za codzienne inspiracje i wsparcie – na różnych, niekiedy trudnych etapach drogi zawodowej.*

*Podziękowania chciałbym także złożyć w tym miejscu wszystkim moim **Koleżankom i Kolegom**, których tutaj nie sposób wymienić z imienia i z nazwiska, a dzięki którym przyjaźni i pomocy jestem w obecnym miejscu rozwoju zawodowego.*

*Na końcu, ale przecież bardzo ważne: dziękuję **Rodzinie, Przyjaciołom i Temu**, który prowadzi ścieżki mojego życia.*

SPIS TREŚCI

Wprowadzenie	4
Założenia	6
Cele pracy	7
Omówienie	8
Wnioski	19
Streszczenie	20
Summary	22
Piśmiennictwo	24
Wykaz publikacji włączonych do rozprawy doktorskiej	26
Praca nr 1	27
Praca nr 2	56
Praca nr 3	66
Oświadczenia współautorów	82
Zgoda komisji bioetycznej	90

WPROWADZENIE

Zwężenie zastawki aortalnej stanowi najbardziej powszechną wadę zastawkową w krajach rozwiniętych. [1, 2] Na przestrzeni ostatnich kilkudziesięciu lat zmianom ulega rozkład częstości występowania poszczególnych typów etiologicznych zwężenia zastawki aortalnej. Zaobserwowano spadek częstości występowania poreumatycznych zwężeń zastawki aortalnej oraz wzrost rozpowszechnienia degeneracyjnej (zwanej również degeneracyjno-zwapnieniową) postaci stenozy aortalnej. W badaniu *Euro Heart Survey on Valvular Heart Disease* zwężenie zastawki aortalnej stanowiło najczęstszą rozpoznawaną wadę zastawkową serca, u większości chorych, a mianowicie u 81,9%, była to właśnie postać degeneracyjno-zwapnieniowa, a tylko u 11,2% chorych rozpoznano poreumatyczny typ wady.

Dane epidemiologiczne wskazują, że w związku z wydłużaniem się średniej czasu trwania życia oraz związanym z powyższym starzeniem się społeczeństw częstość występowania zwężenia zastawki aortalnej będzie wzrastać, jednocześnie narastać będzie rozpowszechnienie ciężkiej postaci stenozy aortalnej.

Leczeniem z wyboru u chorych z ciężką stenozą aortalną jest implantacja protezy zastawki w pozycję aortalną. [2] **Dla dużej grupy osób starszych, obarczonych licznymi schorzeniami towarzyszącymi, ryzyko klasycznego zabiegu kardiochirurgicznego wymiany zastawki aortalnej jest zbyt duże. Dla tej grupy chorych rozwiązaniem jest przeszskórne (przezcewnikowe) wszczepienie zastawki aortalnej (*Transcatheter Aortic Valve Implantation - TAVI* lub inaczej *Transcatheter Aortic Valve Replacement - TAVR*).** [3, 4]

W procedurze kwalifikacji chorych do przeszskórnego wszczepienia zastawki aortalnej rutynowo wykonuje się badania obrazowe, na podstawie których precyzyjnie określa się wymiary zastawki aortalnej, topografię ujścia aortalnego, a także możliwość wykorzystania poszczególnych dostępów tętniczych. Standardem na obecną chwilę jest wykonywanie w tym celu badań tomografii komputerowej serca i dużych naczyń. [5, 6]

Badania tomografii komputerowej wiążą się z narażeniem pacjenta, a także potencjalnie personelu wykonującego na promieniowanie jonizujące. Promieniowanie jonizujące poprzez bezpośrednie oddziaływanie na dwuniciową cząsteczkę DNA, a także

poprzez generowanie, w wyniku radiolizy wody, wolnych rodników tlenowych oddziaływujących z DNA (czyli poprzez mechanizm pośredni) powoduje zmiany materiału genetycznego komórki, które mogą skutkować następstwami deterministycznymi i stochastycznymi. [7, 8, 9]

Zastosowanie promieniowania jonizującego w metodach radiologicznych i radioizotopowych stosowanych w diagnostyce medycznej oraz w terapii (badania radiologii klasycznej, tomografii komputerowej, medycyny nuklearnej, radioterapia) stanowi niewątpliwy sukces nauki XX wieku. Dostępność do urządzeń diagnostycznych wykorzystujących promieniowanie jonizujące ciągle się poprawia, co stanowi oczywiste osiągnięcie organizacyjne opieki zdrowotnej. Według danych Organizacji Współpracy Gospodarczej i Rozwoju (*Organisation for Economic Co-operation and Development*, OECD) w 2010 roku w krajach Unii Europejskiej na milion osób przypadało 20,4 urządzeń tomografii komputerowej. Z kolei według danych z 2020 roku najwięcej było ich w Grecji (42,50) i Danii (40,6); w Polsce wskaźnik ten wyniósł odpowiednio 20,1. Pamiętać należy, że poprawa dostępności przekłada się na ciągły wzrost liczby wykonywanych procedur tego typu. W 2020 roku w niektórych populacjach krajów Unii Europejskiej roczny wskaźnik liczby wykonywanych badań tomografii komputerowej na milion osób przekroczył 200 (w Luksemburgu wyniósł 210, w Belgii 205). W Polsce było to odpowiednio 89,9 badań. **Coraz powszechniejsze stosowanie metod wykorzystujących promieniowanie jonizujące skutkuje wyraźnie rosnącą wielkością ekspozycji populacji na promieniowanie.**

ZAŁOŻENIA

Zgodnie z zasadami ochrony radiologicznej, sformułowanymi przez Międzynarodową Komisję Ochrony Radiologicznej (*International Commission on Radiological Protection*, ICRP), nie wolno dopuścić żadnej praktyki związanej z ekspozycją na promieniowanie jonizujące, dopóki praktyka ta nie przyniesie dostatecznej korzyści osobom eksponowanym lub społeczeństwu, przewyższając straty w postaci radiacyjnego uszczerbku na zdrowiu związanego z tą praktyką. [10] W przypadku dodatniego bilansu zysków i strat związanych z wykonywaniem procedur medycznych wykorzystujących promieniowanie jonizujące **niezbędne jest poszukiwanie możliwości optymalizacji dawki promieniowania jonizującego**. Z punktu widzenia zasad ochrony radiologicznej, zgodnie z zasadą *ALARA* (*As Low As Reasonably Achievable*), należy poszukiwać sposobów redukcji dawki promieniowania jonizującego podczas wykonywania procedur z wykorzystaniem promieniowania jonizującego, optymalnie przy zachowaniu odpowiedniej jakości uzyskanych obrazów diagnostycznych, a czasem nawet kosztem nieistotnej redukcji jakości takich obrazów. [11, 12]

Szczególnie istotne wydaje się **minimalizowanie stosowanych dawek w przypadku badań, które wykonywane są z generowaniem wysokich dawek promieniowania**, np. takich jak badanie tomografii komputerowej serca i dużych naczyń w procedurze kwalifikacji do zabiegu TAVI. W przypadku następstw stochastycznych promieniowania jonizującego występuje bowiem prosta proporcjonalność między dawką promieniowania a ryzykiem ich wystąpienia. Natomiast koszty związane ze zmniejszaniem wielkości narażenia przy coraz niższych wartościach dawek ekspozycyjnych rosną w sposób nieproporcjonalny do stopnia obniżenia dawki efektywnej. [13] Nie można tym samym uznać za społecznie pożądane i ekonomicznie opłacalne unikanie każdego bardzo małego ryzyka, a więc działania należy koncentrować na optymalizacji dawek wysokich, ewentualnie pośrednich. [14]

CELE PRACY

Zasadniczym celem badań było poszukiwanie możliwości optymalizacji dawki promieniowania jonizującego w badaniach tomografii komputerowej w procedurze kwalifikacji do zabiegu TAVI.

Do celów szczegółowych badań należało:

1. udokumentowanie w oparciu o *evidence-based medicine* średnich dawek promieniowania jonizującego w standardowych badaniach tomografii komputerowej serca i dużych naczyń wykonywanych w procedurze kwalifikacji do zabiegu TAVI;
2. poszukiwanie zależności pomiędzy dawką promieniowania jonizującego a powtarzalnością pomiarów wymiarów zastawki aortalnej w badaniach tomografii komputerowej wykonywanych w procedurze kwalifikacji do zabiegu TAVI oraz ocena wpływu potencjalnej redukcji dawki w tego typu badaniach na omawianą powtarzalność wymiarowania zastawki;
3. ocena możliwości estymacji wartości wskaźnika uwapnienia zastawki aortalnej (AVCS) w oparciu o fazę angiograficzną badania wielorzędowej tomografii komputerowej wykonywanego w procedurze kwalifikacji do zabiegu TAVI oraz ocena wielkości redukcji dawki promieniowania jonizującego w wyniku takiej estymacji.

OMÓWIENIE

W pierwszej pracy cyklu doktorskiego pt. „**Radiation Doses in Cardiovascular Computed Tomography**” omówiono współczesne poglądy na temat wpływu promieniowania jonizującego na organizmy żywe oraz proces oszacowania dawek promieniowania w badaniach TK i definicje określeń: tomograficzny wskaźnik dawki (CTDI), objętościowy tomograficzny wskaźnik dawki (CTDIvol), iloczyn dawka-długość (DLP), dawka specyficzna dla wielkości ciała (SSDE), dawka skuteczna (ED). Dokonano przeglądu doniesień z dużych analiz dotyczących dawek promieniowania w badaniach TK tętnic wieńcowych oraz przed zabiegami TAVI, w tym z badań CRESCENT, PROTECTION, German Cardiac CT Registry. Badania te zostały przeprowadzone w ciągu ostatnich 10 lat i w większości ośrodków, w konfrontacji z codzienną praktyką wykonywania badań TK układu krążenia, mogą pomóc w udoskonalaniu ich protokołów. Zebrano również poziomy dawek referencyjnych dla tych badań.

W każdym badaniu TK do problemu klinicznego i właściwości pacjenta należy dostosować możliwości sprzętu i umiejętności korzystania z protokołów zgodnie z zasadą ALARA (*As Low As Reasonably Achievable* – tak nisko jak jest to możliwe w rozsądny sposób). Możliwości optymalizacji dawki promieniowania mogą być rozmaite, zależnie od warunków wykonania badania i rodzaju sprzętu. Do metod optymalizacji – obniżenia dawki promieniowania w badaniach TK należą:

- obniżenie napięcia lampy aparatu TK,
- monitorowana zapisem ekg modulacja promieniowania (natężenia prądu lampy)
- iteracyjne rekonstrukcje obrazów,
- oparte na głębokim uczeniu sztucznej inteligencji rekonstrukcje obrazu oraz redukcja szumów obrazu,
- redukcja zakresu badania (długości skanu),
- prospektywne protokoły badań,
- modulacja natężenia prądu zależna od osłabienia promieniowania,
- regulacja częstości akcji serca,
- racjonalne stosowanie badania stopnia uwapnienia tętnic wieńcowych (Calcium Score),
- zastosowanie tomografii wielorzędowej, dwuzródłowej i szerokozakresowej.

Badania TK przed zabiegami przezcewnikowej wymiany zastawki aortalnej – TAVI stały się „złotym standardem”. Wymagają one uzyskania obrazów opuszki aorty przy użyciu akwizycji monitorowanych zapisem ekg oraz obrazów dostępow naczyniowych od tętnic szyjnych do tętnic udowych, wykonywanych bez synchronizacji z zapisem ekg. W konstruowaniu protokołów badań TK przed zabiegami TAVI stosuje się dwa sposoby uzyskiwania zbiorów danych obrazowych:

1) Akwizycja z monitorowaniem zapisu ekg, obejmująca okolicę serca i opuszki aorty, a następnie akwizycja bez monitorowania zapisu ekg, obejmująca dostępy naczyniowe w obszarze szyi, klatki piersiowej, jamy brzusznej, miednicy i pachwin do poziomu krętarzy mniejszych kości udowych. Wadą tego rozwiązania jest dwukrotna akwizycja w zakresie obejmującym okolice opuszki aorty i serca, co zwiększa dawkę promieniowania. Zaletą jest jednak tutaj fakt, że czasochłonna akwizycja synchronizowana z ekg jest ograniczona do minimum. Skrócenie czasu badania pozwala na zmniejszenie objętości podanego środka kontrastującego. Pamiętać należy, że badania te dotyczą pacjentów w starszym wieku, u których najczęściej funkcja nerek jest – nawet znacznie – obniżona. Ponadto ograniczenie zakresu akwizycji synchronizowanej z ekg zmniejsza tę część badania, która wymaga dużej dawki promieniowania, pomimo że zakresy skanowania częściowo się pokrywają.

2) Akwizycja z monitorowaniem zapisu ekg, obejmująca dolną część szyi i klatkę piersiową, a następnie akwizycja bez monitorowania zapisu ekg, obejmująca jamę brzuszną, miednicę i pachwiny do poziomu krętarzy mniejszych kości udowych. Wadą tego rozwiązania jest wyższa dawka promieniowania i wydłużony czas akwizycji dla całej klatki piersiowej. Wydłużony czas akwizycji może wymagać większej objętości środka kontrastującego oraz wstrzymania oddechu na dłuższy czas, co może powodować u mniej wytrzymałych pacjentów wystąpienie artefaktów oddechowych.

W celu optymalizacji dawki promieniowania autorzy wytycznych Towarzystwa Tomografii Komputerowej Układu Krążenia (*Society of Cardiovascular Computed Tomography – SCCT*) zalecają u pacjentów z masą ciała do 90 kg lub wartościami BMI do 30 kg/m² akwizycję z napięciem lampy aparatu 100 kVp, natomiast u pacjentów z masą ciała > 90 kg lub wartościami BMI > 30 kg/m² – akwizycję z napięciem lampy aparatu 120 kVp. Jeśli pozwalają na to parametry aparatury, u pacjentów z wartościami BMI < 26 kg/m² należy prowadzić akwizycję z napięciem lampy aparatu 80 kVp.

W narodowym badaniu ankietowym, przeprowadzonym w 2018 roku w Wielkiej Brytanii, uzyskano odpowiedzi z 47 ośrodków, z których większość wykonywała poniżej 100 badań miesięcznie. Mediana iloczynu dawka-długość (DLP) wynosiła 675 mGy*cm. Mediana DLP w protokołach prospektywnych z monitorowaniem ekg, z wąskim zakresem cyklu serca objętym akwizycją (*padding*) wyniosła 423 mGy*cm. Zastosowanie szerokich wartości *padding* – obejmujących 30%-80% odstępu R-R – powodowało ponad dwukrotne zwiększenie DLP – do 921 mGy*cm. Akwizycja retrospektywna wiązała się z wysoką medianą DLP, wynoszącą 882 mGy*cm.

Wpływ trybu skanowania badano w pracy przeprowadzonej przez autorów z Ośrodka Charité (Berlin), wykonywanych aparatem 80-rzędowym Aquillion Prime (*Canon Medical Systems, Otawara, Japan*). W pierwszym z protokołów akwizycja obejmowała odcinek klatki piersiowej od szczytów płuc do łuku aorty bez synchronizowania z ekg, następnie odcinek od łuku aorty do przepony z synchronizowaniem z ekg i wreszcie odcinek od przepony do pachwin ponownie bez synchronizowania z ekg. W drugim z protokołów akwizycja prowadzona była jednolicie od szczytów płuc do pachwin bez synchronizacji z ekg, z wysokim współczynnikiem skoku (*pitch factor*) = 1,388. Średnia DLP wynosiła $790,90 \pm 238,15$ mGy*cm protokole z synchronizacją z ekg w porównaniu do $357,10 \pm 200,25$ mGy*cm w protokole z wysokim współczynnikiem skoku bez synchronizacji z ekg. Protokół TK o wysokim współczynniku skoku bez synchronizacji z ekg umożliwił zmniejszenie ekspozycji na promieniowanie o 55% w porównaniu z protokołem z synchronizacją z ekg.

W badaniu obejmującym 30 przypadkowo wybranych pacjentów, u których wykonywano badanie aparatem Somatom Force (*Siemens Healthcare, Erlangen, Germany*) DLP wyniósł $217,6 \pm 12,1$ mGy*cm (zakres 178-248 mGy*cm).

Również aparatem Somatom Force (*Siemens Healthcare, Erlangen, Germany*) badano 226 pacjentów w latach 2018-2019, w protokole, który obejmował w pierwszym etapie badanie stopnia uwapnienia zastawki aortalnej z zastosowaniem napięcia 120 kVp od poziomu rozwidlenia tchawicy do przepony, w drugim etapie akwizycję prospektywną w 30% odstępu R-R, z monitorowaniem ekg, z zastosowaniem wysokiego współczynnika skoku = 3,2 i napięcia 100 kVp. Średnia wartość DLP w tym badaniu wyniosła $201,1 \pm 22,7$ mGy*cm.

W pracy obejmującej 115 badań wykonanych 256-rzędowym aparatem Revolution CT (*GE Healthcare, Milwaukee, USA*) w latach 2016-2017 autorzy raportowali średnią wartość DLP $479,1 \pm 45,7$ mGy*cm. Protokół badania obejmował klatkę piersiową od szczytów płuc do przepony z monitorowaniem ekg oraz akwizycję spiralną bez monitorowania ekg od przepony do proksymalnej trzeciej części ud; badanie wykonywano z napięciem 100 kVp.

Jeszcze inny protokół zastosowano u 42 pacjentów, badanych aparatem Somatom Definition Flash (*Siemens Healthcare, Forchheim, Germany*). Akwizycja struktur serca od łuku aorty do przepony synchronizowana była z ekg w 60% odstępu R-R, następnie skanowanie prowadzono kraniokaudalnie od szczytów płuc do pachwin bez synchronizowania z ekg, akwizycją spiralną. W zależności od wartości BMI stosowano napięcia 100 kVp i 120 kVp. Średnia wartość DLP wyniosła 241 ± 27 mGy*cm.

W końcowej części pracy poglądowej przedstawione zostały badania, które wskazują na potrzebę podniesienia wartości współczynnika konwersji narządowej dla badań układu krążenia z dotychczas stosowanego $0,014-0,017$ mSv/mGy*cm, zaimplementowanego z badań klatki piersiowej, do wartości $0,0264-0,03$ mSv/mGy*cm.

W drugiej pracy cyklu doktorskiego pt. „**Radiation dose and repeatability of aortic valve measurement by multidetector row computed tomography to assess eligibility for transcatheter aortic valve implantation**” dokonano oceny zależności między dawką promieniowania jonizującego a powtarzalnością pomiarów wymiarów aorty za pomocą wielorzędowej tomografii komputerowej (MSCT) serca i dużych naczyń, w ramach standardowej kwalifikacji do zabiegów przezcewnikowej implantacji zastawki aortalnej (TAVI).

Badaniem objęto grupę 60 kolejnych pacjentów, u których w latach 2012-2016 wykonano TK serca i dużych naczyń w procesie kwalifikacji do zabiegów TAVI. Średni wiek badanych wynosił $79,60 \pm 9,17$ lat, a średni wskaźnik masy ciała (BMI) $27,85 \pm 3,99$ kg/m². 63,3% badanych stanowili mężczyźni, a 36,7% kobiety. Tylko 25,0% badanych miało prawidłową masę ciała, 51,7% miało nadwagę, a 23,3% było otyłych.

Wszystkie badania TK serca i dużych naczyń wykonano przy użyciu tomografu komputerowego Somatom Definition Dual-Source (*Siemens Healthcare, Kemnath, Niemcy*) zgodnie ze standardowym protokołem, który obejmował topogram, monitorowanie

wzmocnienia kontrastowego na poziomie rozwidlenia tchawicy, angiografię klatki piersiowej w tętnicznej fazie zakontrastowania z synchronizowaniem akwizycji z zapisem ekg oraz angiografię tętnic jamy brzusznej i miednicy bez synchronizowania z zapisem ekg. Zakres badania sięgał od szczytów płuc do połowy trzonów kości udowych, z napięciem lampy 120 kVp i zmiennymi wartościami mAs.

Dawka promieniowania jonizującego określona została na podstawie raportów aparatury TK jako tomograficzny wskaźnik dawki (CTDIvol) oraz iloczyn dawka-długość (DLP) dla serii obejmującej zakresem klatkę piersiową w tętnicznej fazie zakontrastowania.

Badania były oceniane niezależnie przez 2 radiologów z 7- i 10-letnim doświadczeniem w ocenie tomografii komputerowej serca zgodnie z zaleceniami opisanymi w dokumencie: *SCCT expert consensus document on computed tomography imaging before transcatheter aortic valve implantation (TAVI) / transcatheter aortic valve replacement (TAVR)*. Wszystkie pomiary były wyrażone w milimetrach z dokładnością do 0,1 mm.

Na podstawie mediany wartości CTDIvol (43,92 mGy) i DLP (1143,00 mGy*cm) wyróżniono podgrupy o niskim CTDIvol (CTDIvol < Me, n = 30) i wysokim CTDIvol (CTDIvol ≥ Me, n = 30) oraz podgrupy o niskim DLP (DLP < Me, n = 29) i wysokim DLP (DLP ≥ Me, n = 31).

Analizy statystyczne przeprowadzono przy użyciu programu Dell Statistica v. 13 (*Dell Inc., Austin, USA*).

Analiza powtarzalności pomiarów zastawki aortalnej wykazała największą bezwzględną różnicę pomiarów w odległości między ujściem lewej tętnicy wieńcowej a pierścieniem aortalnym ($1,77 \pm 0,96$ mm), natomiast najmniejszą bezwzględną różnicę pomiarów w średnim wymiarze pierścienia aortalnego ($0,97 \pm 0,60$ mm). Największą względną różnicę pomiarów i największe wartości współczynnika zmienności pomiaru (CV) stwierdzono w odległości między ujściem lewej tętnicy wieńcowej a pierścieniem aortalnym (odpowiednio $0,13 \pm 0,07\%$ i $9,24 \pm 5,17\%$). Najmniejszą względną różnicę pomiarów i najmniejszy CV stwierdzono w średnim wymiarze opuszki aorty (odpowiednio $0,03 \pm 0,02\%$ i $2,39 \pm 1,72\%$).

Analiza porównawcza nie wykazała istotnych statystycznie różnic w średnich wartościach parametrów, charakteryzujących powtarzalność poszczególnych pomiarów zastawki aortalnej pomiędzy grupami wyodrębnionymi na podstawie mediany CTDIvol. Analiza porównawcza wykazała, że bezwzględna różnica pomiaru, względna różnica pomiaru oraz CV w przypadku średniego wymiaru zastawki aortalnej były istotnie wyższe w podgrupie o niskim DLP niż w podgrupie o wysokim DLP.

Analiza korelacji wykazała istotne statystycznie ujemne korelacje liniowe pomiędzy wartością DLP a różnicą bezwzględną (AD), różnicą względną (RD) i CV pomiaru minimalnego wymiaru pierścienia aortalnego (odpowiednio $r = -0,26$, $r = -0,25$ i $r = -0,25$; $p < 0,05$). Ponadto wykazano dodatnie korelacje liniowe między BMI a AD, RD i CV pomiaru minimalnego wymiaru opuszki aorty (odpowiednio $r = 0,28$, $r = 0,31$ i $r = 0,31$; $p < 0,05$), a także między BMI a AD, RD i CV odległości między ujściem lewej tętnicy wieńcowej a pierścieniem aortalnym (odpowiednio $r = 0,33$, $r = 0,28$ i $r = 0,28$; $p < 0,05$).

Analiza regresji wykazała, że płeć żeńska i niższe wartości DLP są czynnikami niezależnie związanymi z wyższym CV dla pomiaru minimalnego wymiaru pierścienia aortalnego. Wyższe BMI i płeć żeńska są niezależnie związane z wyższym CV dla pomiaru minimalnego wymiaru opuszki aorty. Wyższe BMI, płeć żeńska i starszy wiek są niezależnie związane z wyższym CV dla pomiaru odległości między lewą tętnicą wieńcową a pierścieniem aortalnym.

Analizując wyniki tego badania nie można stwierdzić jednoznacznych zależności między dawką promieniowania jonizującego a powtarzalnością pomiarów wymiaru aorty za pomocą tomografii komputerowej.

Należy jednak pamiętać o wykazanych pojedynczych, istotnych statystycznie zależnościach, tj.:

- istotnie większych: bezwzględnej różnicy pomiarów, względnej różnicy pomiarów i CV dla średniej wartości średnicy zastawki aortalnej w podgrupie o niskim DLP w porównaniu do podgrupy o wysokim DLP;
- istotne ujemnych zależnościach liniowych pomiędzy wartością DLP a bezwzględną różnicą pomiarów, względną różnicą pomiarów i CV dla minimalnego wymiaru pierścienia aortalnego;

- niższym DLP jako niezależnym czynnikiem związanym z wyższym CV dla minimalnego wymiaru pierścienia aortalnego.

Niezależnie od dawki promieniowania, wyższe BMI, płeć żeńska i starszy wiek wpływają niekorzystnie na CV dla pomiarów zastawki aortalnej. Wydaje się, że w tych grupach chorych należy zachować większą ostrożność podczas wykonywania badań TK z zastosowaniem niższych dawek promieniowania.

Warto podkreślić, że przedstawione wyniki badań są pierwszą naukową próbą określenia zależności pomiędzy dawką promieniowania jonizującego a powtarzalnością pomiarów aorty za pomocą badań TK, wykonywanych w celu standardowej oceny kwalifikacji do TAVI. W dostępnym piśmiennictwie problem powtarzalności wymiarowania zastawki aortalnej za pomocą tomografii komputerowej przed TAVI był dotąd poruszany sporadycznie.

Wielkość dawki promieniowania w rutynowych badaniach TK wykonywanych w procesie kwalifikacji do TAVI zasadniczo nie wpływa na powtarzalność pomiarów zastawki aortalnej, co uzasadnia próby wykonywania tych badań z zastosowaniem niższych dawek promieniowania. Ze względu na wykazane pojedyncze korelacje pomiędzy dawką promieniowania w badaniach TK, wykonywanych w procesie kwalifikacji do TAVI a stopniem powtarzalności pomiarów zastawki aortalnej i opuszki aorty proponuje się, aby po badaniach z niższymi dawkami promieniowania następowała kontrola stopnia powtarzalności tych pomiarów.

W trzeciej pracy cyklu doktorskiego pt. „**Estimation of Aortic Valve Calcium Score Based on Angiographic Phase Versus Reduction of Ionizing Radiation Dose in Computed Tomography**” dokonano oceny wartości oszacowania wskaźnika uwapnienia zastawki aortalnej (AVCS) na podstawie fazy angiograficznej metodą wielorzędowej tomografii komputerowej. Na podstawie tego oszacowania dokonano oceny możliwości obniżenia dawki promieniowania jonizującego.

AVCS jest matematycznie oszacowanym, ilościowym, niejednostkowym parametrem, charakteryzującym całkowitą ilość zwapnień w obrębie zastawki aortalnej, koreluje ze stopniem jej zwyrodnienia oraz zwężenia i jest parametrem uwzględnianym w kwalifikacji pacjentów do TAVI. Zgodnie z wytycznymi Europejskiego Towarzystwa Kardiologicznego

(*European Society of Cardiology – ECS*) i Europejskiego Stowarzyszenia Kardiologii i Torakochirurgii (*European Association for Cardio-Toracic Surgery – EACTS*) AVCS uznano za parametr, który można wykorzystać do różnicowania stopnia stenozы aortalnej u pacjentów z powierzchnią ujścia aortalnego $<1,0 \text{ cm}^2$, niskim gradientem ($<40 \text{ mmHg}$) i zachowaną frakcją wyrzutową lewej komory. Wartości AVCS_{native3.0} wg Agatstona powyżej 2000 u mężczyzn i 1200 u kobiet stanowią kryterium wysoce prawdopodobnej ciężkiej stenozы aortalnej.

Określenie AVCS wymaga wykonania badania TK w warunkach analogicznych jak przy badaniu wskaźnika uwapnienia tętnic wieńcowych: w fazie natywnej (bez podania środka kontrastującego), w warstwach o grubości 3 mm, przy napięciu lampy aparatu TK 120 kVp. W algorytmach wg Agatstona ocenie podlegają wszystkie zwapnienia o gęstości $\geq 130 \text{ j. H.}$, o powierzchni ≥ 3 pikseli. Ocena AVCS wymaga odrębnej serii badania w protokole kwalifikacji do TAVI i wiąże się z dodatkowym narażeniem pacjenta na promieniowanie jonizujące.

Badaniem objęto kolejnych 51 pacjentów w wieku $78,59 \pm 5,72$ lat, badanych w 2019 roku, kwalifikowanych do przezcewnikowej implantacji zastawki aortalnej (TAVI). Ze względu na zmierzone parametry antropometryczne wyodrębniono podgrupy kobiet i mężczyzn, pacjentów z prawidłową masą ciała, nadwagą i otyłością oraz pacjentów w wieku podeszłym i starszym.

Badania wykonywano na 128-rzędowym aparacie Somatom Definition AS+ (*Siemens Healthcare, Erlangen, Niemcy*), zgodnie ze standardowym protokołem, który obejmował: topogram, fazę natywną dla oceny AVCS, monitorowanie wysycenia aorty środkiem kontrastującym oraz akwizycję w tętniczej fazie zakontrastowania w warstwach o grubości 3,0 mm i 0,6 mm w części poświęconej ocenie zastawki aortalnej i opuszki aorty oraz o grubości 3,0 mm i 1,0 mm w części poświęconej obrazowaniu dostępów tętniczych.

W oparciu o fazę natywną przeprowadzono ocenę AVCS dla rekonstrukcji osiowych o grubości warstwy 3,0 mm i 2,0 mm (AVCS_{native3.0} i AVCS_{native2.0}). Na podstawie fazy angiograficznej oszacowano AVCS dla rekonstrukcji osiowych o grubości 0,6 mm ze zwiększonymi do 500 j. H. i 600 j. H. (AVCS_{CTA0.6 500 HU} i AVCS_{CTA0.6 600 HU}) wartościami odcięcia dla gęstości zmian w płatkach zastawki aortalnej/pierścieniu aortalnym,

uważanych za zwapnienia. Wartości 500 j. H. i 600 j. H. zostały wybrane subiektywnie w celu odróżnienia zwapnień w zastawce aortalnej od zakontrastowanego światła drogi odpływu lewej komory i/lub opuszki aorty. W momencie oceny AVCS w fazie angiograficznej badacze nie mieli informacji o wartości AVCS w fazie natywnej.

Ocenę AVCS przeprowadzono retrospektywnie przy użyciu aplikacji syngo.CT CaScoring (*Siemens Healthcare, Erlangen, Niemcy*). Na podstawie fazy natywnej badania TK dokonano półautomatycznej oceny AVCS dla rekonstrukcji osiowych o grubości 3,0 mm i 2,0 mm (odpowiednio $AVCS_{\text{native}3,0}$ i $AVCS_{\text{native}2,0}$). Zmiany uznawano za zwapnienia, zgodnie z algorytmem Agatstona, jeśli ich gęstość wynosiła ≥ 130 j. H. Zmiany sugerowane przez aplikację jako zwapnienia były kategoryzowane jako zmiany w obrębie płatków zastawki aortalnej lub pierścienia aortalnego, albo jako zmiany poza tymi strukturami. Kategoryzacja zwapnień dla każdego pacjenta była weryfikowana przez konsensus tych samych dwóch oceniających radiologów.

Dawkę promieniowania jonizującego w analizowanych badaniach TK określono na podstawie odczytu pomiarów dokonywanych podczas akwizycji obrazu przez aparat TK. Oznaczono objętościowy wskaźnik dawki (CTDIvol) oraz iloczyn dawka-długość (DLP) dla fazy natywnej, poświęconej ocenie AVCS oraz fazy angiograficznej służącej do oceny zastawki aortalnej i opuszki aorty. Ponadto wyznaczono całkowitą wartość DLP dla badania TK serca i dużych naczyń z oceną AVCS.

Analizę statystyczną przeprowadzono przy użyciu narzędzia "Dell Statistica 13" (*Dell Inc., Round Rock, TX, USA*).

AVCS, w zależności od grubości natywnych rekonstrukcji obrazu, w badanej grupie pacjentów wynosił: $3690,54 \pm 2378,82$ w przypadku grubości warstwy 3,0 mm ($AVCS_{\text{native}3,0}$) i $3457,03 \pm 2190,81$ w przypadku grubości warstwy 2,0 mm ($AVCS_{\text{native}2,0}$). Wartości $AVCS_{\text{native}3,0}$ powyżej 3000 u mężczyzn i 1600 u kobiet przyjęto jako wskaźniki wysoce prawdopodobnej ciężkiej stenozы aortalnej, a wartości $AVCS_{\text{native}3,0}$ powyżej 2000 u mężczyzn i 1200 u kobiet uznano za wskaźniki prawdopodobnej ciężkiej stenozы aortalnej. Pacjenci, u których wartości $AVCS_{\text{native}3,0}$ były niższe niż 1600 u mężczyzn i 800 u kobiet zostali zakwalifikowani jako osoby, u których wystąpienie ciężkiej stenozы aortalnej nie jest prawdopodobne. Średnia wartość gęstości zakontrastowanej krwi

w świetle lewej komory i opuszki aorty wynosiła $380,84 \pm 113,33$ j. H. i $392,21 \pm 129,12$ j. H. AVCS oszacowany na podstawie angiografii TK wynosił $2068,62 \pm 1422,23$ przy progu detekcji zwapnień podwyższonym do 500 j. H. ($AVCS_{CTA0,6\ 500HU}$) oraz $1372,39 \pm 1044,53$ przy progu detekcji zwapnień podwyższonym do 600 j. H. ($AVCS_{CTA0,6\ 600HU}$). Przy obu wyżej wymienionych progach detekcji zwapnień oszacowanie wartości AVCS było możliwe odpowiednio w 76,47% i 98,04% badań. W pozostałych przypadkach wskazane progi detekcji były niewystarczające do odróżnienia zwapnień od zakontrastowanej krwi, w związku z czym aplikacja syngo.CT CaScoring nie umożliwiała generowania wyników AVCS.

Na podstawie jednoczynnikowej analizy regresji wyodrębniono formuły matematyczne, pozwalające na obliczenie natywnego AVCS na podstawie wartości AVCS, oszacowanych z obrazów fazy angiograficznej badań TK:

$$AVCS_{native3.0} = 813.920 + 1.510 AVCS_{CTA0.6\ 500\ HU}$$

$$AVCS_{native3.0} = 1235.863 + 1.817 AVCS_{CTA0.6\ 600\ HU}$$

$$AVCS_{native2.0} = 797.471 + 1.393 AVCS_{CTA0.6\ 500\ HU}$$

$$AVCS_{native2.0} = 1228.310 + 1.650 AVCS_{CTA0.6\ 600\ HU}$$

W grupie kobiet największą dokładność predykcyjną uzyskano przy przyjęciu wartości $AVCS_{CTA0,6\ 500\ HU} = 1569,00$ jako predyktora wysoce prawdopodobnej ciężkiej stenozы aortalnej. Dokładność tak przyjętego kryterium wynosiła 100%. Natomiast w grupie mężczyzn najwyższą dokładność predykcyjną uzyskano przy przyjęciu wartości $AVCS_{CTA0,6\ 600\ HU} = 1234,00$ jako predyktora wysoce prawdopodobnej ciężkiej stenozы aortalnej oraz $AVCS_{CTA0,6\ 600\ HU} = 899,10$ jako predyktora prawdopodobnej ciężkiej stenozы aortalnej. Dokładność obu tych kryteriów wynosiła 92,3%.

W związku z pominięciem fazy natywnej badania, określona parametrem DLP wielkość potencjalnej redukcji dawki promieniowania jonizującego – w przypadku szacowania wartości AVCS na podstawie fazy angiograficznej – wyniosła średnio $30,50 \pm 26,85$ mGy*cm. Stanowi to $4,45 \pm 1,54\%$ całkowitej dawki promieniowania zastosowanej w badaniu TK serca i dużych naczyń przed TAVI. Przy ograniczeniu badania jedynie do

zastawki aortalnej (badanie obejmujące fazę natywną, poświęconą ocenie AVCS, oraz fazę angiograficzną, poświęconą ocenie zastawki aortalnej i opuszki aorty, z wyłączeniem fazy angiograficznej, poświęconej ocenie wszystkich potencjalnych dostępow tętnicznych do zabiegu TAVI) redukcja dawki promieniowania stanowi $11,03 \pm 7,96\%$.

Szacowana wartość AVCS jest niższa od rzeczywistej ze względu na utracone w tej metodzie zwapnienia o gęstościach pomiędzy 130 a 500 lub 600 j. H. W niniejszej pracy udowodniono jednak, że uzyskane wartości szacowanej AVCS silnie korelują z rzeczywistymi wartościami AVCS (r pomiędzy 0,78 a 0,85). Przy zastosowaniu równań regresji przeliczenie wartości szacowanych na rzeczywiste można przeprowadzić z dopasowaniem 70%, a po uwzględnieniu płci pacjentów z 73% dopasowaniem.

Przeprowadzone badania prowadzą do wniosku, że opierając się wyłącznie na fazie angiograficznej badania TK serca i dużych naczyń można ocenić stopień uwapnienia zastawki aortalnej – AVCS. Oszacowanie AVCS na podstawie fazy angiograficznej badania TK – ze względu na pominięcie natywnej fazy badania – skutkuje mniejszą dawką promieniowania jonizującego.

WNIOSKI

- 1.1. Z przeprowadzonego przeglądu literatury wynika, że badanie TK przed zabiegami TAVI stanowi „złoty standard” w ocenie zastawki aortalnej i opuszki aorty oraz dostępow naczyniowych. Wskazania do TAVI ulegają poszerzeniu, w związku z czym rośnie liczba pacjentów, u których będą wykonywane te badania.
- 1.2. W każdym badaniu TK do problemu klinicznego i właściwości pacjenta należy dostosować możliwości sprzętu i umiejętności korzystania z protokołów zgodnie z zasadą ALARA. Do sposobów optymalizacji dawki promieniowania należy m. in. racjonalne korzystanie z protokołów oceny stopnia uwapnienia – Calcium Score.
- 2.1. Wielkość dawki promieniowania w rutynowych badaniach TK wykonywanych w procesie kwalifikacji do TAVI zasadniczo nie wpływa na powtarzalność pomiarów zastawki aortalnej, co uzasadnia próby wykonywania tych badań z zastosowaniem niższych dawek promieniowania.
- 2.2. Ze względu na wykazane pojedyncze korelacje pomiędzy dawką promieniowania w badaniach TK wykonywanych w procesie kwalifikacji do TAVI a stopniem powtarzalności pomiarów zastawki aortalnej i opuszki aorty proponuje się, aby po badaniach z niższymi dawkami promieniowania następowała kontrola stopnia powtarzalności tych pomiarów.
- 3.1. Opierając się wyłącznie na fazie angiograficznej badania TK serca i dużych naczyń można ocenić stopień uwapnienia zastawki aortalnej – AVCS.
- 3.2. Oszacowanie AVCS na podstawie fazy angiograficznej badania TK – ze względu na pominięcie natywnej fazy badania – skutkuje mniejszą dawką promieniowania.
- 3.3. Wielkość potencjalnej redukcji dawki promieniowania, określona parametrem DLP, w przypadku szacowania wartości AVCS na podstawie fazy angiograficznej badania, w związku z pominięciem fazy natywnej wyniosła średnio $30,50 \pm 26,85$ mGy*cm. Stanowi to $4,45 \pm 1,54\%$ całkowitej dawki promieniowania zastosowanej w badaniu TK serca i dużych naczyń przed TAVI.

STRESZCZENIE:

Zwężenie zastawki aortalnej – stenoza aortalna – jest najbardziej powszechną wadą zastawkową w krajach rozwiniętych. 81,9% zwężeń zastawki aortalnej ma postać degeneracyjno-zwapnieniową. W związku z wydłużaniem się średniej czasu trwania życia oraz starzeniem się społeczeństw częstość występowania zwężenia zastawki aortalnej będzie wzrastać, jednocześnie narastać będzie rozpowszechnienie ciężkiej postaci stenozy aortalnej. Leczeniem z wyboru u chorych z ciężką stenozą aortalną jest wszczepienie protezy zastawki w pozycję aortalną. Dla dużej grupy osób starszych, obciążonych licznymi schorzeniami towarzyszącymi, ryzyko klasycznego zabiegu kardiochirurgicznego wymiany zastawki aortalnej jest zbyt duże. Dla tej grupy chorych rozwiązaniem jest przeszskórne (przecewnikowe) wszczepienie zastawki aortalnej (ang. *Transcatheter Aortic Valve Implantation*, TAVI).

W procedurze kwalifikacji do zabiegów TAVI rutynowo wykonuje się badania obrazowe, które mają na celu określenie wymiarów zastawki aortalnej i opuszki aorty oraz możliwości wykorzystania poszczególnych dostępów tętniczych. „Złotym standardem” jest obecnie wykonywanie w tym celu badań tomografii komputerowej (TK) serca i dużych naczyń.

Pamiętać należy, że badania tomografii komputerowej wiążą się z narażeniem pacjenta na promieniowanie jonizujące. Najpoważniejszym źródłem narażenia na promieniowanie jonizujące we współczesnym świecie są właśnie ekspozycje medyczne, a rozpowszechnienie badań TK powoduje, że metoda ta zajmuje tutaj znaczące miejsce. Zgodnie z zasadą ALARA (*As Low As Reasonably Achievable*) podczas wykonywania procedur z wykorzystaniem promieniowania jonizującego należy poszukiwać sposobów redukcji jego dawki, optymalnie przy zachowaniu odpowiedniej jakości uzyskanych obrazów diagnostycznych, a czasem nawet kosztem nieistotnego obniżenia jakości takich obrazów.

Celem niniejszej pracy było poszukiwanie możliwości optymalizacji dawki promieniowania jonizującego w badaniach tomografii komputerowej w procedurze kwalifikacji do zabiegu TAVI.

Rozprawę doktorską stanowi cykl trzech artykułów naukowych składający się z jednej pracy przeglądowej oraz dwóch prac oryginalnych.

W pracy przeglądowej na podstawie dostępnego piśmiennictwa omówiono współczesne poglądy na temat wpływu promieniowania jonizującego na organizmy żywe, zagadnienie dawek promieniowania w badaniach oraz dokonano przeglądu doniesień z dużych analiz dotyczących dawek promieniowania w badaniach układu sercowo-naczyniowego, w tym badaniach przed zabiegami TAVI z ostatnich 10 lat. Przedstawiono wielkości dawek promieniowania przy zastosowaniu różnych protokołów badań. Dokonano również analizy sposobów obniżenia dawki promieniowania w badaniach TK.

W pierwszej pracy oryginalnej dokonano oceny zależności między dawką promieniowania jonizującego a powtarzalnością pomiarów aorty w badaniach TK serca i dużych naczyń w ramach standardowej kwalifikacji do zabiegów TAVI. Na podstawie analizy statystycznej wykazano, że wielkość dawki promieniowania w rutynowych badaniach TK w kwalifikacji do TAVI zasadniczo nie wpływa na powtarzalność pomiarów zastawki aortalnej i opuszki aorty, co uzasadnia próby wykonywania tych badań z zastosowaniem niższych dawek promieniowania. Jednakże ze względu na pojedyncze, istotne statystycznie zależności pomiędzy dawką promieniowania a stopniem powtarzalności wymiarowania zastawki aortalnej i opuszki aorty proponuje się, aby po badaniach z niższymi dawkami promieniowania następowała kontrola stopnia powtarzalności tych pomiarów.

W drugiej pracy oryginalnej dokonano oceny możliwości obniżenia dawki promieniowania jonizującego w badaniach TK przed zabiegami TAVI na podstawie oszacowania wskaźnika uwapnienia zastawki aortalnej z obrazów fazy angiograficznej, zamiast dedykowanej do tego osobnej, natywnej serii badania. Wskaźnik ten wykorzystywany jest jako dodatkowy parametr w kwalifikacji do zabiegów TAVI u pacjentów z niskogradientowym zwężeniem zastawki aortalnej i zachowaną frakcją wyrzutową lewej komory. W pracy wykazano, że w oparciu o obrazy fazy angiograficznej badania TK można ocenić stopień uwapnienia zastawki aortalnej, co – ze względu na pominięcie natywnej fazy badania – skutkuje mniejszą dawką promieniowania jonizującego. Wielkość osiągniętej w ten sposób potencjalnej redukcji dawki promieniowania jonizującego określona parametrem DLP w niniejszej pracy wyniosła średnio $30,50 \pm 26,85$ mGy*cm, co stanowi $4,45 \pm 1,54\%$ całkowitej dawki promieniowania zastosowanej w badaniu TK serca i dużych naczyń przed TAVI.

SUMMARY

Aortic valve stenosis - aortic stenosis - is the most common valvular defect in developed countries. 81.9% of aortic valve stenosis is degenerative and calcified. With increasing life expectancy and an aging population, the incidence of aortic valve stenosis will increase, at the same time, the prevalence of severe aortic stenosis will increase. The treatment of choice for patients with severe aortic stenosis is implantation of a valve prosthesis in the aortic position. For a large group of elderly patients, burdened by numerous comorbidities, the risk of classical cardiac surgery for aortic valve replacement is too high. For this group of patients, the solution is percutaneous (transcatheter) aortic valve implantation (TAVI).

In the qualification procedure for TAVI, imaging studies are routinely performed to determine the dimensions of the aortic valve and aortic leaflet, as well as the feasibility of using particular arterial accesses. "The gold standard" nowadays is to perform computed tomography (CT) scans of the heart and great vessels for this purpose.

It should be remembered that CT scans involve patient exposure to ionizing radiation. The most serious source of exposure to ionizing radiation in the modern world is just medical exposures, and the prevalence of CT examinations makes this method occupy a significant place here. According to the ALARA (As Low As Reasonably Achievable) principle, when performing procedures with ionizing radiation, one should look for ways to reduce its dose, optimally while maintaining the quality of the obtained diagnostic images, and sometimes even at the expense of a negligible reduction in the quality of such images.

The purpose of this dissertation was to seek ways to optimize the dose of ionizing radiation in CT scans in the qualification procedure for TAVI.

The dissertation is a series of three scientific articles consisting of one review paper and two original papers.

The review paper, on the basis of the available literature, discusses contemporary views on the effects of ionizing radiation on living organisms, the issue of radiation doses in examinations, and reviews reports of large studies on radiation doses in cardiovascular examinations, including examinations before TAVI procedures from the last 10 years. The

magnitudes of radiation doses using different study protocols are presented. Ways to reduce radiation dose in CT examinations were also analyzed.

In the first original study, the relationship between the dose of ionizing radiation and the repeatability of aortic dimension measurements using cardiac and large vessel CT as part of the standard qualification for TAVI procedures was evaluated. Based on statistical analysis, it was shown that the amount of radiation dose in routine CT examinations in TAVI qualification generally does not affect the repeatability of aortic valve measurements, justifying attempts to perform these examinations with lower radiation doses. However, because of the single statistically significant relationship between radiation dose and the degree of reproducibility of aortic valve sizing, it is proposed that examinations with lower radiation doses should be followed by a check of the degree of reproducibility of aortic valve sizing.

The second original paper evaluates the possibility of lowering the radiation dose in CT examinations before TAVI procedures based on the estimation of the aortic valve calcification index from angiographic phase images, instead of a dedicated separate native examination series. This index is used as an additional parameter in the qualification for TAVI procedures in patients with low-grade aortic valve stenosis and preserved left ventricular ejection fraction. The study shows that based on the angiographic phase images of the CT scan, it is possible to assess the degree of calcification of the aortic valve, which, due to the omission of the native phase of the scan, results in a lower dose of ionizing radiation. The magnitude of the potential reduction in ionizing radiation dose thus achieved, as determined by the DLP parameter in the present study, averaged 30.50 ± 26.85 mGy*cm, or $4.45 \pm 1.54\%$ of the total radiation dose applied to CT examination of the heart and great vessels before TAVI.

PIŚMIENNICTWO

1. Thaden JJ, Nkomo VT, Enriquez-Sarano M. The global burden of aortic stenosis. *Prog Cardiovasc Dis.* 2014;56(6):565–571.
2. Bajona P, Suri RM, Greason KL, Schaff HV. Outcomes of surgical aortic valve replacement: The benchmark for percutaneous therapies. *Prog Cardiovasc Dis.* 2014;56(6):619–624.
3. Krasopoulos G, Falconieri F, Benedetto U, et al. European real world trans-catheter aortic valve implantation: Systematic review and meta-analysis of European national registries. *J Cardiothorac Surg.* 2016;11(1):159.
4. Davlouros PA, Mplani VC, Koniari I, Tsigkas G, Hahalis G. Transcatheter aortic valve replacement and stroke: A comprehensive review. *J Geriatr Cardiol.* 2018;15(1):95–104.
5. Achenbach, S.; Delgado, V.; Hausleiter, J.; Schoenhagen, P.; Min, J.K.; Leipsic, J.A. SCCT expert consensus document on computed tomography imaging before transcatheter aortic valve implantation (TAVI) / transcatheter aortic valve replacement (TAVR). *J. Cardiovasc. Comput. Tomogr.* 2012, 6, 366-380.
6. Blanke, P.; Weir-McCall, J.R.; Achenbach, S.; Delgado, V.; Hausleiter, J.; Jilaihawi, H.; Marwan, M.; Nørgaard, B.; Piazza, N.; Schoenhagen, P.; et al. Computed tomography imaging in the context of transcatheter aortic valve implantation (TAVI) / transcatheter aortic valve replacement (TAVR): An expert consensus document of the Society of Cardiovascular Computed Tomography. *J. Cardiovasc. Comput. Tomogr.* 2019, 13, 1-20.
7. Mettler FA. Medical effects and risks of exposure to ionising radiation. *J Radiol Prot.* 2012;32(1):N9–N13.
8. Liu, X.-C.; Zhou, P.-K. Tissue Reactions and Mechanism in Cardiovascular Diseases Induced by Radiation. *Int. J. Mol. Sci.* 2022, 23, 14786.
9. Baselet, B.; Rombouts, C.; Benotmane, A.M.; Baatout, S.; Aerts, A. Cardiovascular diseases related to ionizing radiation: The risk of low-dose exposure (Review). *Int. J. Mol. Med.* 2016, 38, 1623–1641.
10. Vano E. Global view on radiation protection in medicine. *Radiat Prot Dosimetry.* 2011;147(1–2):3–7.

11. Cohen MD. ALARA, image gently and CT-induced cancer. *Pediatr Radiol.* 2015;45(4):465–470.
12. Shnayien, S.; Bressemer, K.K.; Beetz, N.L.; Asbach, P.; Hamm, B.; Niehues, S.M. Radiation Dose Reduction in Preprocedural CT Imaging for TAVI/TAVR Using a Novel 3-Phase Protocol: A Single Institution's Experience. *RöFo* 2020, 192, 1174–1182.
13. Kalra MK, Sodickson AD, Mayo-Smith WW. CT radiation: Key concepts for gentle and wise use. *Radiographics.* 2015;35(6):1706–1721.
14. Soschynski, M.; Hagen, F.; Baumann, S.; Hagar, M.T.; Weiss, J.; Krauss, T.; Schlett, C.L.; Mühlen, C.V.Z.; Bamberg, F.; Nikolaou, K.; et al. High Temporal Resolution Dual-Source Photon-Counting CT for Coronary Artery Disease: Initial Multicenter Clinical Experience. *J. Clin. Med.* 2022, 11, 6003.

WYKAZ PUBLIKACJI WŁĄCZONYCH DO ROZPRAWY DOKTORSKIEJ


1. Bartłomiej Kędziński; Piotr Macek; Barbara Dziadkowiec-Macek; Krystian Truskiewicz; Rafał Poręba; Paweł Gać. **Radiation Doses in Cardiovascular Computed Tomography**. *Life* 2023, 13, 990.
2. Bartłomiej Kędziński, Paweł Gać, Martyna Głońska, Rafał Poręba, Krystyna Pawlas. **Radiation dose and repeatability of aortic valve measurement by multidetector row computed tomography to assess eligibility for transcatheter aortic valve implantation**. *Adv Clin Exp Med*. 2020 Aug;29(8):983-992. doi: 10.17219/acem/123624. PMID: 32853487.
3. Paweł Gać, Bartłomiej Kędziński, Piotr Macek, Krystyna Pawlas, Rafał Poręba. **Estimation of Aortic Valve Calcium Score Based on Angiographic Phase Versus Reduction of Ionizing Radiation Dose in Computed Tomography**. *Life (Basel)*. 2021 Jun 23;11(7):604. doi: 10.3390/life11070604. PMID: 34201824; PMCID: PMC8305341.

PRACA NR 1



Review

Radiation Doses in Cardiovascular Computed Tomography

Bartłomiej Kędzierski ¹, Piotr Macek ², Barbara Dziadkowiec-Macek ², Krystian Truskiewicz ¹, Rafał Poręba ² and Paweł Gać ^{3,*} 

¹ Department of Radiology and Imaging Diagnostics, Emergency Medicine Center, Marciniak Lower Silesian Specialist Hospital, Fieldorfa 2, 54-049 Wrocław, Poland

² Department of Internal Medicine, Occupational Diseases, Hypertension and Clinical Oncology, Wrocław Medical University, Borowska 213, 50-556 Wrocław, Poland

³ Department of Population Health, Division of Environmental Health and Occupational Medicine, Wrocław Medical University, Mikulicza-Radeckiego 7, 50-368 Wrocław, Poland

* Correspondence: pawelgac@interia.pl or pawel.gac@umw.edu.pl

Abstract: We discussed the contemporary views on the effects of ionising radiation on living organisms and the process of estimating radiation doses in CT examinations and the definitions of the CTDI, CTDIvol, DLP, SSDE, ED. We reviewed the reports from large analyses on the radiation doses in CT examinations of the coronary arteries prior to TAVI procedures, including the CRESCENT, PROTECTION, German Cardiac CT Registry studies. These studies were carried out over the last 10 years and can help confront the daily practice of performing cardiovascular CT examinations in most centres. The reference dose levels for these examinations were also collected. The methods to optimise the radiation dose included tube voltage reduction, ECG-monitored tube current modulation, iterative and deep learning reconstruction techniques, a reduction in the scan range, prospective study protocols, automatic exposure control, heart rate control, rational use of the calcium score, multi-slices and dual-source and wide-field tomography. We also present the studies that indicated the need to raise the organ conversion factor for cardiovascular studies from the 0.014–0.017 mSv/mGy*cm used for chest studies to date to a value of 0.0264–0.03 mSv/mGy*cm.

Keywords: computed tomography; cardiovascular system; radiation dose; TAVI procedures



Citation: Kędzierski, B.; Macek, P.; Dziadkowiec-Macek, B.; Truskiewicz, K.; Poręba, R.; Gać, P. Radiation Doses in Cardiovascular Computed Tomography. *Life* **2023**, *13*, 990. <https://doi.org/10.3390/life13040990>

Academic Editor: Dimitris Tousoulis

Received: 16 February 2023

Revised: 3 April 2023

Accepted: 7 April 2023

Published: 11 April 2023



Copyright: © 2023 by the authors. Licensee MDPI, Basel, Switzerland. This article is an open access article distributed under the terms and conditions of the Creative Commons Attribution (CC BY) license (<https://creativecommons.org/licenses/by/4.0/>).

1. Introduction

Fifty years have passed since the invention of computed tomography by Sir Godfrey Hounsfield in 1972. During this time, this method has revolutionised imaging diagnostics in medicine [1]. The first application of computed tomography with ECG acquisition monitoring was implemented by George Harell and Diana Guthaner from Stanford University [2] in 1978, and the images of the heart obtained by this team, including the coronary vessels in computed tomography, were published in 1979 [3]. Today we would judge these images as very imperfect, as they were created using sequential computed tomography. The extensive use of computed tomography in heart diagnostics became possible only after the introduction of the helical acquisition method and the improvement of the temporal and spatial resolution of CT machines in the following years. In 1992, the images from the one-slice camera were published. In 1994, a retrospective reconstruction technique was developed from the ECG-gated studies. In 1999, four-slice computed tomography was introduced, followed by 16-slice in 2002 [4,5].

Currently, cardiac computed tomography is part of the guidelines of the European Society of Cardiology and repeated by the Polish Society of Cardiology. In the diagnosis of chronic coronary syndromes, CT is recommended as an initial test for the diagnosis of coronary artery disease for symptomatic patients when coronary artery disease with stenoses in the coronary arteries cannot be ruled out by clinical assessment alone. It is recommended that CT be considered as an alternative to invasive coronary angiography

(ICA) if the results of the other non-invasive tests are inconclusive or non-diagnostic [6]. On the other hand, in the diagnosis of acute coronary syndromes, CT is recommended as an alternative to ICA to exclude the acute coronary syndrome if the probability of coronary artery disease is low or moderate and when the cardiac troponin levels and/or ECG results are normal or inconclusive [7].

As a result of significant technological development of the apparatus, cardiac CT achieves a temporal resolution of 76 ms and a spatial resolution of 0.5 mm. However, it still lags behind the capabilities of ICA, which allows for a time resolution of 8 milliseconds and a spatial resolution of 0.2 mm [8].

It should be remembered that the dissemination of CT examinations are the most serious source of exposure to ionising radiation in the modern world. In the 20 years following 1990, the use of CT in the United States has increased approximately 20-fold. The share of radiation from diagnostic imaging sources in the total radiation exposure has increased from 20% of the total effective radiation dose (ERD) per capita to over 50%, half of which was related to CT [9].

In computed tomography, we use Roentgen rays (X-rays). They are a type of non-particle electromagnetic radiation with a wavelength of 5 pm to 10 nm, located in the electromagnetic radiation spectrum above ultraviolet, partially overlapping with gamma radiation. They are formed in X-ray tubes during the braking of the stream of accelerated electrons that are released from the cathode at the anode of the tube. Braking radiation (involving characteristic radiation, depending on the anode material) is ionising radiation, which means it can cause the release of free electrons as they pass through matter and can cause damaging effects to the tissues of the living organisms exposed to them.

The harmful effects of ionising radiation can be divided into stochastic and deterministic, or early and late, according to another division. Stochastic radiation causes effects where the likelihood (but not severity) is directly proportional to the dose. This includes malignant tumours and damage to the genetic material. If they arise in the reproductive cells of the body, they can lead to genetic disorders in offspring. These effects occur after a long latency period—from five to 20 or even 40 years after the exposure to the radiation. Deterministic radiation causes effects that are dose-dependent in their likelihood and severity, but do not occur below a certain dose level (threshold dose). These include, among others, cataracts, hair loss, pulmonary fibrosis, necrosis of the digestive tract, skin erythema, skin necrosis and radiation sickness. These effects occur immediately after the exposure to the radiation, most often within 2 to 4 weeks. They are associated with an exposure to high doses above 100 mGy. With regard to the stochastic effects, the concept of a linear, non-threshold probability of their occurrence is adopted, where even the lowest dose of radiation causes a certain risk of cancer. The doses used in diagnostic imaging, referred to as low linear energy transfer (LET) radiation, are typically below 100 mSv and have stochastic effects [8,10]. It is assumed that the stochastic effects occur randomly and that the risk of their occurrence depends on the type of ionising radiation, the type of tissue irradiated and the age of the examined person. It is believed that the dose fractionation does not significantly modify the stochastic risk and that the stochastic risk is cumulative, increasing with subsequent exposures [8].

Determining the degree of risk for the doses used in diagnostic imaging is not easy. Researchers have learned about the effects of ionising radiation on the human body from catastrophic events, such as the analysis of the effects of the nuclear explosions in Hiroshima and Nagasaki and atmospheric nuclear test explosions; disasters related to damaged nuclear reactors, in particular in Chernobyl (1986) and Fukushima (2011); and errors in imaging diagnostics related to exceeding radiation doses. The source of this information is also stems from research on the occupational exposure to radiation; the exposure from medical sources, e.g., in patients with tuberculosis who received high doses of X-rays as a result of repeated fluoroscopy; the analysis of natural environmental exposures related to living in areas with high background radiation; and artificial exposures, e.g., related to the use

of building materials containing radioactive elements. Based on such data analysis, risk models were constructed [8].

The most widely accepted cancer risk models are presented in the Biologic Effects of Ionizing Radiation (BEIR) Committee report. The committee is part of the American National Research Council, operating under the auspices of the US National Academy of Sciences. It publishes reports on ionising radiation effects. In the VII Report of 2006, a linear, no-threshold correlation was assumed between the exposure to radiation and the risk of cancer. According to this model, even the lowest dose of radiation carried some risk of cancer [11].

According to the BEIR VII report, for every 100,000 people who received an overdose of ionising radiation of 100 mSv, the lifetime attributable risk (LAR) was 510 in 100,000. Therefore, five out of 1000 people exposed to such radiation would die from malignant tumours caused by this radiation. For a radiation dose of 10 mSv, the lifetime LAR would be approx. one in 1000. On the other hand, the number of all the cases of malignant neoplasms, not only the fatal cases, predicted in this model was twice as high [9].

A significant proportion of the 25,000 survivors of the Hiroshima and Nagasaki nuclear explosions received radiation doses below 50 mSv. This group included individuals of all age categories and who had not been selected based on any underlying disease. However, it was an ethnically homogeneous group. The main negative effect in this group was an increase in the number of malignancies [8].

In 2007, the observations of 407,391 nuclear industry workers from 15 countries were published. The period covered by the study was as much as 20 years, which resulted in over five million person-years of observation. It involved the largest cohort to date, was conducted using accurate dosimetry and involved employees from many ethnic groups. The disadvantage of this study was that 90% of the study group was comprised of men who received as much as 98% of the cumulative dose of radiation. Additionally, it had lack of reference to the time when the cumulative dose was received by each of the participants. However, people employed for less than 1 year were excluded from the study. Most of the workers were employed in nuclear energy production facilities; the remaining plants specialised in various types of activities, including scientific research, waste management and the production of nuclear fuel, isotopes and weapons. The workers were exposed to X-rays and gamma rays. Approx. 90% of the people received cumulative doses below 50 mSv and the average dose was 19.4 mSv. Less than 0.1% received cumulative doses greater than 500 mSv. The study, therefore, provided information on the effects of the exposure to radiation doses similar to those used in cardiac CT scans. The authors reported an excessive relative risk of all-cause mortality of 0.42/Sv (0.00042/mSv) and a statistically significant increase in the excessive relative risk with the increasing radiation doses. The increased risk of all-cause mortality was mainly due to the increases in mortality from all cancers except for leukaemia and lung cancer. Among the 31 types of malignancies that were analysed, a significant relationship was identified for lung cancer and a borderline significant relationship for multiple myeloma as well as unspecified and secondary cancers. The doses received before age of 35 were associated with a lower risk for all cancers, except for leukaemia, than the doses received later [8,12].

The authors of a paper published in 2005 presented three cases of transient, bandage-shaped hair loss in the patients who underwent two DSA studies of cerebral vessels, two or more cerebral CT perfusion examinations with a tube current of 200 mA and several CT scans of the brain without CM within 15 days of subarachnoid haemorrhage. The radiation exposure to the scalp was estimated to be approximately 1.93 Gy in each cerebral CT perfusion study with a 200 mA tube current. The DLP of the cerebral CT perfusion protocol was 6.04 Gy·cm. The hair loss started on day 22 after the first CT scan. The loss was transient and lasted the longest at 92 days [13].

The harmful effects of ionising radiation are associated not only with an increased risk of developing cancer, but also with direct effects on the tissues and organs of the cardiovascular system. The importance of this problem is increasing due to the growing

number of patients who have undergone radiotherapy, going on to live their lives as cured cancer patients, and due to an increasing exposure to ionising radiation associated with medical diagnostics.

Most experimental and clinical studies relating to the effects of radiation on the cardiovascular system involve doses above 2 Gy. The excess relative risk per Gy for cardiovascular disease is estimated to be in the range of 0.1–0.2 1/Gy and is lower than the cancer risk [14].

Cardiovascular disease caused by high doses of ionising radiation has been observed in American radiologists, emergency workers who entered the Chernobyl zone in 1986–1987 and were exposed to doses above 150 mSv, British Nuclear Fuels Plc employees, adults who were treated using radiotherapy in childhood and adolescence for cancer, women after radiotherapy treatment for breast cancer and in survivors of a nuclear explosion with a radiation exposure above 500 mSv [15]. A study involving a group of more than 70,000 women diagnosed with breast cancer in Denmark and Sweden between 1976 and 2006 showed an increased risk of ischaemic heart disease, pericarditis and valvular disease in the patients treated for left breast tumours who received higher radiation doses to the heart area (mean 6.3 Gy) compared to the women treated for right breast tumours (mean cardiac dose 2.7 Gy) [16,17]. The cardiovascular mortality was also significantly higher in a case-control study of Chernobyl clean-up workers between 1992 and 2006 who were exposed to an average external gamma radiation dose of 128 mSv. A possible association between increased cardiovascular mortality and low radiation doses (with mean cumulative radiation doses of 20.7, 24.9 and 21.5 mSv, respectively) was evident from studies of nuclear workers [15,17]. In an analysis of the studies on the effects of whole-body irradiation with an average cumulative dose of less than 0.5 Sv or less than 10 mSv/day, four categories of cardiovascular diseases were assessed, namely ischaemic heart disease, non-ischaemic heart disease, cerebrovascular disease and other cardiovascular diseases. The relative excess risk values were 0.1/Sv, (95% CI) for ischaemic heart disease, 0.21/Sv, (95% CI), for cerebrovascular disease and 0.19/Sv, (95% CI) for non-ischaemic cardiovascular disease and stroke [17]. A study on the association between occupational exposure to low-dose ionising radiation in 11,500 workers in diagnostic medical facilities in South Korea and the incidence of cardiovascular disease estimated the relative excess risk for all cardiovascular diseases at ERR/100 mGy to be 0.14 [17].

The primary and initial cause of cardiovascular disease induced by ionising radiation is vascular endothelial damage. The primary mechanism of endothelial damage is oxidative stress, defined as an imbalance between the formation of oxygen free radicals and the activity of enzymatic and non-enzymatic antioxidant mechanisms. Its consequences are DNA damage, changes in the gene expression (epigenetic), mitochondrial dysfunction, increased production of pro-inflammatory cytokines, activation of the mechanisms of cell ageing (senescence) and cell apoptosis.

In the first stage of the interaction between radiation and tissue, the water radiolysis products are formed, including hydroxyl radicals ($\cdot\text{OH}$), hydroperoxyl radicals ($\text{HO}_2\cdot$) and hydrogen peroxide (H_2O_2). They are rapidly degraded, but the oxidative stress persists after the irradiation due to the endogenous cellular production of the reactive oxygen species mediated by the mitochondria [16].

Ionising radiation also causes reduced proliferation and apoptosis of the smooth vascular wall muscle cells [17].

In the next stage, these processes contribute to the formation and progression of atherosclerosis. The radiation-induced atherosclerotic plaques show a high inflammatory activity and have a reduced fibrous cap [14]. Following atherosclerosis, vascular stenosis develops for up to several decades after the exposure to ionising radiation. The atherosclerotic plaques can cause acute coronary syndromes, cerebrovascular incidents and peripheral ischaemia in the large and medium-sized arteries, and coronary microvascular dysfunction can lead to heart failure with a preserved ejection fraction [17].

Ionising radiation also leads to damage of the microcirculation. The radiation-induced damage of the capillary bed causes fragile and bleeding-prone telangiectasias, which develop 6 months to years after the radiation exposure. The radiation-induced damage of the renal microcirculation, or atherosclerosis of the renal artery, can lead to renin hypertension. Damage to the microcirculation in the lungs can lead to pulmonary hypertension and additional myocardial strain [14].

The radiation-induced fibrotic processes are a consequence of an inflammatory response involving the mast cells mediating the collagen deposition in the cardiac tissues. This process produces senescent fibroblasts that are metabolically active for many decades and produce increased amounts of collagen. Such reactions to radiation are observed in all tissues, including the heart. They can lead to cardiac arrhythmias [14].

After high-dose irradiation above 40 Gy, one of the earliest adverse effects is pericarditis, which appears after a few months and is characterised by the exudation of protein-rich fluid in the pericardial sac. In the subsequent course, it can lead to chronic constrictive pericarditis due to the formation of fibrous tissue, causing the thickening and rigidity of the pericardial sac. However, this is now extremely rare during radiotherapy due to the early initiation of prophylaxis [16].

Ionising radiation induces the osteogenic transformation of the valve interstitial cells and increases the production of osteogenic enzymes and cytokines and the deposition of the calcium phosphate deposits, with a consequent impairment of the valve function (insufficiency and/or stenosis) [14].

2. Dose Definitions and Applications in Computed Tomography

In radiological practice, we encounter the terms CTDI_{vol}, the volumetric computed tomography dose index, and DLP, the dose-length product, which are calculated using the algorithms of the CT machine, presented on the screen of the CT scanner work console and saved in the DICOM format in the radiation dose structured report (RDSR). In 1981, the definitions of the computed tomographic dose index (CTDI) and the multiple scan average dose (MSAD) were introduced. The definition of the CTDI has changed as a new generation of CT technologies have developed. The implementation of multi-slice CT scanners and CT scanners that use wide beams of radiation has affected the CTDI's ability to determine the radiation dose accurately. Since 2002, device manufacturers have been required to display the tomographic volumetric dose index (CTDI_{vol}) and the dose-length product (DLP) on the operator's console. The predicted value of the CTDI_{vol} appears on the console after the topogram is executed and before starting the actual study. It can be used to estimate the dose even before the test is performed [1,18,19]

2.1. MSAD—Multiple Scan Average Dose

The MSAD determines the average radiation dose delivered during the examination to the covered area when scanning in multiple, continuous layers. It is a measure of the average absorbed dose, expressed in mGy. It is defined as the average dose in the central layer of a series of multiple layers (each of a certain thickness) when there is a constant gap between the successive layers. To measure the MSAD, one would place the radiation detector in a phantom simulating the patient (an anthropomorphic phantom) and perform a CT scan according to a specific protocol, taking the dose readings layer by layer. The MSAD value is the average dose in the centre area of the study. It is typically 1.25–1.4 times the dose of a single layer because it includes the measurements resulting from the exposure of the overlapping adjacent layers and from the diffuse radiation. This parameter did not catch on because the direct measurement of the MSAD requires multiple exposures, and in the early years of CT, testing was very time consuming. In practice, the tomographic dose index (CTDI), an alternative, more convenient way of dose estimation, is preferred, which saves a significant amount of time. In this case, the MSAD is defined as the ratio of the ply

width to the ply spacing multiplied by the CTDI. If the pitch factor is one, then the MSAD = the CTDI [1,1,18].

$$\text{MSAD} = T/I \text{ CTDI}$$

2.2. CTDI—Computed Tomography Dose Index

This is the dose measured during a single rotation of the lamp detector system using a pencil ionisation chamber with a measuring part length of 10 cm. The ionisation chamber is placed in a 14 cm-long cylindrical phantom, composed of plastic (PMMA) with a diameter of 16 cm (head phantom) or 32 cm (torso phantom), as shown in Figure 1.

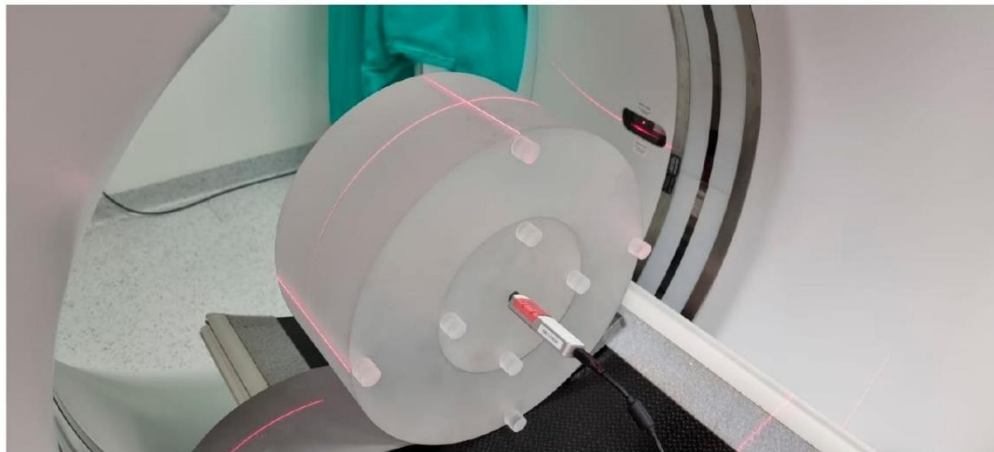


Figure 1. Acrylic phantom used for dosimetry in CT. Here, a 32 cm diameter phantom (torso) with nine holes. A pencil probe sits in the central hole with an ionization chamber. The visible laser lines position the phantom in the gantry.

The measurements are taken in the holes located along the axis of the phantom and in the four holes on its perimeter, 1 cm below the surface of the phantom at every 90 degrees. It is not an anthropomorphic phantom as the measured dose is the dose absorbed in the air, not in the human body. The weighted average is calculated from the measurement in the centre of the phantom and the arithmetic mean of the measurements from the four circumferential holes. The current definition of the index was standardised by the International Electrotechnical Commission (IEC) in 2002. Its main advantage is that it can be used to estimate further indexes used in CT dosimetry, such as the volumetric tomographic dose index (CTDIvol) and the dose-length product (DLP) [1,1,12,18].

2.3. CTDIvol—Volumetric Computed Tomography Dose Index

The CTDI value is determined by measuring the ionisation chamber during a single revolution. In the sequential mode testing, the lower the dose, the greater the table travel between the successive layers. In the spiral (helical) mode testing, the lower the dose, the greater the spiral pitch (pitch factor) [19]. While the CTDI refers well to the sequential scanning modes, the helical (spiral, or otherwise: volumetric) mode of scanning is so different that the measurements from a dose during a single revolution are insufficient. In 2002, the concept of the volumetric computed tomography dose index (CTDIvol) was introduced, which takes into account, among other things, the pitch factor during the helical scanning. A requirement has also been introduced for the CTDIvol value to be presented on the tomograph operator's console. This value does not have to be obtained on a specific camera. Instead, it may simply be the typical value for a specific camera model. During the specialist tests, in the case of the measurements for the spiral mode of acquisition, the measurements are taken using the sequential mode. For all the other

parameters (voltage, current, collimation, etc.) the measurements are taken in the spiral mode, and the calculations are made depending on the pitch [19].

$$\text{CTDI} = \text{CTDIvol if pitch} = 1$$

The formula $\text{CTDIvol} = n - \text{CTDIw}$ is used for the mode in which the camera performs n lamp revolutions in one table position, without moving the table.

The 2002 definition for the pitch can be stated as $\text{CTpitch factor} = \Delta d/\text{NT}$

With the advent of multi-slice computed tomography and the extension of the radiation beam—now up to 16 cm—the method of measuring the dose in specialised tests had to be modified. In the case of wide radiation beams, a 10 cm-long ionisation chamber does not register a large part or even most of the scattered radiation. Sometimes it even registers a part of the radiation beam itself, which can exceed 10 cm in width. Thus, the dose is underestimated. This is not significant in the case of beams up to 4 cm wide, while in the case of wider beams, underdosing is significant. This problem is addressed by the 2012 standard. The measurement must be taken using an ionization chamber with a length of at least 4 cm greater than the beam width. Therefore, 10 cm chambers can be used for beam widths up to 6 cm. In the case of wider beams, e.g., a 16 cm beam, longer ionisation chambers should be used, in this case 20 cm. If such a chamber is not available, then a standard chamber with a length of 10 cm can be used, but the measurements should be taken several times. The ionisation chamber should be shifted in relation to the axis of the gantry, and the measurement results should be added. The 2012 standard also defines the CTDIvol definition for the shuttle acquisition method used in the organ perfusion studies. The device console should also display information about the diameter of the phantom (16 cm or 32 cm) used for the CTDIvol measurement. The smaller the phantom, the greater the marked dose. The dose for the same exposure parameters will be approximately twice as high when using the 16 cm phantom compared to the 32 cm phantom. In the specialised testing, the deviation of the CTDIvol from the value displayed on the CT console is expected to be less than $\pm 20\%$.

2.4. DLP—Dose-Length Product

The dose-length product (DLP) values are usually presented to the CT operator at the end of the examination and provide a convenient summary of the total amount of radiation that has been emitted to the patient. The DLP was defined as the product of the CTDIvol and the scan length (L), expressed in milligrays \times centimetres. The DLP determines the radiation dose used in the examination, depending on the scope of the study, which is not taken into account by the CTDI and CTDIvol. It is important to note that this is still not the patient dose. When examining the different body regions, the DLP values should not be added together to calculate the patient dose. The DLP value obtained from each of the study ranges should be multiplied each time by a different organ conversion k-factor [1,8,19,20].

2.5. SSDE—Size-Specific Dose Estimates

The SSDE is expressed in milligrays (mGy) and requires the determination of the patient's body size. The bilateral dimension (LAT) can be determined from the topogram. If two topograms are planned in the study protocol for the orthogonal projections, then the anteroposterior dimension (AP) can be determined from the second topogram. After the examination, the AP and LAT dimensions can be marked from the CT scan axial images. The dimensions of the AP and LAT are added together or the effective diameter is determined, i.e., the square root of the product of the AP and LAT. Then, from the appropriate tables, the conversion factor for the LAT dimensions or the converted AP and LAT are multiplied by the CTDIvol values from the CT device for a given examination. The coefficients are the same for all the study types but different for the different phantoms used for the dose estimation. They were created based on the Monte Carlo calculations for anthropomorphic phantoms [1,18].

2.6. ED—Effective Dose

The effective dose (ED) reflects the biological risk of the radiation exposure and corresponds to the dose received by the whole body. Uniform irradiation is needed to generate the same stochastic risk as the dose delivered to a part of the body during a particular CT scan. It is used to relate the different doses received by the different tissues to the total sum of the stochastic effects. It allows for the dose in a CT scan to be compared to the doses received in the other medical tests [8,21].

Its definition was introduced by the ICRP in 1991. It is calculated by adding the doses absorbed by all the organs under examination and multiplying them by the appropriate weighting factors, taking into account their sensitivity to radiation [5,8,19,21].

The unit of measurement for the effective dose is the sievert (Sv) or millisievert (mSv) [5,8,19,21], as shown in Figure 2.

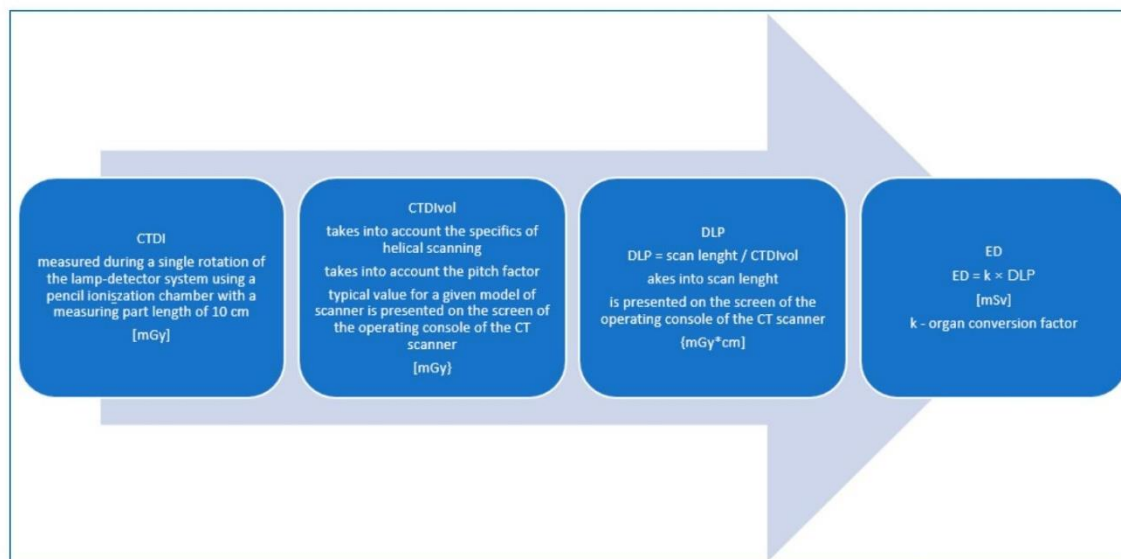


Figure 2. Methodology of the radiation dose estimation in the CT examinations.

The effective dose is considered the best parameter to quantify the radiation received by the patients undergoing the ionising radiation testing and to compare the risks associated with the different types of examinations. In the CT scans, the effective dose is most commonly estimated by multiplying the dose-length product (DLP) value displayed on the dose report of each CT scan by the organ conversion k-factor.

$$ED = k \times DLP$$

The methods for determining the tissue conversion factors (k) can be varied. They can be determined by dividing the effective doses, calculated using the Monte Carlo simulations performed in math or voxel phantoms, by the DLP values for the relevant studies [19,22]. Commercial CT dosimetry software packages can be used [20]. The direct radiation measurements in the anthropomorphic phantoms can also be employed by using radiochromic films (RCF) or metal-oxide-semiconductor field-effect transistor (MOSFET) radiation detectors [23].

The normalised organ conversion k-factor has different values for the different body regions and takes into account the radiosensitivity of the organs in the body region that is under examination. The adopted conversion factors are independent of sex and age, and they determine the risk for the theoretical body of a 30-year-old hermaphrodite. They are

also independent of the patient size. However, in the case of a specific patient, the actual risk of cancer may be up to three times higher or lower [8,23].

The definition of the effective dose introduced by the ICRP refers to the weighting factors that take into account the sensitivity of the organs to radiation. They have already been modified and will most likely continue to be changed in the future as knowledge advances. Published in 2007 (ICRP publication 103), a new set of tissue weighting factors increased the effective dose value for cardiac imaging by approximately 30–50% compared to the previous versions from 1996. This was mainly due to an increase in the tissue weighting factor for breast tissue, the value of which increased from 0.05 to 0.12. Previously, it was 0.15 in 1977, but was reduced to 0.05 in 1991. Since the breasts are directly irradiated by the X-ray beam during CT scans of the heart, together with the lung dose, they are the main dose-determining organs that are effective in cardiac CT scans. In cardiac CT scans, the equivalent organ dose (expressed in mSv) to the breast may be significantly higher than the effective dose (also expressed in mSv). Therefore, confusion between these terms should be avoided [8,19,21,23].

Due to its imperfections, the effective dose cannot be used to assess the radiation risk for a particular patient. The ICRP emphasises that the effective dose is intended for use in radiation protection and should not be used for the epidemiological assessment or the estimation of specific human exposures. Nevertheless, it remains the most widely used parameter to compare radiation exposure across the test methods and protocols [19,21,23].

3. Radiation Doses in Cardiovascular CT Scans—A Review of Reports

The radiation doses used in cardiovascular CT scans are not low. During these examinations, the largest doses of radiation are absorbed by the lungs and breasts, which are the organs most sensitive to radiation-related damage. Younger patients are clearly more sensitive to radiation and are more likely to develop lymphoma and breast cancer, so attention should be paid to the radiation doses used during cardiac CT scans in children and young adults. Women who are screened during breastfeeding are particularly at risk of developing breast cancer. The radiation doses to which the breasts are exposed in cardiac CT examinations exceed the doses associated with mammography in two projections (3 mGy). In turn, the risk of lung cancer is potentially higher in the elderly due to advanced age and the possible synergistic carcinogenic effects of tobacco smoke and ionising radiation [8,10].

In the CORE-64 study, the mean effective dose on the coronary CT scans was 19 mSv (range 16–26 mSv), as determined by the Monte Carlo simulations for the 64-slice Aquilion scanner and calculated according to the ICRP report 103 of 2007. The mean effective dose for the entire cardiac CT protocol, including the topograms, calcium score, contrast bolus monitoring and coronary vessels CT was 22 mSv (range 18–30 mSv). The calcium score doses ranged from 1.7 to 2.6 mSv. The contribution of the topograms and contrast agent bolus monitoring was very small, at ≤ 0.3 mSv. The highest mean organ equivalent doses associated with the cardiac CT scans for the normal body patient models were observed as 38 mSv for the breasts, 35 mSv for the lungs, 32 mSv for the liver, 29 mSv for the stomach and 27 mSv for the oesophagus. In the case of distant organs, the dose was 0.2 mSv or less for the bladder, ovaries—0.2 mSv or less for the ovaries and 0.02 mSv or less for the testicles [24].

For the study, the doses of over 35,000 coronary artery CT scans that were performed at the University Center in Nanjing (China) in 2007–2016 with the use of 1st- and 2nd-generation dual-source scanners (Somatom Definition and Somatom Flash, Siemens Healthineers, Forchheim, Germany) were analysed. I median values were 47.4 mGy for the CTFIvol (value range 25.1–61.1 mGy), 661.2 mGy*cm for the DLP (value range 315.2–940.0 mGy*cm) and 66.9 mGy for the SSDE (value range 38.5–97.3 mGy). The radiation doses decreased after the implementation of the 2nd-generation dual-source computed tomography (Definition Flash) and reached the lowest level in the last year of the analysed period, where the CTDIvol was 23.1 mGy (value range 15.7–32.4 mGy), the DLP was 268.2 mGy*cm (value range 183.0–393.6 mGy*cm) and the SSDE was 32.5 mGy (value range 22.9–45.2 mGy). The

median CTDI_{vol} for the studies in the retrospective acquisition protocol was 57.9 mGy (range 47.2–59.0 mGy), approximately 116.9% higher compared to the prospective sequential acquisition and 185.2% higher compared to the prospective helical with the use of a high pitch. After the CABG, the patients received higher radiation doses than a classic coronary CT scan, while the highest doses were received by the patients with arrhythmia. The calcium score studies were excluded from the dose analysis in this study [25].

In the analysis of 5000 patients examined in German centres from the years 2009–2014, the median DLP in the calcium score scan was 40 mGy*cm. In the case of the CCTA, it was 255 mGy*cm, which decreased from 397 mGy*cm at the turn of 2009 and 2010 to 176 mGy*cm from 2011–2017. In this study, a significant percentage of coronary CT examinations in the prospective acquisition protocol was noteworthy, which increased from 67.5% to 82.2% in the analysed period, while the share of the studies with retrospective acquisition without the dose modulation decreased from 5.3% to 1.6% [26].

In a paper from 2012, A. Sarma et al. provided the estimated radiation doses for the calcium score scans at an average of 3.0 mSv (dose range 1.0–12.0 mSv), for coronary CT at an average of 8.7–16 mSv (dose range 1.0–32.0 mSv) and for the triple rule-out study at an average of 4.0–31.8 mSv (range 7.5–19.4 mSv). These doses, converted to the DLP using the value of the coefficient $k = 0.017$ were 214 mGy*cm for the calcium score, 621–1143 mGy*cm for the coronary arteries CT and 286–1386 mGy*cm for the triple rule-out study [10].

When comparing the doses used in the studies pooled from the four centres in Saudi Arabia, the median DLP values were 320–432 mGy*cm on the Siemens Somatom scanners and 1112 mGy*cm on the Philips Ingenuity scanner (Philips Healthcare, Amsterdam, The Netherlands). The authors mentioned that the exposure parameters, such as the tube voltage (kVp), exposure time product (mAs), pitch settings, layer thickness and scan length, may have affected the patient radiation exposure and image quality. One of the labs (equipped with the Somatom scanner), regardless of the patient's BMI and clinical conditions, used a constant tube voltage, rotation time, pitch and layer thickness, which overexposed the patient to the radiation dose. The high dose at the Philips facility was not associated with high DLP_{vol} value (33.1 mGy) but with the use of long scan ranges. The mean effective dose on a coronary CT scan was 15.2 ± 8 mSv and ranged from 1.2 to 61.8 mSv. The highest DLP value in the analysed studies was 3277 mGy*cm. Since the average expected radiation risk from the coronary CT scans was one in 1000, the risk from this highest dose could be estimated as one case of malignancy in 300 scans. This increased cancer risk was due to the non-optimised irradiation procedures and was immediately corrected [27].

In the CRESCENT study, conducted from April 2011 to July 2013, the coronary artery calcium score was performed on a group of 242 patients with stable angina pectoris referred to the outpatient clinics of four Dutch hospitals. This was followed by the CCTA if the calcium score did not exceed 400. In this study, 117 patients were included. The mean radiation dose from the calcium score was 2.4 mSv and 8.5 mSv from the full cardiac CT scan [28].

In the 2017 PROTECTION VI study (the prospective multicentre study on radiation dose estimates of cardiac CT angiography), the median total DLP of all 4502 patients was 252 mGy*cm (IQR 154–412 mGy*cm). This was a prospective, worldwide, multicentre, observational, survey-based study to assess the radiation exposure during the cardiac CT examinations in everyday practice. It involved 4502 patients from around 70 centres in Europe, North America, South America, Asia and Australia. It did not benefit from financing from its equipment suppliers. A total of 435 radiologists and cardiologists from 62 different countries were invited to participate in the study. The DLP values for the coronary CT alone were 195 mGy*cm, corresponding to an effective dose of 2.7 mSv using the conversion k-factor for the chest CT scans (0.014 mSv/mGy*cm) or an effective dose of 5.1 mSv using the conversion k-factor recently postulated for the cardiac CT scans (0.026 mSv/mGy*cm). In 2017, compared to the 2007 study, a significant 78% reduction in the DLP was observed ($p < 0.001$) [29]. The difference in the median dose from the

individual centres was as much as 37-fold (from 57 to 2090 mGy*cm). The reduction in the radiation dose did not increase the rate of the non-diagnostic coronary artery CT scans (1.9%). It should be noted that 78% of the studies were performed using prospective, sequential acquisition protocols. [29–31] The median radiation dose for the studies using a conventional tube voltage (120 kVp) was estimated to be 4.3 or 8.1 mSv, using the thoracic or the recently published cardiac DLP to effective dose conversion factor of 0.014 or 0.026 mSv/mGy*cm, respectively [29].

A summary of the dose values from the publications in question is shown in Table 1.

Table 1. Radiation doses in the cardiovascular CT scans—a review of the reports.

Study	Year of the Survey/Publication	Kind of Protocol	Radiation Doses
CORE-64 study	2010 (publication)	CCTA	ED 19 mSv (range: 16–26 mSv) DLP 633.3 mGy*cm (range: 533.3–866.6 mGy*cm) (mean) k = 0.030 mSv/mGy*cm
		CS	ED 1.7–2.6 mSv DLP 56.6–86.6 mGy*cm (mean) k = 0.030 mSv/mGy*cm
University Center in Nanjing (China)	2007–2016 (survey)	CS+CCTA	DLP 661.2 mGy*cm (range: 315.2–940.0 mGy*cm) (median)
	2016 (survey)	CS+CCTA	DLP 268.2 mGy*cm (range: 183.0–393.6 mGy*cm) (median)
German Cardiac CT Registry	2009–2014 (survey)	CCTA	DLP 255 mGy*cm (median) k = 0.014 mSv/mGy*cm
		CS	DLP 40 mGy*cm (median) k = 0.014 mSv/mGy*cm
	2014 (survey)	CCTA	DLP 176 mGy*cm (median) k = 0.014 mSv/mGy*cm
USA multicentre data	2012 (publication)	CCTA	DLP 621–1143 mGy*cm (mean) k = 0.014 mSv/mGy*cm
		CS	DLP 214 mGy*cm (mean) k = 0.014 mSv/mGy*cm
		TROCT	DLP 286–1386 mGy*cm (mean) k = 0.014 mSv/mGy*cm
Saudi Arabia four centres	2020 (publication)	CS+CCTA	DLP 383.8 ± 354 mGy*cm (mean)
CRESCENT	2011–2013 (survey)	CS+CCTA	ED 8.5 mSv DLP 607.1 mGy*cm (mean) k = 0.014 mSv/mGy*cm
		CS	ED 2.4 mSv DLP 171.4 mGy*cm (mean) k = 0.014 mSv/mGy*cm
PROTECTION VI	2017 (survey)	CCTA	195 mGy*cm (range: 110–338 mGy*cm) (median)
		CS+CCTA	252 mGy*cm (range: 154–412 mGy*cm)

CCTA—coronary computed tomography angiography; CS—calcium score; k—organ conversion factor.

In the conclusion of the PROTECTION VI study, a diagnostic reference level for the coronary CT scans was proposed. This value was usually set at the 75th percentile of the dose for a typical patient size and for a particular radiological procedure. It was not a recommended or preferred dose, but rather a value to aim for. The authors suggested that a new DLP diagnostic reference level of 400 mGy*cm should be considered [29]. As a reminder, in the PROTECTION I study conducted 10 years earlier, the DLP reference level for the angio-CT of the coronary vessels was set at 1200 mGy*cm (17 mSv) [19]. The achievable dose, on the other hand, was the level set at the 50th percentile [25].

The reference levels of the radiation doses for the coronary CT under the Ionising Radiation (Medical Exposure) Regulations in the UK were 380 mGy*cm for the retrospective acquisitions with ECG monitoring and 170 mGy*cm for the prospective acquisitions without padding [32].

Based on a survey conducted in 2016/2017 under the ICRP rules in 55 centres on 338 patients in Australia, the national dose reference levels were established for the CCTA with a DLP of 268 mGy*cm and for the CS with a DLP of 137 mGy*cm [33].

A similar study was conducted in France in 2013 in eight hospitals. A total of 460 CCTA studies were analysed. The reference dose levels were proposed for the retrospective studies with an ECG-gating DLP of 870 mGy*cm and a DLP of 393 mGy*cm for the prospective studies with an ECG-gating DLP of 370 mGy*cm [34].

In 2016, a similar study was carried out in 11 centres in Saudi Arabia, analysing information from the RIS and PACS data of the studies of 197 patients. The studies in the prospective protocol were used in 55% of the patients. The reference dose levels were set at a DLP of 395 mGy*cm for the studies in the prospective protocol and at 1057 mGy*cm for studies in the retrospective protocol [35].

The more recent data came from a single-centre analysis in Taiwan involving 445 patients that was studied from February 2017 to December 2019. The following reference levels were established—for the CCTA, a DLP of 560.1 mGy*cm and for the calcium score, a DLP of 39.2 mGy*cm [36].

The dose reference values (DRLs) are shown in Table 2.

Table 2. Cardiovascular CT scans—dose reference values (DRLs).

Study	Year of the Survey/Publication	Reference Level
PROTECTION I	2007	DLP 1200 mGy*cm
PROTECTION VI	2017	DLP 400 mGy*cm
DRL in CCTA in Australia	2018	DLP 268 mGy*cm for the CCTA DLP 137 mGy*cm for the CS
DRL in CCTA in France	2013	DLP 370 mGy*cm for the prospective protocols DLP 870 mGy*cm for the retrospective protocols
DRL in CCTA in Saudi Arabia	2016	DLP 393 mGy*cm for the prospective protocols DLP 1057 mGy*cm for the retrospective protocols
DRL in CCTA in Taiwan	2017–2019	DLP 560.1 mGy*cm for the CCTA DLP 39.2 mGy*cm for the CS
Ionising Radiation (Medical Exposure) Regulations UK	2017	DLP 380 mGy*cm for the retrospective acquisitions with an ECG gating
		DLP 170 mGy*cm for the prospective acquisitions without padding

CCTA—coronary computed tomography angiography; CS—calcium score; DRL—dose reference values.

Einstein et al. estimated the lifetime risk of cancer in a 20-year-old woman as 0.7%, following a single coronary CT scan in a protocol without applying a dose reduction. Hurwitz et al., in turn, estimated that the excess relative risk in a 25-year-old woman

who underwent a coronary CT scan ranged from 1.4% to 2.6% for breast cancer and from 2.4% to 3.8% for lung cancer [10,37,38]. In the whole coronary CT cohort, the estimated mean lifetime risk of radiation-induced cancer was 0.13% [10,39]. In comparison, the relative risk of lung cancer associated with an effective dose of 1000 mSv (approximately 50–100 coronary CT scans) was 2.9. They can be compared to the relative risk of lung cancer in tobacco smokers, which—according to the statistics of the US National Cancer Institute—was 4.9 in people who smoked up to 15 cigarettes per day and 13.3 in people who smoked up to 25 cigarettes per day [21].

It should be noted that multiple, repeated CT scans can lead to high cumulative ERDs (50–200 mSv). Compared to the dose from a single CT scan, a cumulative dose of 120 mSv (equivalent to 12 coronary angio-CT scans) can increase the lifetime cancer risk from 1/1000 to 1/82 [9].

The effect of the length of the imaging interval on the risk of developing malignancies remains unclear, partly because of the undefined effect of the cellular repair mechanisms. However, it is assumed that the radiation risk of two CT scans is approximately twice that of a single scan, regardless of the time interval between them [10].

The median age in the PROTECTION VI study was 60 years. An effective dose of 5 mSv at this age increased the additional lifetime risk of malignancy only marginally, and the benefits of the coronary CT information significantly outweighed this risk. The estimated risk of lethal malignancy due to CT with a dose of 10 mSv was 0.05%. In contrast, the benefits of coronary CT were an estimated 50% reduction in the number of fatal and non-fatal myocardial injuries observed in the 3-year period following a CT scan [29].

In comparison, the median effective dose for a frequently performed SPECT study was approx. 10 mSv worldwide, 7 mSv in conventional chest CT scans, 14 mSv in 18F PET cardiac scans, 10 mSv in cardiac stress tests with ^{99m}Tc sestamibi, 40 mSv in thallium stress tests 210 Tl and 7 mSv in diagnostic coronary angiography [20,29,40].

The radiation doses from medical sources are often referred to as ‘background radiation’. Over one year, patients receive slightly less than half the dose associated with a routine chest CT scan (3 mSv) from background sources, including cosmic rays and radon gas. Compared to a chest X-ray in two projections, the radiation dose in a chest CT is 100 to 400 times higher [10]. The average dose level from background radiation in Poland is 2.5 mSv per year [41].

The comparison of the CT protocols should be conducted using the DLP values as all the CT systems share the same dosimetry system. Comparing the equipment or test protocols on the basis of the effective dose expressed in millisieverts (mSv) always requires the use of the same conversion k-factor. Different publications use different values, from 0.014–0.017 for chest examinations to 0.024 to 0.030 mSv/mGy*cm for postulated cardiac examinations [24,27].

Assuming there is a linear, no-threshold concept of ionising radiation harm, the estimated lifetime risk of death from cancer associated with the radiation dose received during a typical coronary CT scan (ok. 10 mSv) is 0.05%. On the other hand, ICA performed for diagnostic purposes only has a “serious” complication rate of 1.7% (including mortality: 0.11%; myocardial infarction: 0.05%; stroke: 0.07%; haemodynamic complications: 0.26% and serious contrast agent reaction: 0.37%). This should be added to the theoretical risk of future malignancy associated with the use of fluoroscopy during ICA, which is 0.02% [19].

In 2018, an expert consensus from the Society of Cardiovascular Computed Tomography (SSCT) was published referring to coronary artery examinations in women. The authors indicated that exposure to ionising radiation was a major safety concern for CT in women, and this was especially true for breast exposure. The paper stated that after a CT scan of the heart of a 60-year-old woman, her LAR rate of malignancy was 0.22% (one in 466). In the estimation of this risk, a higher number of effective doses resulting from the study were assumed than are currently commonly used. In the studies on an anthropomorphic phantom performed using a 64-slice apparatus in a retrospective spiral protocol with ECG monitoring but without dose modulation, the absorbed dose in the

breast was 82.9 mGy. On the same phantom, using dose modulation on a 320-slice device, the dose was reduced by 79%—to 17.5 mGy. This showed how modern dose reduction techniques can reduce radiation exposure. With a skilful use of the CT study protocols, the dose is more of a concern for certain studies, such as myocardial perfusion imaging using SPECT, PET and ICA [40].

The authors of the study do not recommend the use of breast shields. However, in the process of positioning the patient, they recommend the manual movement of the movable part of the breast outside the field of CT imaging of the heart. This makes it possible to reduce the dose absorbed by the breasts, reduce the absorption of the radiation during acquisition and allows for the use of a lower CT tube current. This reduces the effective radiation dose to 33% compared to men with similar BMI values [40].

The discussed publication also raised the important problem of CT examinations during pregnancy. The authors confirmed that examinations that use ionising radiation during pregnancy may be performed only when the expected results may change the medical management. The radiation risk to the foetus was mainly due to the diffuse radiation from within the imaged part of the patient's body. The radiation doses to the foetus during chest CT or CT lung angiography to exclude pulmonary embolism were low. In the case of testing to exclude pulmonary embolism, it was estimated to be within 0.02 mGy, so the risk of non-stochastic foetal damage in the case of CT limited to the chest was negligible. Higher doses were associated with the studies that directly involve the foetus. The foetal dose for the CT angiography of the chest, abdomen and pelvis was 13 mGy. The authors of the guidelines referred to the opinion of the American College of Obstetrics and Gynecology (ACOG), which states that, if clinically indicated, angio-CT should not be withheld in pregnant patients. Instead, before the test is performed, the risks and benefits should be considered and discussed. The assessment of stochastic risk to the foetus is very difficult. The authors of the study referred to the models that allowed for estimating the excess risk of malignant neoplasm associated with a radiation dose of 10 mGy on the foetus from one in 4545 in the high-risk model to one in 1667 in the low-risk model. It should be noted that, although the iodinated contrast agents may cross the placenta into the foetal circulation during pregnancy and may be detectable in the amniotic fluid, there is no evidence of teratogenic, mutagenic or other foetal harm [40].

4. Optimization Methods—Reduction in the Radiation Dose

In each study, the capabilities of the equipment and the ability to use the protocols should be adapted to the clinical problem and the patient characteristics in accordance with the ALARA (as low as reasonably achievable) principle. The opportunities to optimise the radiation dose may vary, depending on the conditions of the examination and the type of equipment.

The optimisation methods and reductions in the radiation dose in the CT examinations include the following.

- CT tube voltage reduction
- ECG-monitored radiation modulation (tube current)
- Iterative image reconstruction
- Deep learning-based image reconstruction and deep learning-based image denoising
- Reduction in the scan range (scan length)
- Prospective study protocols
- Modulation of the current intensity depends on the attenuation of the radiation
- Heart rate control
- Rational use of the calcium score coronary artery calcification test
- Multi-slice, dual-source and wide-field tomography

4.1. CT Tube Voltage Reduction

A lot of information regarding the possibility of adjusting the tube voltage was provided by the PROTECTION studies. They were prospective, multicentre, survey studies based

on the analysis of the radiation doses in CT scans of coronary arteries. Lowering the tube voltage is extremely effective in lowering the radiation dose due to its exponential reduction.

In the PROTECTION I study, the results of which were published in 2009, the radiation doses and image quality from the cardiac CT scans were compared in a group of 82 patients using a 100 kVp voltage and 239 patients using a 120 kVp voltage. At that time, out of 50 centres, only eight used a reduced tube voltage. The effective dose of radiation was estimated on the basis of the DLP values. The quality of the study was assessed by an experienced researcher on a four-point scale. The authors of the study found that the application of the voltage of 100 kVp was associated with a reduction in the median radiation dose by 53% compared to the tests with the voltage of 120 kVp. Although the image noise increased by 26.3% in the 100 kVp tests, the signal-to-noise ratio (SNR) increased by 7.9% and the contrast-to-noise ratio (CNR) increased by 10.8% due to the reduced tube voltage increased the density of the contrasted vascular lumen. Reducing the tube voltage did not impair the diagnostic quality of the image. The median estimated radiation dose was reduced from 14 mSv for 120 kVp to 6 mSv for 100 kVp [42].

In 2019, the results of the PROTECTION VI study were published, which analysed, among other things, the impact of very low (80 kVp), low (90–100 kVp), conventional (110–120 kVp) and high (130 kVp) voltages on the radiation dose in the CT scans coronary arteries. A total of 61 international research centres from 32 countries provided the imaging data and protocols for the CCTA studies performed during the 1 month period between March and December 2017. Approx. 91% of the examinations were performed using cameras with at least 128 slices [29]. Nearly 10 years after the PROTECTION I trial, the low tube voltage was used in 56% of the trials (80 kVp in 9%; 90 to 100 kVp in 47%) [29,30]. The low tube voltage protocols, 90 to 100 kVp, were less frequently used in the GE equipment (42% CCTA) compared to the others (Toshiba: 45%, Philips: 49%, Siemens: 50%). The frequency of use of the 80 kVp ultra-low potential tube was significantly higher in the Siemens scanners (17% CCTA) compared to all the other suppliers (GE: 1%, Philips: 3%, Toshiba: 4%) [30]. The radiation doses were read for each study from the DLP reports [29]. The use of the low tube voltage protocols significantly reduced the median CTDIvol to 11.1 mGy when using 90 to 100 kVp and 6.9 mGy when using 80 kVp. The application of the voltage of 80 kVp resulted in a reduction in the average DLP by 68% compared to the tests with the voltage of 120 kVp, while at the voltage of 90 to 100 kVp, the reduction in the DLP was 50% on average [19,30]. It should be mentioned that the CT examinations conducted in the process of the qualification for the TAVI procedures were excluded from the analysis due to the heterogeneity of the acquisition protocols [29,30].

The authors of the analysis of the PROTECTION VI study concluded that, taking the BMI criteria into account (80 kVp for a BMI < 25 and 90–100 kVp for a BMI 25–30), 58% of the patients tested using the conventional tube voltage were able to use the protocols with a low tube potential (90 to 100 kVp), and 44% of the patients tested at 90–100 kVp would qualify for the protocols with a very low tube potential (80 kV). The PROTECTION VI trial data showed that the dose reduction strategy of lowering the tube voltage was still underutilised in daily practice. The four centres participating in this study carried out the tests using the 120 kVp voltage only. The women and patients with a lower cardiovascular risk and lower BMI values were more often referred for the studies using the lower-than-conventional tube voltages. A strict implementation of the criteria of a BMI < 25 kg/m² in the qualification for the 80 kVp test and a BMI between 25 and 30 kg/m² in the qualification for the 90 to 100 kVp test would reduce the median DLP in the PROTECTION VI population by an additional 23% (up to 150 mGy*cm) [30].

In the PROTECTION VI study, lowering the tube voltage also reduced the contrast medium volume by 25% for 80 kVp (to 55–79 mL) and 13% for 90–100 kVp (to 60–80 mL) [29,30]. Some of the data indicated that reducing the volume of the iodinated contrast medium not only helped protect kidney function, but also reduced the potential effects of irradiation. In a study conducted on 245 patients in whom lymphocytes were collected before and after the chest CT scans and evaluated using fluorescence microscopy,

it was shown that the patients who underwent CT with an iodinated contrast agent had a 107% increase in the amount of radiation damage to their DNA compared to the study group that was not administered a contrast agent [43].

In turn, Huda et al. performed simulations using the IMPACT program, which showed that reducing the X-ray tube voltage from 140 to 80 kV while maintaining constant mAs values will reduce the radiation dose five times [20].

4.2. ECG-Monitored Radiation Modulation (Tube Current)

In cardiac CT, the time of the data acquisition during the diastole, when the movement of the heart and coronary vessels is minimal, is most desirable. The earliest acquisition protocols using ECG monitoring in the cardiac studies generated a constant radiation intensity throughout the cardiac cycle. However, the modification of the radiation dose has been used for many years so that it is maximal in the diastole and minimal (approx. 20% of the maximum value) during the contraction, achieved by changing the CT tube current. This procedure can reduce the radiation dose by up to 50% without a significant loss in the image quality [19]. In the radiation modulation protocols, there is a risk of an incorrect determination of the optimal timing for the acquisition in patients with sinus tachycardia, arrhythmias or ectopic beats. The use of the maximum and minimum tube currents at the inappropriate phases of the heart cycle may cause difficulties in interpreting the images or make diagnostic examination completely impossible. Since the concept of ECG-monitored radiation modulation works most effectively in the patients with a regular, slow heart rate, a pharmacological slowing of the heart rate is recommended [19]. The radiation modulation can be omitted in the studies where cine imaging is necessary, e.g., when the valve movement or heart muscle function must be assessed. The time resolution of the apparatus should also be taken into account each time. Although there are constructions of CT machines that ensure a good examination quality even at a beat rate of 80 bpm and higher, most centres do not yet have such scanners.

4.3. Iterative Image Reconstructions

Until the beginning of the 21st century, CT images were obtained using filtered back projection (FBP) algorithms. The main advantages of this algorithm were the low computational power requirements and the speed of reconstruction, while the disadvantages were the rather significant image noise, especially when using low tube current intensities, poor contrast resolution and streak artefacts. Increasing the signal-to-noise ratio (SNR) required an increase in the radiation dose. The new iterative reconstruction algorithms, used in nuclear medicine since the 1980s, then came to the rescue. The advances in computational technology made it possible to implement them in CT image reconstruction.

The term 'iterative' (from Latin "*iteratio*" meaning repetition) means repeating the same operation in a loop until a certain condition is met. Iterative reconstruction algorithms perform calculations in a loop in a way that allows for a significant noise reduction, preserving the information about the edges and the contrast of the anatomical structures [44]. In these calculations, the data with a low statistical uncertainty are assigned a higher weight than the data with a higher statistical uncertainty. This is overlaid with the algorithms for modelling the photon interaction between the X-ray tube, the isocentre and the detector. The first iterative reconstruction algorithm used in cardiac CT was ASiR (GE Healthcare, Chicago, IL, USA), implemented in 2008. In the same year, Siemens Healthcare (Forchheim, Germany) introduced the IRIS algorithm, which was later replaced in 2010 by the SAFIRE (sinogram affirmed iterative reconstruction) algorithm, which works in both the raw data and image domains [45].

In the iterative reconstruction methods, the noise does not depend as strongly on the CT scanner tube voltage as in the FBP methods. Therefore, the IR algorithms allowed for the use of strategies to reduce the radiation dose by lowering the tube voltage. In addition, they allowed for coronary artery CT to be performed in patients with high BMI values, who previously could not be examined with high image quality due to the significant noise,

and in patients with a high calcium score and implanted stents, who previously could not be examined effectively using CT due to the blooming artefacts [45].

One study showed a 24% dose reduction in the coronary artery CT with ASiR (adaptive statistical iterative reconstruction, GE Healthcare, USA) compared to the FBP, with no difference in the signal-to-noise ratio (SNR) or the contrast-to-noise ratio (CNR), but with a comparable diagnostic quality [46].

The use of the IRIS algorithm (Siemens Healthcare, Erlangen, Germany) in the cardiac CT examinations allowed for the use of a tube voltage of 80/100 kVp. In these studies, the average ED was 3.7 mSv. This was compared to the average ED of 9.7 mSv in the studies reconstructed using the FBP with the same diagnostic quality and a 120 kVp tube voltage. This represented a reduction in the radiation dose of 62% [47].

The ADMIRE (advanced model iterative reconstruction, Siemens Healthcare, Germany) algorithm uses advanced modelling to improve the image resolution and edge detection, as well as the noise reduction. This algorithm enables coronary artery CT to be performed with a low radiation dose of 0.3 mSv [45].

The PROTECTION VI study showed that the combination of the iterative image reconstruction and the reduced X-ray tube voltage resulted in a reduction in the radiation dose without compromising the quality of the examination images. The use of the iterative image reconstruction resulted in a 33% reduction in the radiation dose compared to the filtered back projection [29–31].

4.4. Deep Learning-Based Image Reconstruction and Deep Learning-Based Image Denoising

The use of artificial intelligence algorithms in image reconstruction and denoising in CT scans has increased significantly in recent years. These algorithms make it possible to obtain diagnostic quality CT images at lower doses than the iterative reconstruction used to date. It has become possible to perform CT examinations using radiation doses that previously did not allow for sufficient diagnostic quality images.

A paper comparing the images of the CT scans of the thorax, abdomen and pelvis at sub-millisievert doses that were reconstructed using iterative reconstruction and deep learning algorithms was published in 2019. The patients for the standard-dose CT examinations were additionally acquired using the low-dose examination protocols (100 kVp, 120 kVp; 30–50 mA). The reconstructions of the images from the standard acquisitions were developed using the iterative algorithms (adaptive iterative dose reduction [AIDR] 3D, Canon Medical Systems, Otawara, Tochigi, Japan), while the reconstructions of the low-dose CT images were created using the iterative algorithms and deep learning artificial intelligence (Advanced Intelligent Clear-IQ Engine [AiCE], Canon Medical Systems). The mean DLP values were 567 ± 249 mGy*cm for the standard CT studies and were significantly lower for the LDCT: 49 ± 13 mGy*cm. In an image comparison conducted in an independent, randomised and blinded trial, the low-dose CT scans of the thorax were found to be 95–100% diagnostic. The quality of the images that were reconstructed using the artificial intelligence algorithms allowed for significant reductions in the radiation doses for the CT scans [48].

As the radiation dose decreased, the noise increased, which manifested itself by blurring the contours of the anatomical structures and producing low-contrast images in which the pathological changes may remain undetected. Over the past few decades, various denoising algorithms have been proposed. They can be divided into three categories: filtering in the sinogram domain (raw data), iterative reconstruction and processing in the image domain. The DLR algorithms enable the image noise reduction, high resolution and lesion recognition [49].

The DLR algorithms are the image domain restoration methods. The machine learning-based methods are aimed at automatically learning and improving the applications through experience, rather than using user-defined programmes. They are effective in denoising, which shows a non-uniform distribution in the CT images. The dynamic development of the hardware and computing techniques has led to the popularity for artificial intelligence

algorithms in denoising based on convolutional neural networks. The network achieves this effect by learning from the training data based on the examinations taken at a conventional radiation dose, then relating this information to the images taken at low doses [49]. Reducing the noise without losing the important image features, such as the edges, angles and other sharp structures, is a difficult task. Kaur et al. reviewed and compared the various noise reduction techniques in abdominal and pelvic CT images [50].

Artificial intelligence algorithms have a high efficiency for denoising images. They also provide a better spatial resolution than the iterative algorithms, while maintaining similar radiation dose levels. Phantom and clinical studies have shown that deep learning reconstructions allow for a dose reduction of 30–80% compared to the current iterative reconstruction algorithms while maintaining a diagnostic image quality. In CT angiography, the artificial intelligence algorithms allow for fine vessel reconstructions with the examinations performed at radiation doses that would not be possible with the iterative reconstructions [51], as shown in Figure 3.

Currently, CT device vendors provide commercial algorithms for image reconstruction or image denoising based on artificial intelligence, such as the Advanced Intelligent Clear-IQ Engine (AiCE) (Canon Medical Systems) and TrueFidelity (GE Healthcare) [51].

The authors of the study, which evaluated the images of the studies of 50 patients who underwent coronary artery CT using standard- and low-dose radiation, showed that the DLR enabled a 43% reduction in the radiation dose in the CCTA with no significant effect on the image noise, stenosis severity, plaque composition or quantitative plaque volume [52].

The use of the DLR algorithm for cardiac CT in a thrombus assessment (in comprehensive stroke diagnosis, in prospective acquisition) reduced the radiation dose by approx. 40% and improved the image quality by approx. 50% compared to the IR algorithm. The mean DLP for the DLR algorithms was 106.4 ± 50.0 mGy*cm compared to the IR (176.1 ± 37.1 mGy*cm). The ED was lower for the DLR and was 1.5 ± 0.7 mSv (for IR 2.5 ± 0.5 mSv). Compared to the IR, an increase in the SNR and the CNR of approximately 51% and 49%, respectively, was shown for the DLR [53].

Kang et al. analysed the cardiac CT images of 50 patients with mitral valve prolapse and 50 patients with coronary artery disease taken using a Somatom Definition Flash scanner, (Siemens Healthineers, Germany). A neural network was involved and subjected to deep learning to reduce the noise. Two networks were subjected to training between two different domains (a low dose and a routine dose). The network designed by the authors did not require exactly matched images of the low and routine doses. It was designed to identify the distributions of the high-dose cardiac phase images and to prevent the generation of artificial features that were not present in the input images. The network performed well in reducing the noise in the input low-dose CT images while retaining the texture and edge information [54].

4.5. Reduction in the Scan Range (Scan Length)

In most cardiac CT scans, the length of the scanning range is 12 to 13 cm for adults, typically extending from the tracheal bifurcation to the diaphragm. The patient dose per procedure (DLP) was found to increase by approximately 5% for every one cm increase in the scan length [8,27]. Applying a “safety margin” above and below the heart for fear of missing important heart structures is not appropriate [19]. However, the scope of the examination should always be extended in the case of a vascular graft examination, simultaneous assessment of the aorta and in studies where there are other relevant clinical indications.

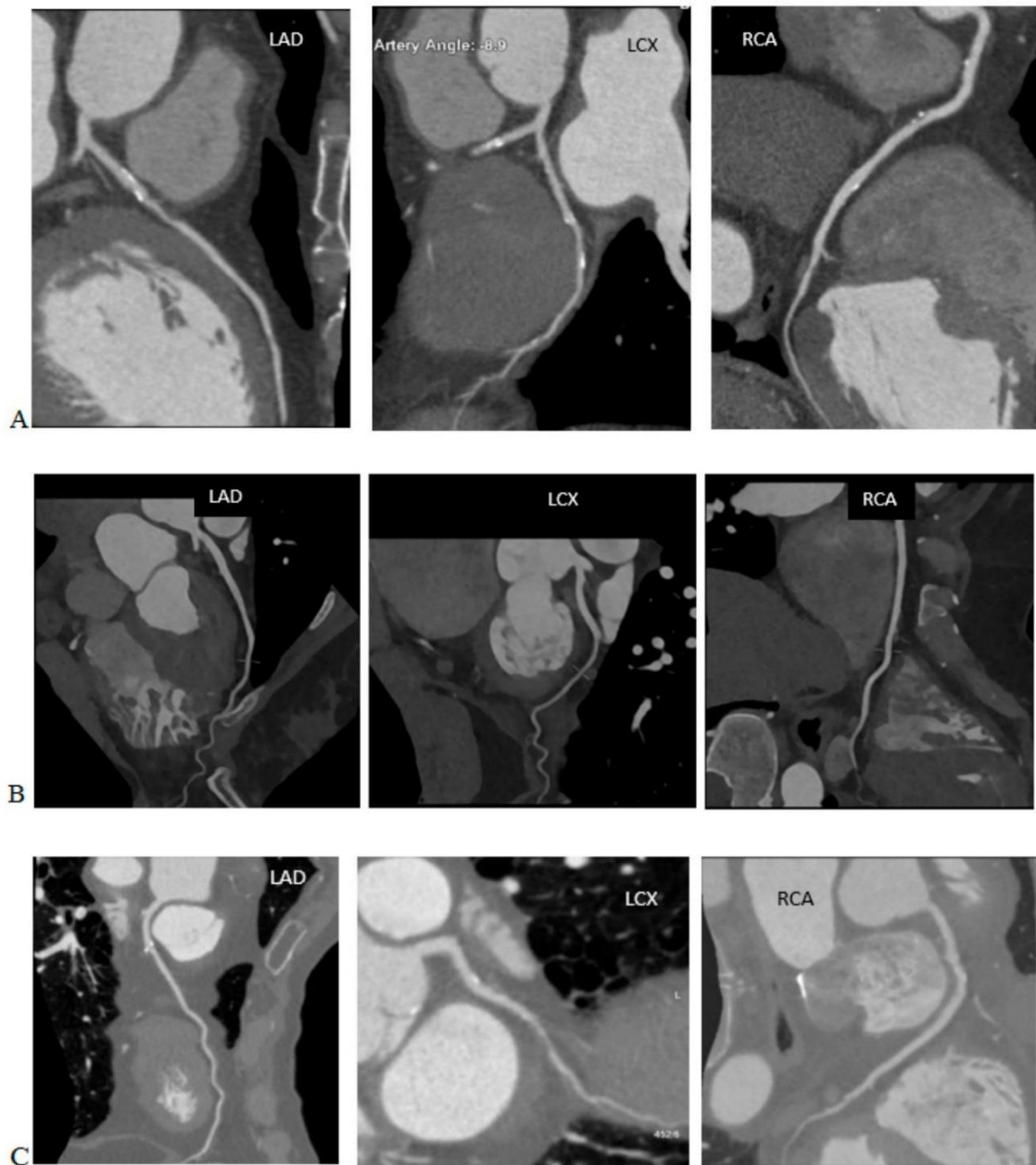


Figure 3. Cont.

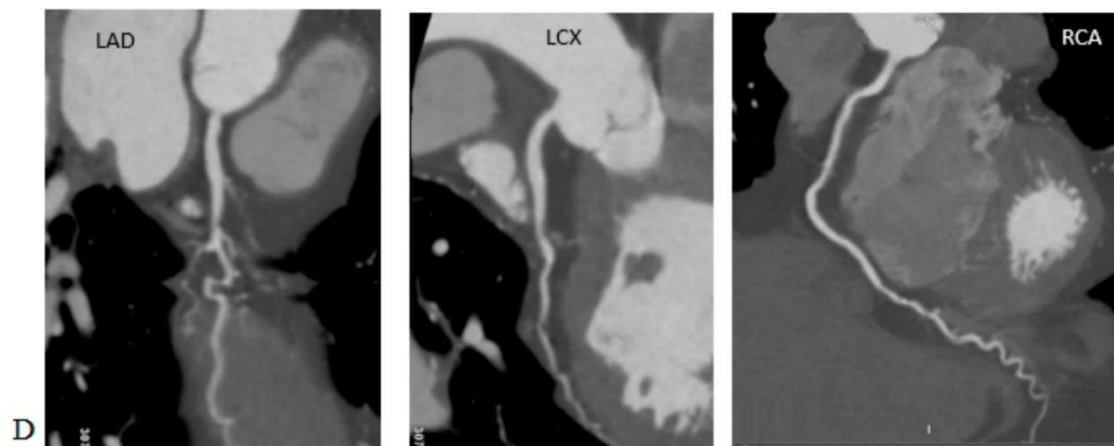


Figure 3. Coronary artery computed tomography scans performed on various scanners, using iterative reconstructions and AI algorithms. Note the DLP and effective dose (ED) of the studies and compare them to the image quality. (A) 120 kVp, DLP 1684.6 mGy*cm, ED = 23.58 mSv ($k = 0.014$ mSv/mGy*cm), iterative reconstruction. (B) 100 kVp, DLP 712.2 mGy*cm, ED = 9.97 mSv ($k = 0.014$ mSv/mGy*cm, reconstruction with AI algorithms). (C) 100 kVp, DLP 715.7 mGy*cm, ED = 10.02 mSv ($k = 0.014$ mSv/mGy*cm), iterative reconstruction. (D) 100 kVp, DLP 99.7 mGy*cm, ED = 1.40 mSv ($k = 0.014$ mSv/mGy*cm), reconstruction with AI algorithms.

4.6. Prospective Study Protocols

In this acquisition mode, the CT X-ray tube is turned on for only a short period—in the middle of the diastolic phase—after which it turns off. During this time, the table with the patient moves to the next position, where a short acquisition in the diastolic phase occurs again. The method was named ‘step-and-shoot’. Limiting the radiation of the CT tube to only a fragment of the diastolic phase of the heart cycle allows for reducing the radiation dose by as much as 78% to 1–5 mSv [19]. The acquisition of the prospective protocol requires a sufficiently long time window for the collection of the image data, in which the movement of the coronary vessels is minimal. Therefore, it cannot be used for a heart rate that is too fast. The optimal moment of acquisition is assumed to be half of the diastolic phase—from 60% to 70% of the R-R cycle—at a heart rate no higher than 60 bpm. Accelerating the heart rate reduces the available acquisition time. Arrhythmia and ectopic beats may result in a non-diagnostic image quality [8,19]. Due to the acquisition of the data from only a small part of the R-R cycle, the prospective study protocols cannot be used where it is necessary to assess the function of the heart valves, myocardium, or the reconstruction of other anatomical structures in motion. In the analysis of the examinations performed using dual-source devices at the University Center in Nanjing (China) in the years 2007–2016, in the first year of the analysis, all the examinations were performed using retrospective protocols with a radiation dose modulation. However, in the last analysed year, approx. 2/5 studies were conducted using the prospective protocols. The median DLP value in these studies was 311.7 mGy*cm [25]. In PROTECION VI, 78% of prospective protocols were used [30].

4.7. The Modulation of the Current Intensity Depends on the Attenuation of the Radiation

The modulation of the current intensity takes into account the fact that the cross-section of the body is usually oval, so in the anterior–posterior dimension the radiation beam has to overcome a smaller layer of tissue compared to the bilateral dimension. In addition, the thickness of the tissue layer also changes with the movement of the table. Equipment manufacturers use software that adjusts the CT tube current intensity to the

thickness of the tissue layers. In the AP dimension, the tube current is lowered, while in the double-sided dimension, it is increased. This technique is called the automatic exposure control (AEC) and can provide a significant reduction in the radiation dose with minimal deterioration in the image quality [27].

4.8. Heart Rate Control

In a large proportion of coronary angio-CT studies, it was necessary to reduce the heart rate to no more than 60 bpm to match the time resolution of the equipment. An increase in the heart rate of 10 beats per minute and an absence of the sinus rhythm were associated with an 8% and 21% increase in the radiation dose, respectively [29]. However, some test protocols used in newer CT scanners, and the radiation dose was lower at the higher heart rates due to a less irradiated layering between the successive rotations of the gantry [19]. The median DLP in the study of the patients with arrhythmias at the Nanjing University Center (China) was 132.6% higher than in the normorhythmic patients [25].

4.9. Rational Use of Calcium Score

The determination of the coronary artery calcification index is a valuable method for the cardiovascular risk stratification. It is a helpful screening tool. Depending on the quality of the equipment, the centres performing the tests use different values of the CS coefficient (from 400 according to Agatston), above which the angiographic phase is abandoned. Some cameras provide a high image quality regardless of the intensity of the calcification in the coronary arteries. The information from the calcium score test can be used to modify the angio-CT protocol of the coronary arteries, e.g., to adjust the scanning range [8,19]. The calcium score is not performed in the patients after the coronary angioplasty (PTCA) and coronary artery bypass grafting (CABG). The doses resulting from the calcium score assessment in the coronary vessels can range from 1.7 to 2.6 mSv, according to the ICRP 103 [24].

4.10. Multi-Slice, Dual-Source and Wide-Field Tomography

In a retrospective analysis of 278 patients performed in the years from 2015–2017, the DLP values for the examined protocols, including the calcium score and CCTA with the use of the 70–120 kVp tube voltage, were 35.4 mGy*cm (28.3–43.9) for the calcium score, 44.8 mGy*cm (36.6–64.6) for high *pitch factor* helical acquisitions, 94.3 mGy*cm (56.4–175.9) for the sequential, prospective acquisitions and 340.4 mGy*cm (215.6–590.4) for the retrospective spiral acquisitions. For the high-pitch spiral acquisitions, the authors determined the effective dose of 0.63 mSv (0.51–0.90) for the CCTA alone, using an organ conversion factor of $k = 0.014$ mSv/mGy*cm. The tests were performed using a third-generation dual-source CT system (Somatom Force, *Siemens Healthineers*) [55]. The use of a high pitch factor scanning technique with ECG monitoring reduced the radiation dose by 30% [29,30].

The CONVERGE study compared groups of 110 patients using 64-slice and 256-slice cameras in each group. The determined mean DLP values in the group tested using the 256-slice instrument (*Revolution CT, GE Healthcare*) were 113.5 ± 53.6 mGy*cm (1.59 ± 0.75 mSv) and were 32% lower than the group tested using the 64-slice instrument for the patients with normal BMI values (18.5–24.9) [56].

In a multicentre study covering 92 patients using scanners equipped with two radiation sources and spectral dual-source photon-counting detector coronary computed tomography angiography (PCD-CCTA) (*Naotom Alpha, Siemens Healthineers*), the mean DLP was 234.1 ± 347.6 mGy*cm and the median DLP was 90.9 mGy*cm (IQR 52.8–235.5 mGy*cm). Using the organ conversion factor $k = 0.015$ mSv/mGy*cm, the authors determined it to be 1.4 mSv (IQR 0.8–3.5 mSv). The dose depended on the acquisition mode of 1.0 ± 0.8 mSv for the spiral acquisitions with a high *pitch factor*, 4.8 ± 4.0 mSv for the sequential, prospective acquisitions and 9.6 ± 4.4 mSv for the retrospective spiral acquisitions with a low *pitch factor* [57].

5. Doses in the TAVI Studies

Transcatheter aortic valve implantation (TAVI) or transcatheter aortic valve replacement (TAVR) was performed for the first time in 2002. The first procedures in Poland were performed in 2008. Initially, this procedure was recommended for patients with severe, symptomatic aortic stenosis who were ineligible for surgery or for whom the surgery was associated with a high risk. Currently, the indications have been extended to patients for whom conventional surgery carries an intermediate risk. In the first period of development for TAVI/TAVR procedures, computed tomography was used to assess the vascular access. Currently, it is also used to accurately image the aortic root with the aortic valve, including determining the dimensions of the aortic annulus, determining the risk of the coronary artery ossification and planning the optimal C-arm angles, which reduces the radiation exposure, the centre volume duration of the procedure and the monitoring of the post-procedural complications, including the prosthetic valve leaflet thickening and possible periarticular leaks. CT has, therefore, become the 'gold standard' for planning TAVI/TAVR procedures [58].

CT scanning prior to the TAVI/TAVR procedures required images of the aortic root to be obtained using ECG-monitored acquisitions and images of the vascular accesses from the carotid arteries to the femoral arteries, which did not require synchronisation with the ECG recording. In the construction of the CT protocols before TAVI/TAVR procedures, two methods for obtaining the image data sets were used.

(1) ECG-gated acquisition covering the region of the heart and aortic root followed by the acquisition without ECG gating covering the vascular accesses in the neck, thorax, abdomen, pelvis and axilla up to the level of the lesser femoral ileum. The disadvantage of this solution was the double acquisition in the area of the aortic root and the heart, which increases the radiation dose. The advantage here, however, was the fact that the time-consuming acquisition of the data synchronised with ECG was reduced to a minimum. By shortening the examination time, the volume of the administered contrast agent could be reduced. It should be remembered that these studies concerned elderly patients, in whom kidney function was most often—even significantly—reduced. In addition, limiting the scope of the ECG-monitored acquisition reduced the part of the examination that required a high dose of radiation, even though the scanning ranges partially overlapped [58], as shown in Figure 4A.

(2) ECG-gated acquisition covering the lower neck and thorax followed by the acquisition without ECG gating covering the abdomen, pelvis and groin to the level of the lesser femoral ileum. The disadvantage of this solution was a higher radiation dose and extended acquisition time for the entire chest. An extended acquisition time may require a larger volume of contrast for the medium and longer breath hold times, which may result in respiratory artifacts in the less resilient patients [58], as shown in Figure 4B.

In order to optimise the radiation dose, the authors of the SSCT guidelines noted that for the patients with a body weight of up to 90 kg or BMI values up to 30 kg/m², the acquisition should use a tube voltage of 100 kVp, and for the patients with a body weight > 90 kg or BMI values > 30 kg/m², the acquisition should use a tube voltage 120 kVp. If the parameters of the scanner allow it, for the patients with BMI values < 26 kg/m², the acquisition should be carried out with an 80 kVp voltage of the apparatus tube [58].

In a national survey conducted in 2018 in Great Britain, 47 responses (12% response rate) were obtained from 40 cardiology centres. A total of 23 centres (58%) also performed TAVI procedures. Most centres (27–59%) performed less than 100 examinations per month. The acquisition protocols varied, where 41% of centres performed retrospective acquisitions with an ECG-monitored radiation dose modulation, 47% performed prospective acquisitions with ECG gating with narrow padding and 12% performed prospective acquisitions with ECG gating and wide padding. The median dose-length product was 675 mGy*cm (IQR 477–954 mGy*cm). The median DLP in the prospective protocols with ECG gating with narrow padding was 423 mGy*cm. The use of a wide padding (30–80% R-R spacing)

more than doubled the DLP to 921 mGy*cm. The retrospective acquisition was associated with a high median DLP of 882 mGy*cm [32].

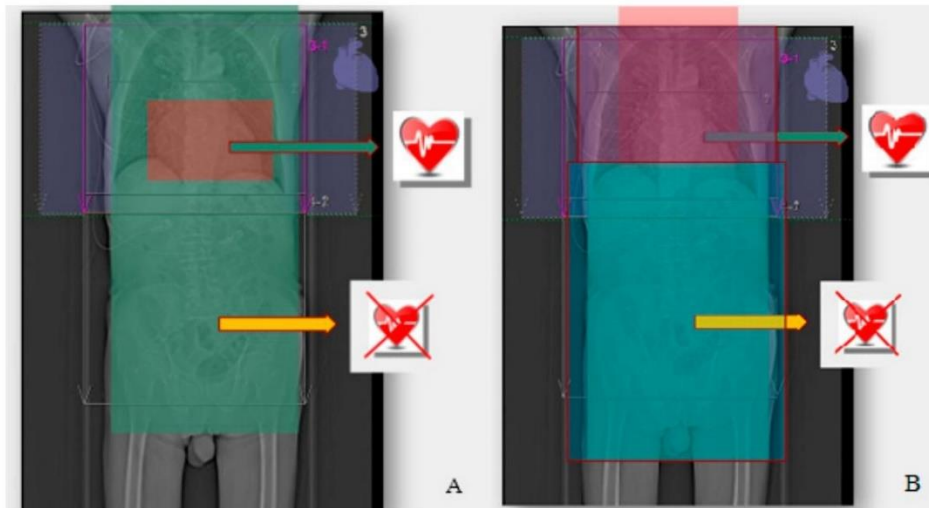


Figure 4. (A) ECG-gated acquisition covering the region of the heart and aortic root, followed by the acquisition without ECG gating, covering the vascular accesses in the neck, thorax, abdomen, pelvis and axilla up to the level of the lesser femoral ileum. (B) ECG-gated acquisition covering the lower neck and thorax, followed by the acquisition without ECG gating covering the abdomen, pelvis and groin to the level of the lesser femoral ileum.

In a study conducted at the Charité University Hospital (Berlin), two study protocols performed on an 80-slice Aquillion Prime instrument (Canon Medical Systems, Otawara, Japan) were compared. In the first of the protocols, the acquisition covered the section of the chest from the top of the lungs to the aortic arch without ECG gating, then the section from the aortic arch to the diaphragm with ECG gating, and finally, the section from the diaphragm to the groin without ECG gating. In the second protocol, the acquisition was carried out uniformly from the lung peaks to the axillae without ECG monitoring with a high *pitch factor* = 1.388). The mean DLP was 790.90 ± 238.15 mGy*cm for the protocol with ECG gating compared to 357.10 ± 200.25 mGy*cm in the high *pitch factor* protocol without ECG monitoring. The mean effective doses were 13.44 ± 4.05 mSv and 6.07 ± 3.40 mSv, respectively, and the mean SSDEs were 13.84 ± 2.94 mGy and 5.69 ± 2.27 mGy, respectively. The high-spike CT protocol without ECG monitoring reduced the radiation exposure by 55% compared to the protocol with ECG monitoring (from 13.44 mSv to 6.07 mSv). The authors reported statistically significant differences in the SNR and CNR values at the aortic root level between the two groups. However, in the subjective assessment of the Likert scale by two radiologists experienced in imaging the cardiovascular system, the quality of the aortic root image did not show any significant differences [59].

In a study involving 30 randomly selected patients who were tested using the Somatom Force scanner (Siemens Healthcare, Erlangen, Germany), the DLP was 217.6 ± 12.1 mGy*cm (range 178–248 mGy*cm). The acquisition was conducted from the level of the aortic root to the axilla, prospectively with ECG triggering and a high *pitch factor*. The acquisition was triggered at 60% of the R-R interval using a voltage of 100 kVp and a current of 350 mAs/rev [60].

Additionally, the Somatom Force scanner (Siemens Healthcare, Erlangen, Germany) was used to examine 226 patients in 2018–2019. The first stage of the protocol included a calcium score scan of the aortic valve with the use of a 120 kVp voltage from the level of

the tracheal bifurcation to the diaphragm. In the second stage, the prospective acquisition was triggered at 30% of the R-R interval with ECG triggering using a high pitch factor = 3.2 and a voltage of 100 kVp. The mean DLP in this study was 201.1 ± 22.7 mGy*cm [61].

In the work covering 115 studies carried out in 2016–2017, the authors reported an average DLP value of 479.1 ± 45.7 mGy*cm. The study was conducted using a 256-slice revolution CT scanner (GE Healthcare, Milwaukee, WI, USA). The study protocol included the thorax from the lung peaks to the diaphragm in two blocks monitored by an ECG. The study was performed at 100 kVp using a retrospective acquisition, with padding at the 500 ms R-R interval, and a spiral acquisition without ECG monitoring from the diaphragm to the proximal third of the thighs [62].

Another protocol was used for 42 patients who were examined using the Somatom Definition Flash device (Siemens Healthcare, Forchheim, Germany). The acquisition of the cardiac structures from the aortic arch to the diaphragm was performed using ECG monitoring at 60% of the R-R interval, followed by craniocaudal scanning from the top of the lungs to the groin without ECG monitoring and spiral acquisition. Depending on the BMI value, the voltages of 100 kVp and 120 kVp were used. The mean DLP value was 241 ± 27 mGy*cm [63].

6. The Postulated New Values of The Organ Conversion Factor—k

In current practice, the effective dose conversion factors for cardiac CT scans are assumed to be the same as for conventional chest CT scans. However, some publications have identified that different, organ-specific conversion factors should be used in cardiac CT scans, which are higher than in conventional chest CT scans.

In one study, the commercial ImPACT CT patient dosimetry calculator program (version 1.0, ImPACT 2009) was used to calculate the CTDIvol, the DLP and the effective dose using the tissue weighting factors, according to the ICRP 103 publication for the cardiac CT model in adult patients with a body weight of 70 kg and a tube voltage from 80 to 140 kV for two systems of 64- and 128-slices (General Electric and Siemens Healthineers). The scope of the survey was 16 cm. The maximum E/DLP values were 0.0375 mSv/mGy*cm and were located in the breast region, which is a particularly sensitive organ. The E/DLP values at the apex of the lung were five times lower and amounted to 0.007 mSv/mGy*cm. The conversion factor developed by the authors for the CT scan of the heart with the examination range of 16 cm and a voltage of 120 kV was 0.0264 mSv/mGy*cm, while the chest CT scan with the examination scope of 36 cm was 0.021 mSv/mGy*cm. It was approximately 70% higher than the current k-factor value adopted for chest CT, which was $\sim 0.014\text{--}0.017$ mSv/mGy*cm [20].

The CORE-64 study (the coronary artery evaluation using 64-slice multidetector computed tomography angiography study) used the Monte Carlo calculations for the studies from the Aquillion 64-slice scanner. The study was performed at nine centres. The organ dose and the effective dose resulting from the cardiac CT protocol were assessed. Six voxel patient models were used, representing the examined three men and three women with different body constitutions, i.e., small, normal and obese. They were performed at a tube voltage of 120 kV in a protocol consisting of topograms, calcium scores and the CCTA triggered by a bolus of the contrast agent. The breast tissue weighting factor of 0.24 (ICRP 103) was used in the women, but not in the men. Using the ICRP 103 standards, the sex-averaged organ conversion k-factor for calculating the effective dose from the DLP was 0.030 mSv/mGy*cm (range 0.019–0.043 mSv/mGy*cm). The authors of the study noted that the use of the organ conversion k-factor of 0.017 mSv/mGy*cm, adapted for conventional thoracic CT examinations to estimate the effective dose, resulted in an underestimation of the effective dose of 43% if ICRP 103 standards were used [24].

In 2017, the results of the work based on dosimetry using radiation detectors with MOSFET field-effect transistors were published. These detectors were placed in the topography of 27 organs contributing to the determination of the effective dose in anthropomorphic phantoms and scanned using numerous cardiological CT protocols. The doses in the larger

or highly radiation-sensitive organs, such as the lungs and breasts in women, were determined on the basis of the measurements in multiple detectors. In total, 41–44 detectors were used. A total of 120 protocols, performed on 12 CT scanners from five manufacturers (GE, Hitachi (Marunouchi, Chiyoda-ku, Tokyo, Japan), Philips, Siemens, Canon), were examined. The study protocol included topograms, calcium scores and the CCTA using a tube voltage of 70–140 kVp and simulating a pulse rate of 60 and 80 bpm. The effective dose measurements in the phantoms and dose-length products reported by the CT scanner were used to determine the k-factors. The organ conversion k-factor was, on average, 0.026 mSv/mGy*cm and ranged from 0.020–0.035 mSv/mGy*cm. The standard k-factor for the conventional chest CT scans underestimated the calculated effective dose by an average of 46%, ranging from 30% to 60%, depending on the scanner, mode and tube voltage of the scanner. The authors of the study identified that the k-factor for the conventional chest CT examinations was not designed for cardiological examinations. It was based on the older (now replaced by the ICRP 130) definition of effective dose according to the ICRP 60 publication and was determined using three single-slice devices, which differed significantly in the technology from the machines currently used for cardiac CT examinations [23].

The authors of these papers concluded that the k-factors for the cardiac CT scans for all the scanners and protocols were higher than the currently used k-factors for the conventional chest CT scans. Therefore, the radiation doses from the cardiac CT scans were significantly and systematically underestimated. The use of new k-factors in cardiac CT scans may provide more precise guidance for determining the benefits and risks of the testing. Other authors also mentioned higher organ conversion k-factors in their publications. [27,29,30]

7. Summary

Cardiovascular CT examinations are becoming increasingly common, and their number and range of indications will continue to increase. The doses of ionising radiation associated with these examinations have always been relatively high, but have been decreasing significantly in recent years, as shown by the studies of the daily practice. This is due both to advances in CT scanner technology and an increase in the ability to optimise the radiation doses. It is important to remember that radiation from medical sources ranks first in possible exposures and that radiation doses are cumulative. Attention should be paid to the radiation doses emitted to the patient in each case. However, it should be kept in mind that some studies indicated that the organ conversion k-factor for cardiac examinations needs to be increased. Therefore we may currently be underestimating the radiation doses in these examinations. The reference dose levels may help to evaluate the CT protocols used in each centre.

Author Contributions: Conceptualization, B.K., R.P. and P.G.; resources, B.K., P.M. and B.D.-M.; writing—original draft preparation, B.K. and P.M.; writing—review and editing, B.D.-M. and K.T.; visualization, B.K.; supervision, P.G. and R.P.; funding acquisition, P.G. All authors have read and agreed to the published version of the manuscript.

Funding: This research received no external funding. The APC was funded by Wrocław Medical University (SUBZ.E264.23.039).

Institutional Review Board Statement: Not applicable.

Informed Consent Statement: Not applicable.

Data Availability Statement: Not applicable.

Conflicts of Interest: The authors declare no conflict of interest.

Abbreviations

ACR	American College of Radiology
AEC	Automatic exposure control
AHA	American Heart Association
ALARA	As low as reasonably achievable
BEIR Committee	Biologic Effects of Ionizing Radiation Committee
BMI	Body mass index
CS	Calcium score
CT	Computed tomography
CTA	Coronary tomography angiography
CTCA	Computed tomography coronary angiography
CTDI	Computed tomography dose index
CTDIvol	Volumetric computed tomography dose index
DLP	Dose-length product
DLR	Deep learning reconstruction
DLIR	Deep learning image reconstruction
ED	Effective dose
ERD	Effective radiation dose
FBP	Filtered back projection
ICA	Invasive coronarography angiography
IEC	International Electrotechnical Commission
IR	Iterative reconstruction
LAR	Lifetime attributable risk
LET	Linear energy transfer
MOSFET	Metal-oxide-semiconductor field-effect transistor
RDSR	Radiation dose structured report
SSCT	Society of Cardiovascular Computed Tomography
TAVI	Transcatheter aortic valve implantation
TAVR	Transcatheter aortic valve implantation replacement
UNSCEAR	United Nations Scientific Committee on the Effects of Atomic Radiation

References

- Kordolaimi, S.D.; Efstathopoulos, E.P. Computed Tomography Radiation Dosimetry: From the indicators to the indications. *J. Comput. Assist. Tomogr.* **2014**, *38*, 807–814. [[CrossRef](#)] [[PubMed](#)]
- Harell, G.S.; Guthaner, D.F.; Breiman, R.S.; Morehouse, C.C.; Seppi, E.J.; Marshall, W.H.; Wexler, L. Stop-Action Cardiac Computed Tomography. *Radiology* **1977**, *123*, 515–517. [[CrossRef](#)]
- Guthaner, D.; Wexler, L.; Harell, G. CT demonstration of cardiac structures. *Am. J. Roentgenol.* **1979**, *133*, 75–81. [[CrossRef](#)] [[PubMed](#)]
- Budoff, M.; Achenbach, S.; Hecht, H.N.J. *Atlas of Cardiovascular Computed Tomography*; Springer: Berlin/Heidelberg, Germany, 2018.
- Achenbach, S.; Giesler, T.; Ropers, D.; Ulzheimer, S.; Derlien, H.; Schulte, C.; Wenkel, E.; Moshage, W.; Bautz, W.; Daniel, W.G.; et al. Detection of Coronary Artery Stenoses by Contrast-Enhanced, Retrospectively Electrocardiographically-Gated, Multislice Spiral Computed Tomography. *Circulation* **2001**, *103*, 2535–2538. [[CrossRef](#)] [[PubMed](#)]
- Knuuti, J.; Wijns, W.; Saraste, A.; Capodanno, D.; Barbato, E.; Funck-Brentano, C.; Prescott, E.; Storey, R.F.; Deaton, C.; Cuisset, T.; et al. 2019 ESC Guidelines for the diagnosis and management of chronic coronary syndromes. *Eur. Heart J.* **2020**, *41*, 407–477. Erratum in *Eur. Heart J.* **2020**, *41*, 4242. [[CrossRef](#)] [[PubMed](#)]
- Collet, J.P.; Thiele, H.; Barbato, E.; Barthélémy, O.; Bauersachs, J.; Bhatt, D.L.; Dendale, P.; Dorobantu, M.; Edvardsen, T.; Folliguet, T.; et al. 2020 ESC Guidelines for the management of acute coronary syndromes in patients presenting without persistent ST-segment elevation. *Eur. Heart J.* **2021**, *42*, 1289–1367, Erratum in *Eur. Heart J.* **2021**, *42*, 1908; Erratum in *Eur. Heart J.* **2021**, *42*, 1925; Erratum in *Eur. Heart J.* **2021**, *42*, 2298. [[CrossRef](#)]
- Mayo, J.R.; Leipsic, J.A. Radiation dose in cardiac CT. *AJR Am. J. Roentgenol.* **2009**, *192*, 646–653. [[CrossRef](#)] [[PubMed](#)]
- Costello, J.E.; Cecava, N.D.; Tucker, J.E.; Bau, J.L. Radiatradiation and chest: Current controversies and dose reduction strategies. *AJR Am. J. Roentgenol.* **2013**, *201*, 1283–1290. [[CrossRef](#)]
- Sarma, A.; Heilbrun, M.E.; Conner, K.E.; Stevens, S.M.; Woller, S.C.; Elliott, C.G. Radiation and chest CT scan examinations: What do we know? *Chest* **2012**, *142*, 750–760. [[CrossRef](#)]
- Committee to Assess Health Risks from Exposure to Low Levels of Ionizing Radiation. *National Research Council. Health Risks from Exposure to low levels of Ionizing Radiation: BEIR VII–Phase 2*; National Academies Press: Washington, DC, USA, 2006.

12. Cardis, E.; Vrijheid, M.; Blettner, M.; Gilbert, E.; Hakama, M.; Hill, C.; Howe, G.; Kaldor, J.; Muirhead, C.R.; Schubauer-Berigan, M.; et al. The 15-Country Collaborative Study of Cancer Risk among Radiation Workers in the Nuclear Industry: Estimates of Radiation-Related Cancer Risks. *Radiat. Res.* **2007**, *167*, 396–416. [[CrossRef](#)]
13. Imanishi, Y.; Fukui, A.; Niimi, H.; Itoh, D.; Nozaki, K.; Nakaji, S.; Ishizuka, K.; Tabata, H.; Furuya, Y.; Uzura, M.; et al. Radiation-induced temporary hair loss as a radiation damage only occurring in patients who had the combination of MDCT and DSA. *Eur. Radiol.* **2004**, *15*, 41–46. [[CrossRef](#)] [[PubMed](#)]
14. Kreuzer, M.; Auvinen, A.; Cardis, E.; Hall, J.; Jourdain, J.-R.; Laurier, D.; Little, M.P.; Peters, A.; Raj, K.; Russell, N.S.; et al. Low-dose ionising radiation and cardiovascular diseases—Strategies for molecular epidemiological studies in Europe. *Mutat. Res. Mol. Mech. Mutagen.* **2015**, *764*, 90–100. [[CrossRef](#)] [[PubMed](#)]
15. Tang, F.R.; Loganovsky, K. Low dose or low dose rate ionizing radiation-induced health effect in the human. *J. Environ. Radioact.* **2018**, *192*, 32–47. [[CrossRef](#)] [[PubMed](#)]
16. Baselet, B.; Rombouts, C.; Benotmane, A.M.; Baatout, S.; Aerts, A. Cardiovascular diseases related to ionizing radiation: The risk of low-dose exposure (Review). *Int. J. Mol. Med.* **2016**, *38*, 1623–1641. [[CrossRef](#)]
17. Liu, X.-C.; Zhou, P.-K. Tissue Reactions and Mechanism in Cardiovascular Diseases Induced by Radiation. *Int. J. Mol. Sci.* **2022**, *23*, 14786. [[CrossRef](#)]
18. Skrzyński, W. Tomograficzny Indeks Dawki CTDI. Available online: https://www.researchgate.net/publication/315658247_Tomograficzny_indeks_dawki_CTDI (accessed on 15 November 2022).
19. Shapiro, B.P.; Young, P.M.; Kantor, B.; Choe, Y.H.; McCollough, C.H.; Gerber, T.C. Radiation Dose Reduction in CT Coronary Angiography. *Curr. Cardiol. Rep.* **2010**, *12*, 59–67. [[CrossRef](#)]
20. Huda, W.; Tipnis, S.; Sterzik, A.; Schoepf, U.J. Computing effective dose in cardiac CT. *Phys. Med. Biol.* **2010**, *55*, 3675–3684. [[CrossRef](#)]
21. Gerber, T.C.; Carr, J.J.; Arai, A.E.; Dixon, R.L.; Ferrari, V.A.; Gomes, A.S.; Heller, G.V.; McCollough, C.H.; McNitt-Gray, M.F.; Mettler, F.A.; et al. Ionizing Radiation in Cardiac Imaging: A science advisory from the American Heart Association Committee on Cardiac Imaging of the Council on Clinical Cardiology and Committee on Cardiovascular Imaging and Intervention of the Council on Cardiovascular Radiology and Intervention. *Circulation* **2009**, *119*, 1056–1065. [[CrossRef](#)]
22. Kalender, W.A. Dose in x-ray computed tomography. *Phys. Med. Biol.* **2014**, *59*, R129–R150. [[CrossRef](#)]
23. Trattner, S.; Halliburton, S.; Thompson, C.M.; Xu, Y.; Chelliah, A.; Jambawalikar, S.R.; Peng, B.; Peters, M.R.; Jacobs, J.E.; Ghesani, M.; et al. Cardiac-Specific Conversion Factors to Estimate Radiation Effective Dose from Dose-Length Product in Computed Tomography. *JACC Cardiovasc. Imaging.* **2018**, *11*, 64–74. [[CrossRef](#)]
24. Geleijns, J.; Joemai, R.M.S.; Dewey, M.; de Roos, A.; Zankl, M.; Cantera, A.C.; Artells, M.S. Radiation Exposure to Patients in a Multicenter Coronary Angiography Trial (CORE 64). *Am. J. Roentgenol.* **2011**, *196*, 1126–1132. [[CrossRef](#)]
25. Lin, Z.X.; Zhou, C.S.; Schoepf, U.J.; Eid, M.; Duguay, T.M.; Greenberg, W.T.; Luo, S.; Quan, W.; Zhou, F.; Lu, G.M.; et al. Coronary CT angiography radiation dose trends: A 10-year analysis to develop institutional diagnostic reference levels. *Eur. J. Radiol.* **2019**, *113*, 140–147. [[CrossRef](#)]
26. Schmermund, A.; Marwan, M.; Hausleiter, J.; Barth, S.; Bruder, O.; Kerber, S.; Korosoglou, G.; Leber, A.; Moshage, W.; Schröder, S.; et al. Declining radiation dose of coronary computed tomography angiography: German cardiac CT registry experience 2009–2014. *Clin. Res. Cardiol.* **2017**, *106*, 905–912. [[CrossRef](#)]
27. Alkhorayef, M.; Sulieman, A.; Alzahrani, K.; Abuzaid, M.; Alomair, O.I.; Almuwannis, M.; Alghamdi, S.; Tamam, N.; Bradley, D.A. Radiation risk for patients undergoing cardiac computed tomography examinations. *Appl. Radiat. Isot.* **2020**, *168*, 109520. [[CrossRef](#)] [[PubMed](#)]
28. Lubbers, M.; Dedic, A.; Coenen, A.; Galema, T.; Akkerhuis, J.; Bruning, T.; Krenning, B.; Musters, P.; Ouhlous, M.; Liem, A.; et al. Calcium imaging and selective computed tomography angiography in comparison to functional testing for suspected coronary artery disease: The multicentre, randomized CRESCENT trial. *Eur. Heart J.* **2016**, *37*, 1232–1243. [[CrossRef](#)]
29. Stocker, T.J.; Deseive, S.; Leipsic, J.; Hadamitzky, M.; Chen, M.Y.; Rubinshtein, R.; Heckner, M.; Bax, J.J.; Fang, X.M.; Grove, E.L.; et al. Reduction in radiation exposure in cardio-vascular computed tomography imaging: Results from the PROSpective multicenter registry on radiation dose Estimates of cardiac CT angiography in daily practice in 2017 (PROTECTION VI). *Eur. Heart J.* **2018**, *39*, 3715–3723. [[CrossRef](#)] [[PubMed](#)]
30. Stocker, T.J.; Leipsic, J.; Hadamitzky, M.; Chen, M.Y.; Rubinshtein, R.; Deseive, S.; Heckner, M.; Bax, J.J.; Kitagawa, K.; Marques, H.; et al. Application of Low Tube Potentials in CCTA: Results from the PROTECTION VI Study. *JACC Cardiovasc. Imaging.* **2020**, *13*, 425–434. [[CrossRef](#)] [[PubMed](#)]
31. Stocker, T.J.; Deseive, S.; Chen, M.; Leipsic, J.; Hadamitzky, M.; Rubinshtein, R.; Grove, E.L.; Fang, X.-M.; Lesser, J.; Maurovich-Horvat, P.; et al. Rationale and design of the worldwide prospective multicenter registry on radiation dose estimates of cardiac CT angiography in daily practice in 2017 (PROTECTION VI). *J. Cardiovasc. Comput. Tomogr.* **2017**, *12*, 81–85. [[CrossRef](#)] [[PubMed](#)]
32. Harries, I.; Weir-McCall, J.R.; Williams, M.C.; Shambrook, J.; Roditi, G.; Bull, R.; Morgan-Hughes, G.J.; Nicol, E.D.; Moss, A.J. CT imaging prior to transcatheter aortic valve implantation in the UK. *Open Hear.* **2020**, *7*, e001233. [[CrossRef](#)]
33. Alhailiy, A.B.; Ekpo, E.U.; A Ryan, E.; Kench, P.L.; Brennan, P.C.; McEntee, M.F. Diagnostic reference levels for cardiac ct angiography in australia. *Radiat. Prot. Dosim.* **2018**, *182*, 525–531. [[CrossRef](#)]

34. Mafalanka, F.; Etard, C.; Rehel, J.L.; Pesenti-Rossi, D.; Amrar-Vennier, F.; Baron, N.; Christiaens, L.; Convers-Domart, R.; Defez, D.; Douek, P.; et al. Establishment of diagnostic reference levels in cardiac CT in France: A need for patient dose optimisation. *Radiat. Prot. Dosim.* **2014**, *164*, 116–119. [[CrossRef](#)] [[PubMed](#)]
35. Alhailiy, A.B.; Kench, P.L.; McEntee, M.F.; Brennan, P.C.; A Ryan, E. Establishing diagnostic reference levels for cardiac computed tomography angiography in Saudi Arabia. *Radiat. Prot. Dosim.* **2018**, *181*, 129–134. [[CrossRef](#)] [[PubMed](#)]
36. Chen, L.-G.; Wu, P.-A.; Tu, H.-Y.; Sheu, M.-H.; Huang, L.-C. Diagnostic reference levels of cardiac computed tomography angiography in a single medical center in Taiwan: A 3-y analysis. *Radiat. Prot. Dosim.* **2021**, *194*, 36–41. [[CrossRef](#)] [[PubMed](#)]
37. Einstein, A.J.; Henzlova, M.J.; Rajagopalan, S. Estimating Risk of Cancer Associated with Radiation Exposure From 64-Slice Computed Tomography Coronary Angiography. *JAMA* **2007**, *298*, 317–323. [[CrossRef](#)] [[PubMed](#)]
38. Hurwitz, L.M.; Reiman, R.E.; Yoshizumi, T.T.; Goodman, P.C.; Toncheva, G.; Nguyen, G.; Lowry, C. Radiation Dose from Contemporary Cardiothoracic Multidetector CT Protocols with an Anthropomorphic Female Phantom: Implications for Cancer Induction. *Radiology* **2007**, *245*, 742–750. [[CrossRef](#)]
39. Huda, W. Radiation Doses and Risks in Chest Computed Tomography Examinations. *Proc. Am. Thorac. Soc.* **2007**, *4*, 316–320. [[CrossRef](#)]
40. Truong, Q.A.; Rinehart, S.; Abbara, S.; Achenbach, S.; Berman, D.S.; Bullock-Palmer, R.; Carrascosa, P.; Chinnaiyan, K.M.; Dey, D.; Ferencik, M.; et al. Coronary computed tomographic imaging in women: An expert consensus statement from the Society of Cardiovascular Computed Tomography. *J. Cardiovasc. Comput. Tomogr.* **2018**, *12*, 451–466. [[CrossRef](#)]
41. Strona Ministerstwa Klimatu i Środowiska Rzeczpospolitej Polskiej. Available online: <https://www.gov.pl/web/klimat/promieniowanie-jonizujace> (accessed on 18 November 2022).
42. Bischoff, B.; Hein, F.; Meyer, T.; Hadamitzky, M.; Martinoff, S.; Schömig, A.; Hausleiter, J. Impact of a reduced tube voltage on CT angiography and radiation dose: Results of the PROTECTION I study. *JACC Cardiovasc. Imaging.* **2009**, *2*, 940–946. [[CrossRef](#)]
43. Piechowiak, E.I.; Peter, J.-F.W.; Kleb, B.; Klose, K.J.; Heverhagen, J. Intravenous Iodinated Contrast Agents Amplify DNA Radiation Damage at CT. *Radiology* **2015**, *275*, 692–697. [[CrossRef](#)]
44. Spears, J.R.; Schoepf, U.J.; Henzler, T.; Joshi, G.; Moscariello, A.; Vliegthart, R.; Cho, Y.J.; Apfaltrer, P.; Rowe, G.; Weininger, M.; et al. Comparison of the Effect of Iterative Reconstruction versus Filtered Back Projection on Cardiac CT Postprocessing. *Acad. Radiol.* **2014**, *21*, 318–324. [[CrossRef](#)]
45. Naoum, C.; Blanke, P.; Leipsic, J. Iterative reconstruction in cardiac CT. *J. Cardiovasc. Comput. Tomogr.* **2015**, *9*, 255–263. [[CrossRef](#)] [[PubMed](#)]
46. Tumur, O.; Soon, K.; Brown, F.; Mykytowycz, M. New scanning technique using Adaptive Statistical Iterative Reconstruction (ASIR) significantly reduced the radiation dose of cardiac CT. *J. Med Imaging Radiat. Oncol.* **2013**, *57*, 292–296. [[CrossRef](#)] [[PubMed](#)]
47. Renker, M.; Ramachandra, A.; Schoepf, U.J.; Raupach, R.; Apfaltrer, P.; Rowe, G.W.; Vogt, S.; Flohr, T.G.; Kerl, J.M.; Bauer, R.W.; et al. Iterative image reconstruction techniques: Applications for cardiac CT. *J. Cardiovasc. Comput. Tomogr.* **2011**, *5*, 225–230. [[CrossRef](#)] [[PubMed](#)]
48. Shin, Y.J.; Chang, W.; Ye, J.C.; Kang, E.; Oh, D.Y.; Lee, Y.J.; Park, J.H.; Kim, Y.H. Low-Dose Abdominal CT Using a Deep Learning-Based Denoising Algorithm: A Comparison with CT Reconstructed with Filtered Back Projection or Iterative Reconstruction Algorithm. *Korean J. Radiol.* **2020**, *21*, 356–364. [[CrossRef](#)]
49. Kulathilake, K.A.S.H.; Abdullah, N.A.; Sabri, A.Q.M.; Lai, K.W. A review on Deep Learning approaches for low-dose Computed Tomography restoration. *Complex Intell. Syst.* **2021**, 1–33. [[CrossRef](#)] [[PubMed](#)]
50. Kaur, R.; Juneja, M.; Mandal, A.K. A comprehensive review of denoising techniques for abdominal CT images. *Multimedia Tools Appl.* **2018**, *77*, 22735–22770. [[CrossRef](#)]
51. Nagayama, Y.; Sakabe, D.; Goto, M.; Emoto, T.; Oda, S.; Nakaura, T.; Kidoh, M.; Uetani, H.; Funama, Y.; Hirai, T. Deep Learning-based Reconstruction for Lower-Dose Pediatric CT: Technical Principles, Image Characteristics, and Clinical Implementations. *Radiographics* **2021**, *41*, 1936–1953. [[CrossRef](#)]
52. Benz, D.C.; Ersözülü, S.; Mojon, F.L.A.; Messerli, M.; Mitulla, A.K.; Ciancone, D.; Kenkel, D.; Schaab, J.A.; Gebhard, C.; Pazhenkottil, A.P.; et al. Radiation dose reduction with deep-learning image reconstruction for coronary computed tomography angiography. *Eur. Radiol.* **2021**, *32*, 2620–2628. [[CrossRef](#)]
53. Bernard, A.; Comby, P.-O.; Lemogne, B.; Haioun, K.; Ricolfi, F.; Chevallier, O.; Loffroy, R. Deep learning reconstruction versus iterative reconstruction for cardiac CT angiography in a stroke imaging protocol: Reduced radiation dose and improved image quality. *Quant. Imaging Med. Surg.* **2021**, *11*, 392–401. [[CrossRef](#)]
54. Kang, E.; Koo, H.J.; Yang, D.H.; Seo, J.B.; Ye, J.C. Cycle-consistent adversarial denoising network for multiphase coronary CT angiography. *Med Phys.* **2018**, *46*, 550–562. [[CrossRef](#)]
55. Kosmala, A.; Petritsch, B.; Weng, A.M.; Bley, T.A.; Gassenmaier, T. Radiation dose of coronary CT angiography with a third-generation dual-source CT in a “real-world” patient population. *Eur. Radiol.* **2018**, *29*, 4341–4348. [[CrossRef](#)] [[PubMed](#)]
56. Madaj, P.; Li, D.; Nakanishi, R.; Andreini, D.; Pontone, G.; Conte, E.; Franzcr, R.O.; Hamilton-Craig, C.; Nimmagadda, M.; Kim, N.; et al. Lower Radiation Dosing in Cardiac CT Angiography: The CONVERGE Registry. *J. Nucl. Med. Technol.* **2020**, *48*, 58–62. [[CrossRef](#)] [[PubMed](#)]
57. Soschynski, M.; Hagen, F.; Baumann, S.; Hagar, M.T.; Weiss, J.; Krauss, T.; Schlett, C.L.; Mühlen, C.V.Z.; Bamberg, F.; Nikolaou, K.; et al. High Temporal Resolution Dual-Source Photon-Counting CT for Coronary Artery Disease: Initial Multicenter Clinical Experience. *J. Clin. Med.* **2022**, *11*, 6003. [[CrossRef](#)] [[PubMed](#)]

58. Blanke, P.; Weir-McCall, J.R.; Achenbach, S.; Delgado, V.; Hausleiter, J.; Jilaihawi, H.; Marwan, M.; Nørgaard, B.L.; Piazza, N.; Schoenhagen, P.; et al. Computed tomography imaging in the context of transcatheter aortic valve implantation (TAVI)/transcatheter aortic valve replacement (TAVR) an expert consensus document of the Society of Cardiovascular Computed Tomography. *JACC: Cardiovasc. Imaging* **2019**, *12*, 1–24. [[CrossRef](#)]
59. Shnayien, S.; Beetz, N.L.; Bressemer, K.K.; Hamm, B.; Niehues, S.M. Comparison of a High-Pitch Non-ECG-Gated and a Prospective ECG-Gated Protocol for Preprocedural Computed Tomography Imaging Before TAVI/TAVR. *Rofo* **2022**, *195*, 139–147. [[CrossRef](#)]
60. Dankerl, P.; Hammon, M.; Seuss, H.; Tröbs, M.; Schuhbaeck, A.; Hell, M.M.; Cavallaro, A.; Achenbach, S.; Uder, M.; Marwan, M. Computer-aided evaluation of low-dose and low-contrast agent third-generation dual-source CT angiography prior to transcatheter aortic valve implantation (TAVI). *Int. J. Comput. Assist. Radiol. Surg.* **2016**, *12*, 795–802. [[CrossRef](#)]
61. Schicchi, N.; Fogante, M.; Pirani, P.E.; Agliata, G.; Piva, T.; Tagliati, C.; Marcucci, M.; Francioso, A.; Giovagnoni, A. Third generation dual source CT with ultra-high pitch protocol for TAVI planning and coronary tree assessment: Feasibility, image quality and diagnostic performance. *Eur. J. Radiol.* **2019**, *122*, 108749. [[CrossRef](#)]
62. Annoni, A.D.; Andreini, D.; Pontone, G.; Mancini, M.E.; Formenti, A.; Mushtaq, S.; Baggiano, A.; Conte, E.; Guglielmo, M.; Muscogiuri, G.; et al. CT angiography prior to TAVI procedure using third-generation scanner with wide volume coverage: Feasibility, renal safety and diagnostic accuracy for coronary tree. *Br. J. Radiol.* **2018**, *91*, 20180196. [[CrossRef](#)]
63. Wuest, W.; Anders, K.; Schuhbaeck, A.; May, M.S.; Gauss, S.; Marwan, M.; Arnold, M.; Ensminger, S.; Muschiol, G.; Daniel, W.G.; et al. Dual source multidetector CT-angiography before Transcatheter Aortic Valve Implantation (TAVI) using a high-pitch spiral acquisition mode. *Eur. Radiol.* **2011**, *22*, 51–58. [[CrossRef](#)]

Disclaimer/Publisher's Note: The statements, opinions and data contained in all publications are solely those of the individual author(s) and contributor(s) and not of MDPI and/or the editor(s). MDPI and/or the editor(s) disclaim responsibility for any injury to people or property resulting from any ideas, methods, instructions or products referred to in the content.

PRACA NR 2

Original papers

Radiation dose and repeatability of aortic valve measurement by multidetector row computed tomography to assess eligibility for transcatheter aortic valve implantation

Bartłomiej Kędziński^{1,A–D,F}, Paweł Gać^{1,2,A–D,F}, Martyna Głońska^{1,B,F}, Rafał Poręba^{3,A,C,E,F}, Krystyna Pawlas^{2,E,F}¹ Centre for Diagnostic Imaging, 4th Military Hospital, Wrocław, Poland² Department of Hygiene, Wrocław Medical University, Poland³ Department of Internal Medicine, Occupational Diseases and Hypertension, Wrocław Medical University, Poland

A – research concept and design; B – collection and/or assembly of data; C – data analysis and interpretation;

D – writing the article; E – critical revision of the article; F – final approval of the article

Advances in Clinical and Experimental Medicine, ISSN 1899–5276 (print), ISSN 2451–2680 (online)

Adv Clin Exp Med. 2020;29(8):983–992

Address for correspondence

Paweł Gać

E-mail: pawelgac@interia.pl

Funding sources

None declared

Conflict of interest

None declared

Received on September 23, 2019

Reviewed on May 17, 2020

Accepted on June 7, 2020

Published online on August 27, 2020

Cite as

Kędziński B, Gać P, Głońska M, Poręba R, Pawlas K. Radiation dose and repeatability of aortic valve measurement by multidetector row computed tomography to assess eligibility for transcatheter aortic valve implantation. *Adv Clin Exp Med.* 2020;29(8):983–992. doi:10.17219/acem/123624

DOI

10.17219/acem/123624

Copyright

Copyright by Author(s)

This is an article distributed under the terms of the Creative Commons Attribution 3.0 Unported (CC BY 3.0) (<https://creativecommons.org/licenses/by/3.0/>)

Abstract

Background. Aortic valve stenosis is among the most common valvular defects in developed countries. In the assessment of eligibility for transcatheter aortic valve implantation (TAVI), multidetector row computed tomography (MDCT) is performed to determine the precise dimensions of the aortic valve, the topography of the aortic ostium and the ability to use various arterial access routes.

Objectives. To evaluate the relationships between the radiation dose and the repeatability of measurements of dimensions of the aortic valve in MDCT performed before TAVI.

Material and methods. The study involved a group of 60 consecutive patients undergoing MDCT before TAVI. The radiation dose was expressed as computed tomography dose index volume (CTDIvol) and dose length product (DLP). The coefficient of variation (CV) of each measurement was defined as the standard deviation (SD) of the measurements/mean measurement × 100%, based on the measurements performed independently by 2 radiologists.

Results. A statistically significant negative linear correlation was observed between the DLP value of the MDCT before TAVI, and the CV of the measurement of the minimum dimension of the aortic annulus ($r = -0.25$; $p < 0.05$). Lower DLP doses of the MDCT before TAVI constitute an independent factor associated with a higher CV for the measurement of the minimum dimension of the aortic annulus.

Conclusions. It is proposed that tests using lower radiation doses should be followed by an assessment of the degree of repeatability of the aortic valve sizing.

Key words: aortic valve, coefficient of variation, radiation dose, TAVI, repeatability of measurement

Introduction

Aortic valve stenosis is among the most common valvular defects in developed countries.¹ The treatment of choice in patients with severe aortic stenosis is implantation of a prosthetic aortic valve.² For a large group of elderly patients with a significant burden of comorbidities, the risk of classic cardiosurgical aortic valve replacement is too high. The solution in these patients is transcatheter (transcatheter) aortic valve implantation (TAVI).^{3,4} In the assessment of eligibility for TAVI, standard imaging tests are performed to determine the precise dimensions of the aortic valve, the topography of the aortic ostium and the ability to use various arterial access routes. Currently, the standard examination is multidetector row computed tomography (MDCT) of the heart and large vessels.^{5,6}

Computed tomography (CT) scans expose patients to ionizing radiation. Due to a direct effect on the double DNA helix, and – as a result of water radiolysis – the formation of free oxygen radicals interacting with the DNA (i.e., an indirect effect), ionizing radiation causes modifications in the cellular genetic material that may be associated with deterministic and stochastic consequences.⁷ Following the principles established by the International Commission on Radiological Protection (ICRP), no procedure involving radiation exposure should be performed unless it provides sufficient benefits to the exposed patients or society, outweighing the radiation-induced damage to the health related to this procedure. If the benefit-to-harm balance associated with procedures using ionizing radiation is positive, it is necessary to find a way to optimize the radiation dose.⁸ Following the rules of radiological protection and the ALARA principle (as low as reasonably achievable), the ionizing radiation dose should preferably be reduced during those procedures using this form of radiation. An adequate level of quality for the diagnostic images should be maintained; however, if a minor loss of quality allows the radiation dose to be reduced, it is justified.^{9,10}

Minimizing the radiation for those studies involving high doses, such as CT of the heart and large vessels during the assessment for TAVI, is particularly important, as there is a direct relationship between the radiation dose and the risk of stochastic consequences from the ionizing radiation.¹¹ However, the costs associated with reduced exposure due to the use of lower exposure doses increase disproportionately to the degree of effective dose reduction.¹² Therefore, it is not socially justified or economically profitable to avoid every small risk. Therefore, efforts should be focused on optimizing high and moderate doses.

It may be interesting to determine whether or not the attempt to decrease the dose used in MDCT studies during the assessment of eligibility for TAVI would result in an overly significant reduction in scan quality, in this case defined primarily as reduced repeatability of aortic valve sizing. To achieve this goal, the hypothesis

regarding the relationship between the ionizing radiation dose in standard MDCT examinations and the repeatability of aortic valve sizing needs to be verified.

Study purpose

The aim of the study was to assess the relationships between the ionizing radiation dose and the repeatability of the aortic dimension measurements using MDCT, as part of a standard assessment of eligibility for TAVI.

Material and methods

Study group

The study involved a group of 60 consecutive patients, who received MDCT of the heart and large vessels as part of the eligibility assessment for TAVI in the years 2012–2016. The mean age of the subjects was 79.60 ± 9.17 years, and mean body mass index (BMI) was 27.85 ± 3.99 kg/m². In the study, 63.3% of the subjects were males and 36.7% were females. Only 25.0% of the subjects had normal body weight, 51.7% were overweight and 23.3% were obese. The clinical characteristics of the study group are presented in Table 1.

Study design

The study was part of the project “Possible optimization of ionizing radiation dose in computed tomography studies during the eligibility assessment for transcatheter aortic valve implantation”. The study protocol was approved by the local bioethics committee (approval No. KB 198/2018). Clinical data of all the subjects were collected, and all the patients received a MDCT examination of the heart and large vessels.

Basic anthropometric parameters

The BMI was calculated using the following formula: $BMI = \text{body weight [kg]} / \text{height [m]}^2$. Body surface area (BSA) was derived on the basis of the DuBois formula: $BSA = 0.007184 \times \text{body weight [kg]}^{0.425} \times \text{height [cm]}^{0.725}$. Normal body weight was defined as $BMI < 25$ kg/m², overweight was defined as $BMI 25–29.9$ kg/m² and obesity was defined as $BMI \geq 30$ kg/m².

MDCT studies

All the MDCT examinations of the heart and large vessels during the eligibility assessment for TAVI were performed using a SOMATOM Definition Dual-Source CT scanner (Siemens Healthcare, Kemnath, Germany), following a standardized angiography protocol. The study protocol included a topogram, pre-monitoring and monitoring

Table 1. Clinical characteristics of the study group (n = 60)

Variable	X	Me	Min	Max	SD
Age [years]	79.60	82.00	44.00	95.00	9.17
Height [cm]	169.55	170.00	148.00	186.00	8.08
Body mass [kg]	80.10	80.00	52.00	112.00	12.84
BMI [kg/m ²]	27.85	28.32	19.27	37.38	3.99
BSA [m ²]	1.91	1.93	1.50	2.30	0.17
Gender, n (%)					
men			38 (63.3)		
women			22 (36.7)		
Body mass, n (%)					
normal body mass			15 (25.0)		
overweight			31 (51.7)		
obesity			14 (23.3)		

BMI – body mass index; BSA – body surface area; Max – maximum value; Min – minimum value; n – number of patients; SD – standard deviation; X – arithmetic mean.

at the level of tracheal bifurcation, with acquisition triggered by the required contrast enhancement of the region of interest (ROI) in the ascending aorta, an electrocardiography (ECG)-gated thoracic arterial phase angiography, and a non-ECG-gated angiography of the abdominal and pelvic arteries. The basic technical parameters of the angiographic phases included: craniocaudal direction of image acquisition, spiral method of image acquisition, study scope from the pulmonary apexes to half the length of the femoral shafts, layer collimation of 0.6 mm, exposure kilovoltage of 120 units, and variable mAs values. The examination involved an intravenous administration of a contrast medium at a volume determined by the patient's body weight. Between 90 mL and 120 mL of iodine-based, non-ionic contrast medium was administered using an automatic syringe into the veins in the cubital fossa with infusion rate of 4.0 mL/s. Reconstructions were performed in axial orientations, in layers of 3.0 mm and 0.75 mm, and secondary multi-planar reconstructions (MPRs) were obtained in the coronal and sagittal planes, using maximum intensity projection (MIP) and volume rendering technique (VRT) algorithms.

Ionizing radiation dose

The ionizing radiation dose was determined by recording automated measurements performed using CT. The radiation dose was expressed as computed tomography dose index volume (CTDI_{vol}) and dose length product (DLP) for the thoracic arterial phase MDCT.

Aortic valve assessment

The CT scans of the heart and large vessels were analyzed in terms of assessing the aortic valve and aortic root sizing, topography of the aortic ostium and the possibility to use various arterial access routes during the TAVI procedure. The tests were evaluated following the recommendations of the Society of Cardiovascular Computed

Tomography expert consensus document on CT imaging before TAVI/transcatheter aortic valve replacement (TAVR).⁶ For the purpose of this project, the tests were assessed independently by 2 radiologists with 7 and 10 years of experience in the assessment of CT heart scans, respectively. The assessment involved the following parameters of the aortic valve and root: type of valve (number of leaflets); maximum, minimum and mean dimension of the aortic annulus; maximum, minimum and mean dimension of the aortic root and its height; and distance between the left and the right coronary artery ostia and the aortic annulus (Fig. 1A–F). All the measurements were expressed in millimeters to an accuracy of 0.1 mm.

Assessment of the repeatability of measurements

The analysis of repeatability of the measurements involved the following quantitative variables, calculated on the basis of the measurement of the aortic valve and aortic root parameters, performed independently by 2 radiologists experienced in the evaluation of the cardiovascular system: measurement mean (X), standard deviation (SD), absolute difference (AD), relative difference (RD), and coefficient of measurement variation (CV). The following mathematical formulas were used to calculate the above characteristics of measurement repeatability: AD = |measurement 1 – measurement 2|; RD = AD of the measurement/X of the measurement; CV = SD of the measurement/X of the measurement × 100%. Absolute difference was expressed in mm, RD had no unit, and CV was expressed as percentage.

Subgroups

In the comparative analyses of the studied group of MDCT examinations conducted to assess eligibility for TAVI, the following subgroups were distinguished, based on the median CTDI_{vol} and DLP values for

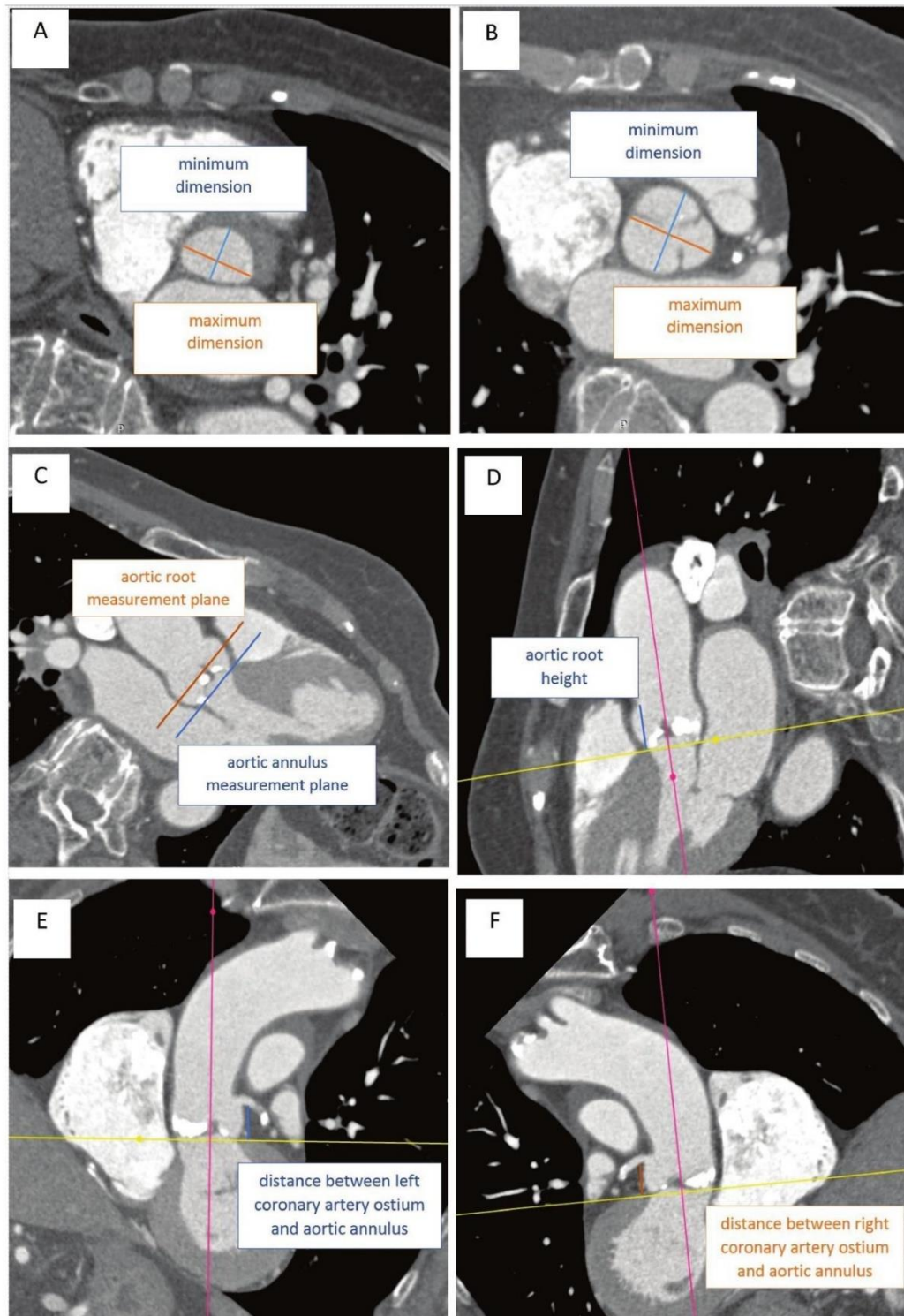


Fig. 1. Computed tomography aortic valve measurements: A) maximum and minimum dimension of the aortic annulus (mean dimension of the aortic annulus = (maximum dimension of the aortic annulus + minimum dimension of the aortic annulus)/2); B) maximum and minimum dimension of the aortic root (mean dimension of the aortic root = (maximum dimension of the aortic root + minimum dimension of the aortic root)/2); C) aortic annulus and aortic root measurement planes; D) height of the aortic root; E) distance between the left coronary artery ostium and the aortic annulus; F) distance between the right coronary artery ostium and the aortic annulus

the thoracic arterial phase of the MDCT. Based on the median CTDIvol (43.92 mGy), a low CTDIvol (CTDIvol < Me, n = 30) and a high CTDIvol (CTDIvol ≥ Me, n = 30) subgroup were identified. Considering the median DLP (1143.00 mGy), a low DLP (DLP < Me, n = 29) and a high DLP (DLP ≥ Me, n = 31) subgroup were identified.

Statistical analysis

Statistical analyses were conducted using Dell Statistica v. 13 software (Dell Inc., Austin, USA). The quantitative variables were characterized with arithmetic means, medians, maximum and minimum values, and SD. The distribution of the variables was verified using the Shapiro–Wilk W test. Due to absence of normal distribution in comparative analyses, the Mann–Whitney U test was used. The results for qualitative variables were characterized by absolute values and percentages. In order to determine the relationships between the analyzed variables, both correlation analysis (2 variables) and multiple regression analyses (more than 2 variables) were conducted. Those results with $p < 0.05$ were considered statistically significant.

Results

The mean CTDIvol and DLP values for the thoracic arterial phase of the MDCT during the eligibility assessment for TAVI were 48.71 ± 20.33 mGy and 1319.98 ± 613.58 mGycm, respectively. In the studied population, 93.3%

of the patients had a tricuspid aortic valve, 5% had a bicuspid aortic valve and 1.7% had a quadricuspid aortic valve. The mean dimensions of the aortic annulus and the aortic root were 24.44 ± 2.50 mm and 32.20 ± 3.95 mm, respectively. The complete results of aortic valve assessment in the MDCT tests for TAVI in the studied group of patients are presented in Table 2.

The analysis of repeatability of aortic valve measurements in the MDCT tests assessing the eligibility for TAVI in the studied subjects showed the greatest absolute measurement difference in the distance between the left coronary artery ostium and the aortic annulus (1.77 ± 0.96 mm), whereas the smallest absolute measurement difference was found in the mean dimension of the aortic annulus (0.97 ± 0.60 mm). The greatest relative measurement difference and the highest CV was observed in the distance between the left coronary artery ostium and aortic annulus ($0.13 \pm 0.07\%$ and $9.24 \pm 5.17\%$, respectively). The smallest relative measurement difference and the smallest CV were found in the mean dimension of the aortic root ($0.03 \pm 0.02\%$ and $2.39 \pm 1.72\%$, respectively). The results of the analysis of aortic valve measurement repeatability in the MDCT tests for TAVI in the studied group of patients are presented in Table 3.

A comparative analysis did not reveal any statistically significant differences in the mean values of the parameters characterizing the repeatability of individual aortic valvular measurements between the groups identified based on the median CTDIvol in the thoracic arterial phase of the MDCT examination used to assess the eligibility for TAVI (Table 4).

Table 2. Aortic valve assessment in MDCT scans evaluating the eligibility for TAVI in the study group (n = 60)

Variable	n		%		
Number of aortic valve leaflets					
2	3		5.0		
3	56		93.3		
4	1		1.7		
Statistical variable	X	Me	Min	Max	SD
Aortic annulus					
maximum dimension [mm]	27.04	27.00	22.50	35.50	3.05
minimum dimension [mm]	21.84	21.50	17.50	31.00	2.83
mean dimension [mm]	24.44	23.88	20.00	31.50	2.50
Aortic root					
maximum dimension [mm]	33.95	33.75	27.50	45.00	4.16
minimum dimension [mm]	30.44	30.00	18.00	44.50	4.33
mean dimension [mm]	32.20	31.75	24.25	44.75	3.95
height [mm]	21.23	20.75	17.00	29.00	2.71
Distance between a coronary artery ostium and the aortic annulus					
left coronary artery [mm]	13.78	14.00	8.25	18.50	2.47
right coronary artery [mm]	15.06	15.00	10.50	20.50	2.51
Radiation dose					
CTDIvol [mGy]	48.71	43.92	24.60	99.14	20.33
DLP [mGycm]	1319.98	1143.00	420.00	2887.00	613.58

Aortic valve dimensions and distances: mean values of measurements conducted by 2 researchers; CTDIvol – computed tomography dose index volume; DLP – dose length product; Max – maximum value; Min – minimum value; n – number of patients; SD – standard deviation; X – arithmetic mean; TAVI – transcatheter aortic valve implantation; MDCT – multidetector row computed tomography.

Table 3. Analysis of repeatability of aortic valve measurements in MDCT scans evaluating the eligibility for TAVI in the study group (n = 60).

Variable	Measurement 1 [mm]	Measurement 2 [mm]	Measurement X [mm]	Measurement SD [mm]	Measurement AD [mm]	Measurement RD	Measurement CV [%]
Aortic annulus							
Maximum dimension	26.72 ±3.11	27.37 ±3.15	27.04 ±3.05	0.95 ±0.53	1.35 ±0.76	0.05 ±0.03	3.58 ±2.12
Minimum dimension	21.60 ±2.78	22.08 ±3.05	21.84 ±2.83	0.84 ±0.63	1.18 ±0.89	0.05 ±0.04	3.83 ±2.92
Mean dimension	24.16 ±2.57	24.73 ±2.53	24.44 ±2.50	0.68 ±0.42	0.97 ±0.60	0.04 ±0.02	2.81 ±1.74
Aortic root							
Maximum dimension	33.48 ±4.18	34.42 ±4.28	33.95 ±4.16	1.01 ±0.66	1.43 ±0.93	0.04 ±0.03	3.03 ±2.00
Minimum dimension	30.45 ±4.35	30.43 ±4.46	30.44 ±4.33	0.93 ±0.73	1.32 ±1.03	0.05 ±0.04	3.20 ±2.59
Mean dimension	31.97 ±3.98	32.43 ±4.01	32.20 ±3.95	0.74 ±0.49	1.04 ±0.69	0.03 ±0.02	2.39 ±1.72
Height	21.87 ±2.80	20.60 ±2.84	21.23 ±2.71	1.24 ±0.71	1.75 ±1.01	0.08 ±0.05	5.87 ±3.34
Distance between coronary artery ostium and aortic annulus							
Left coronary artery	14.43 ±2.73	13.12 ±2.44	13.78 ±2.47	1.25 ±0.68	1.77 ±0.96	0.13 ±0.07	9.24 ±5.17
Right coronary artery	14.47 ±2.58	15.65 ±2.73	15.06 ±2.51	1.24 ±0.79	1.75 ±1.11	0.12 ±0.07	8.29 ±5.22

Values are expressed as mean ± standard deviation (SD); AD – absolute difference; CV – coefficient of variation; RD – relative difference; X – arithmetic mean; TAVI – transcatheter aortic valve implantation; MDCT – multidetector row computed tomography.

Table 4. Analysis of repeatability of aortic valve measurements in MDCT scans evaluating the eligibility for TAVI in subgroups identified based on median CTDIvol

Variable		Low CTDIvol (CTDIvol < Me, n = 30)	High CTDIvol (CTDIvol ≥ Me, n = 30)	p-value
Aortic annulus				
Maximum dimension	measurement AD [mm]	1.33 ±0.76	1.37 ±0.76	0.866
	measurement RD	0.05 ±0.03	0.05 ±0.03	0.878
	measurement CV [%]	3.63 ±2.18	3.54 ±2.10	0.878
Minimum dimension	measurement AD [mm]	1.17 ±0.91	1.20 ±0.89	0.886
	measurement RD	0.05 ±0.04	0.06 ±0.04	0.801
	measurement CV [%]	3.73 ±2.92	3.93 ±2.96	0.801
Mean dimension	measurement AD [mm]	0.88 ±0.52	1.05 ±0.66	0.282
	measurement RD	0.04 ±0.02	0.04 ±0.03	0.290
	measurement CV [%]	2.57 ±1.50	3.05 ±1.95	0.290
Aortic root				
Maximum dimension	measurement AD [mm]	1.47 ±0.94	1.40 ±0.93	0.783
	measurement RD	0.05 ±0.03	0.04 ±0.03	0.458
	measurement CV [%]	3.22 ±2.19	2.83 ±1.81	0.458
Minimum dimension	measurement AD [mm]	1.40 ±0.93	1.23 ±1.14	0.537
	measurement RD	0.05 ±0.03	0.04 ±0.04	0.510
	measurement CV [%]	3.42 ±2.34	2.97 ±2.84	0.510
Mean dimension	measurement AD [mm]	1.17 ±0.75	0.92 ±0.62	0.163
	measurement RD	0.04 ±0.03	0.03 ±0.02	0.147
	measurement CV [%]	2.71 ±1.91	2.07 ±1.47	0.147
Height	measurement AD [mm]	1.87 ±1.05	1.63 ±0.96	0.374
	measurement RD	0.09 ±0.05	0.08 ±0.04	0.449
	measurement CV [%]	6.20 ±3.61	5.54 ±3.08	0.449
Distance between the coronary artery ostium and the aortic annulus				
Left coronary artery	measurement AD [mm]	1.82 ±0.97	1.72 ±0.97	0.691
	measurement RD	0.13 ±0.07	0.13 ±0.08	0.827
	measurement CV [%]	9.10 ±5.11	9.39 ±5.32	0.827
Right coronary artery	measurement AD [mm]	1.60 ±1.16	1.90 ±1.06	0.301
	measurement RD	0.11 ±0.08	0.13 ±0.07	0.234
	measurement CV [%]	7.48 ±5.35	9.10 ±5.04	0.234

Values are expressed as mean ± standard deviation (SD); AD – absolute difference; CTDIvol – computed tomography dose index volume; TAVI – transcatheter aortic valve implantation; MDCT – multidetector row computed tomography; CV – coefficient of variation; RD – relative difference.

Table 5. Analysis of repeatability of aortic valve measurements in MDCT scans evaluating the eligibility for TAVI in subgroups identified based on median DLP

Variable		Low DLP (DLP < Me, n = 29)	High DLP (DLP ≥ Me, n = 31)	p-value
Aortic annulus				
Maximum dimension	measurement AD [mm]	1.38 ± 0.78	1.32 ± 0.75	0.774
	measurement RD	0.05 ± 0.03	0.05 ± 0.03	0.782
	measurement CV [%]	3.66 ± 2.23	3.51 ± 2.06	0.782
Minimum dimension	measurement AD [mm]	1.38 ± 0.98	1.00 ± 0.77	0.100
	measurement RD	0.06 ± 0.05	0.05 ± 0.03	0.121
	measurement CV [%]	4.44 ± 3.27	3.26 ± 2.47	0.121
Mean dimension	measurement AD [mm]	0.97 ± 0.63	0.97 ± 0.58	0.989
	measurement RD	0.04 ± 0.03	0.04 ± 0.02	0.833
	measurement CV [%]	2.76 ± 1.84	2.86 ± 1.68	0.833
Aortic root				
Maximum dimension	measurement AD [mm]	1.41 ± 0.87	1.45 ± 0.99	0.876
	measurement RD	0.04 ± 0.03	0.04 ± 0.03	0.831
	measurement CV [%]	3.09 ± 2.08	2.97 ± 1.96	0.831
Minimum dimension	measurement AD [mm]	1.38 ± 1.08	1.26 ± 1.00	0.654
	measurement RD	0.05 ± 0.04	0.04 ± 0.03	0.600
	measurement CV [%]	3.38 ± 2.77	3.02 ± 2.44	0.600
Mean dimension	measurement AD [mm]	1.35 ± 0.68	0.73 ± 0.65	0.018 *
	measurement RD	0.05 ± 0.03	0.02 ± 0.02	0.020 *
	measurement CV [%]	2.90 ± 1.81	1.88 ± 1.49	0.020 *
Height	measurement AD [mm]	1.84 ± 1.11	1.66 ± 0.91	0.485
	measurement RD	0.09 ± 0.05	0.08 ± 0.04	0.441
	measurement CV [%]	6.22 ± 3.73	5.55 ± 2.97	0.441
Distance between the coronary artery ostium and the aortic annulus				
Left coronary artery	measurement AD [mm]	1.74 ± 1.07	1.79 ± 0.86	0.846
	measurement RD	0.12 ± 0.07	0.14 ± 0.07	0.430
	measurement CV [%]	8.69 ± 5.26	9.76 ± 5.12	0.430
Right coronary artery	measurement AD [mm]	1.69 ± 1.07	1.81 ± 1.17	0.689
	measurement RD	0.11 ± 0.07	0.12 ± 0.08	0.644
	measurement CV [%]	7.96 ± 4.74	8.59 ± 5.69	0.644

Values are expressed as mean ± standard deviation (SD); *p < 0.05; AD – absolute difference; DLP – dose length product; CV – coefficient of variation; RD – relative difference; TAVI – transcatheter aortic valve implantation; MDCT – multidetector row computed tomography.

A comparative analysis of the mean values of the parameters characterizing the repeatability of various aortic valve measurements between the subgroups, based on the median DLP for the thoracic arterial phase of the MDCT examination in the assessment of eligibility for TAVI, revealed significant statistical differences regarding the measurement of the mean aortic root dimension. In the low DLP subgroup (DLP value < the median), the absolute measurement difference, the relative measurement difference and the CV in the case of the mean dimension of the aortic valve were significantly higher than in the high DLP subgroup (DLP value ≥ of the median) (Table 5).

A correlation analysis of the investigated group of tests demonstrated statistically significant negative linear correlations between the DLP value in the thoracic arterial phase of the MDCT during the assessment of eligibility for TAVI, and the AD, RD and CV of the measurement of the minimum dimension of the aortic annulus ($r = -0.26$, $r = -0.25$ and $r = -0.25$, respectively; $p < 0.05$). In addition, positive linear correlations were presented between BMI and AD, RD and CV of the measurement of the minimum dimension of the aortic root ($r = 0.28$, $r = 0.31$ and $r = 0.31$, respectively; $p < 0.05$), as well as between BMI and AD,

RD and CV of the distance between the left coronary artery ostium and the aortic annulus ($r = 0.33$, $r = 0.28$ and $r = 0.28$, respectively; $p < 0.05$).

A multiple stepwise forward-regression analysis determined the relationships between the basic anthropological parameters (age, sex, BMI, and BSA) or the parameters characterizing the radiation dose in the thoracic arterial phase of the MDCT examination assessing the eligibility for TAVI (CTDIvol and DLP), and the CVs for the consecutive aortic valve measurements in these tests. The conducted estimations resulted in the following statistically significant models:

- CV of the measurement of the aortic annular minimum dimension = $5.898 + 0.779$ female – 0.001 DLP;
- CV of the measurement of the aortic root minimum dimension = $-1.789 + 0.206$ BMI + 1.198 female;
- CV of the measurement of the distance between the left coronary artery and the aortic annulus = $4.948 + 0.394$ BMI + 2.283 female + 0.102 age.

The models obtained in the regression analysis indicate that female sex and lower DLP doses in the thoracic arterial phase of the MDCT used to assess the eligibility for TAVI are factors independently associated with a higher CV for

Table 6. Results of multiple regression analysis in the study group (n = 60)

A. Model of relationship determining the independent predictors of higher CV of the measurement of the aortic annular minimum dimension

Model for: CV of the measurement of the aortic annular minimum dimension			
variable	intercept	female	DLP [mGycm]
Regression coefficient	5.898	0.779	-0.001
SEM of Rc	0.989	0.362	0.001
p-value	<0.001	0.009	0.042

DLP – dose length product; CV – coefficient of variation; SEM – standard error of the mean; Rc – regression coefficient.

B. Model of the relationship determining independent predictors of higher CV for the measurement of the aortic root minimum dimension

Model for: CV of the measurement of the aortic root minimum dimension			
variable	intercept	BMI [kg/m ²]	female
Regression coefficient	-1.789	0.206	1.198
SEM of Rc	1.262	0.079	0.552
p-value	0.043	0.012	0.041

CV – coefficient of variation; SEM – standard error of the mean; Rc – regression coefficient; BMI – body mass index.

C. Model of relationship determining independent predictors of higher CV of the measurement of the distance between the left coronary artery ostium and the aortic annulus

Model for: CV of the measurement of the distance between the left coronary artery ostium and the aortic annulus				
variable	intercept	BMI [kg/m ²]	female	age [years]
Regression coefficient	4.948	0.394	2.283	0.102
SEM of Rc	2.603	0.163	1.324	0.031
p-value	0.046	0.008	0.040	0.047

CV – coefficient of variation; SEM – standard error of the mean; Rc – regression coefficient; BMI – body mass index.

the measurement of the minimum dimension of the aortic annulus. Higher BMI and female sex are independently associated with a higher CV for the measurement of the minimal aortic root dimension, whereas higher BMI, female sex and older age are independently associated with a higher CV for the measurement of the distance between the left coronary artery and the aortic annulus. The results of the estimation for significant models obtained in the regression analysis are presented in Table 6.

Discussion

In analyzing the results of this study, it is impossible to identify unequivocally a relationship between the ionizing radiation dose and repeatability of the aortic dimension measurements using MDCT performed for the standard assessment of eligibility for TAVI. The size of the radiation dose in routine MDCT tests to assess eligibility for TAVI did not affect the repeatability of the aortic valve measurements, which justifies the attempts to perform these tests using lower radiation doses. However, it is important to bear in mind the demonstrated individual statistically significant correlations, i.e., considerably higher absolute measurement difference, relative measurement difference and CV of the mean aortic valve diameter in the low DLP subgroup (DLP values < the median) compared

to the high DLP subgroup (DLP values \geq the median); statistically significant negative linear relationships between the DLP value and the absolute measurement difference, relative measurement difference and CV for the minimum aortic annular dimension; as well as a lower DLP dose as an independent factor associated with a higher CV for the minimum aortic annular dimension. Therefore, it is suggested that the MDCT tests using lower radiation doses in the assessment of eligibility for TAVI should be followed by a control of the degree of repeatability of the aortic valve sizing measurements. Based on the conducted studies, it is possible to identify groups of patients in which the variations in aortic valve sizing using MDCT may be higher. Regardless of the radiation dose, higher BMI, female sex, and elderly age affect the CV for individual measurements of the aortic valve. It seems that in these groups of patients, greater caution should be taken while performing MDCT tests using lower radiation doses in the assessment of eligibility for TAVI.

It is worth emphasizing that the presented study results are the first scientific attempt to find a relationship between the ionizing radiation dose and repeatability of aortic dimension measurements using MDCT performed for a standard assessment of eligibility for TAVI.

In the available literature, the problem of repeatability of aortic valve sizing using MDCT before a TAVI procedure was mentioned only occasionally. Schmidkonz et al.

demonstrated that MDCT offers repeatable measurements of aortic annulus and aortic root geometry in patients eligible for TAVI. They also revealed that the highest degree of concordance was obtained for the measurements of the aortic annulus diameter estimated secondarily on the basis of the aortic annulus circumference.¹³ The study did not compare the repeatability of the aortic annulus circumference measurement; among the analyzed parameters, the highest concordance (the lowest CV) was obtained for the mean diameter of the aortic root.

The comparability of the aortic valve assessment was evaluated much more frequently using other diagnostic methods: echocardiography, CT and magnetic resonance imaging (MRI). A study by Bernhardt et al. compared the usefulness of aortic valve sizing prior to a TAVI procedure using non-contrast enhanced MRI with the gold standard, i.e., MDCT examination. In a group of 52 patients who underwent both tests, it was demonstrated that an MRI examination including a 3D steady-state free-precession sequence covering the entire ascending aorta was highly concordant with aortic annulus assessment using MDCT. The mean aortic annular circumference in the measurement with multi-slice computed tomography (MSCT) was 76.7 ± 6.9 mm, whereas in the MRI test it was 76.5 ± 6.7 mm, with a high correlation coefficient for the measurements ($r = 0.93$, $p < 0.0001$).¹⁴ Husser et al. compared the results of aortic valve assessments in patients eligible for TAVI which had been obtained using 3D transesophageal echocardiography (3D-TEE) with the results obtained with the use of MDCT. Based on the comparison of results in a group of 57 patients, the aortic annular diameters and surface areas assessed using 3D-TEE are clearly lower than those obtained in MSCT, with the exception of diameters measured in the sagittal planes. Only in these planes did both methods determine the final size of the prosthesis with a similar accuracy.¹⁵ Other studies by the same researchers compared the results of aortic valve sizing using 2D transesophageal echocardiography (2D-TEE) with 3D-TEE. They demonstrated that the mean aortic annulus diameters were significantly greater in 3D-TEE than in 2D-TEE, with a mean difference of 1.2 mm. The size of the prosthetic valvular implant was correctly determined based on 67% of 2D-TEE tests and 80% of 3D-TEE tests. Discrepancies between 2D-TEE and 3D-TEE test results were observed in 26% of the analyzed cases.¹⁶ The presented study results seem to demonstrate that the use of TEE for the aortic valve sizing in patients eligible for TAVI is limited. The non-contrast enhanced MRI method is promising, but its accessibility is lower compared to MDCT, and the duration of the test is longer, which may be of key importance for patients with severe aortic stenosis. In this context, the authors believe that it is increasingly important to refine the MDCT method in the assessment of eligibility for TAVI.

In relation to the discussed parameters, the significance of the morphological type of the aortic valve should be

mentioned. In the studied group of patients, 93.3% had a tricuspid aortic valve, 5.0% had a bicuspid aortic valve and 1.7% had a quadricuspid aortic valve. The above distribution is similar to the literature data regarding the frequency of individual aortic valve types. Based on the epidemiological studies, the tricuspid aortic valve is considered to be the most common type (98–99.5% of individuals), the bicuspid valve is found in 0.5–2% of individuals and other types are observed only occasionally.¹⁷ The bicuspid aortic valve is often associated with abnormalities, mainly with a predisposition for aortic stenosis.^{18,19} The distribution obtained in the presented study, including 5.0% of patients with bicuspid valves in the group of patients diagnosed with aortic stenosis eligible for a valve replacement procedure, may be considered typical for the population.

This study has certain significant limitations, including a relatively low number of patients participating in the project, a lack of complete clinical characteristics of the patients, including cardiovascular comorbidities and risk factors, considerations related to tests performed using a single tomography scanner, a lack of tests conducted with reduced ionizing radiation doses, a lack of dose determination using size-specific dose estimate (SSDE), a lack of determination of intrapersonal repeatability of the measurements, and the subjective selection of the analyzed aortic valve dimensions. However, the authors believe that these limitations do not undermine the usefulness of the study, which may be considered in further research associated with the presented issue.

Conclusions

The size of the radiation dose in routine MDCT tests assessing eligibility for TAVI essentially does not affect the repeatability of the aortic valve measurements, which justifies the attempts to perform these tests using lower radiation doses.

Due to the demonstrated individual correlations between the radiation dose in MDCT studies performed during the assessment of eligibility for TAVI and the repeatability of aortic valve sizing, it is proposed that tests at lower radiation doses should be followed by a control of the degree of repeatability of the aortic valve sizing.

ORCID iDs

Bartłomiej Kędziński  <https://orcid.org/0000-0002-9109-0368>
Paweł Gać  <https://orcid.org/0000-0001-8366-0239>
Martyna Głońska  <https://orcid.org/0000-0001-9271-7401>
Rafał Poręba  <https://orcid.org/0000-0002-5109-8023>
Krystyna Pawlas  <https://orcid.org/0000-0001-5485-7649>

References

1. Thaden JJ, Nkomo VT, Enriquez-Sarano M. The global burden of aortic stenosis. *Prog Cardiovasc Dis.* 2014;56(6):565–571.
2. Bajona P, Suri RM, Greason KL, Schaff HV. Outcomes of surgical aortic valve replacement: The benchmark for percutaneous therapies. *Prog Cardiovasc Dis.* 2014;56(6):619–624.

3. Krasopoulos G, Falconieri F, Benedetto U, et al. European real world trans-catheter aortic valve implantation: Systematic review and meta-analysis of European national registries. *J Cardiothorac Surg.* 2016;11(1):159.
4. Davlouros PA, Mplani VC, Koniari I, Tsigkas G, Hahalis G. Transcatheter aortic valve replacement and stroke: A comprehensive review. *J Geriatr Cardiol.* 2018;15(1):95–104.
5. Debonnaire P, Katsanos S, Delgado V. Computed tomography to improve TAVI outcomes. *EuroIntervention.* 2012;8(5):531–533.
6. Achenbach S, Delgado V, Hausleiter J, Schoenhagen P, Min JK, Leipsic JA. SCCT expert consensus document on computed tomography imaging before transcatheter aortic valve implantation (TAVI)/transcatheter aortic valve replacement (TAVR). *J Cardiovasc Comput Tomogr.* 2012;6(6):366–380.
7. Mettler FA. Medical effects and risks of exposure to ionising radiation. *J Radiol Prot.* 2012;32(1):N9–N13.
8. Vano E. Global view on radiation protection in medicine. *Radiat Prot Dosimetry.* 2011;147(1–2):3–7.
9. Newman B, Callahan MJ. ALARA (as low as reasonably achievable) CT 2011: Executive summary. *Pediatr Radiol.* 2011;41(Suppl 2):453–455.
10. Cohen MD. ALARA, image gently and CT-induced cancer. *Pediatr Radiol.* 2015;45(4):465–470.
11. Niwa O, Barcellos-Hoff MH, Globus RK, et al. ICRP Publication 131: Stem cell biology with respect to carcinogenesis aspects of radiological protection. *Ann ICRP.* 2015;44(3–4):347–357.
12. Kalra MK, Sodickson AD, Mayo-Smith WW. CT radiation: Key concepts for gentle and wise use. *Radiographics.* 2015;35(6):1706–1721.
13. Schmidkonz C, Marwan M, Klinghammer L, et al. Interobserver variability of CT angiography for evaluation of aortic annulus dimensions prior to transcatheter aortic valve implantation (TAVI). *Eur J Radiol.* 2014;83(9):1672–1678.
14. Bernhardt P, Rodewald C, Seeger J, et al. Non-contrast-enhanced magnetic resonance angiography is equal to contrast-enhanced multislice computed tomography for correct aortic sizing before transcatheter aortic valve implantation. *Clin Res Cardiol.* 2016;105(3):273–278.
15. Husser O, Holzamer A, Resch M, et al. Prosthesis sizing for transcatheter aortic valve implantation: Comparison of three dimensional transesophageal echocardiography with multislice computed tomography. *Int J Cardiol.* 2013;168(4):3431–3438.
16. Husser O, Rauch S, Endemann DH, et al. Impact of three-dimensional transesophageal echocardiography on prosthesis sizing for transcatheter aortic valve implantation. *Catheter Cardiovasc Interv.* 2012;80(6):956–963.
17. Ko SM, Song MG, Hwang HK. Bicuspid aortic valve: Spectrum of imaging findings at cardiac MDCT and cardiovascular MRI. *AJR Am J Roentgenol.* 2012;198(1):89–97.
18. Siu SC, Silversides CK. Bicuspid aortic valve disease. *J Am Coll Cardiol.* 2010;55(25):2789–2800.
19. Roberts WC, Ko JM. Frequency by decades of unicuspid, bicuspid, and tricuspid aortic valves in adults having isolated aortic valve replacement for aortic stenosis, with or without associated aortic regurgitation. *Circulation.* 2005;111(7):920–925.

PRACA NR 3



Article

Estimation of Aortic Valve Calcium Score Based on Angiographic Phase Versus Reduction of Ionizing Radiation Dose in Computed Tomography

Paweł Gać^{1,2,*} , Bartłomiej Kędzierski³, Piotr Macek⁴, Krystyna Pawlas¹  and Rafał Poreba⁴

¹ Department of Hygiene, Wrocław Medical University, Mikulicz-Radeckiego 7, PL 50-368 Wrocław, Poland; krystyna.pawlas@umed.wroc.pl

² Centre for Diagnostic Imaging, 4th Military Hospital, Weigla 5, PL 50-981 Wrocław, Poland

³ Center for Diagnostic Imaging, University Clinical Hospital in Wrocław, Borowska 213, PL 50-556 Wrocław, Poland; bkedzierski@usk.wroc.pl

⁴ Department of Internal Medicine, Occupational Diseases, Hypertension and Clinical Oncology, Wrocław Medical University, Borowska 213, PL 50-556 Wrocław, Poland; piotr.macek@student.umed.wroc.pl (P.M.); rafal.poreba@umed.wroc.pl (R.P.)

* Correspondence: pawel.gac@umed.wroc.pl; Tel.: +48-261-660-480



Citation: Gać, P.; Kędzierski, B.; Macek, P.; Pawlas, K.; Poreba, R. Estimation of Aortic Valve Calcium Score Based on Angiographic Phase Versus Reduction of Ionizing Radiation Dose in Computed Tomography. *Life* **2021**, *11*, 604. <https://doi.org/10.3390/life11070604>

Academic Editors:
Fabrizio Montecucco and
Chang-min Lee

Received: 24 May 2021
Accepted: 22 June 2021
Published: 23 June 2021

Publisher's Note: MDPI stays neutral with regard to jurisdictional claims in published maps and institutional affiliations.



Copyright: © 2021 by the authors. Licensee MDPI, Basel, Switzerland. This article is an open access article distributed under the terms and conditions of the Creative Commons Attribution (CC BY) license (<https://creativecommons.org/licenses/by/4.0/>).

Abstract: The aim of the study was to evaluate the estimation efficacy of aortic valve calcium score (AVCS) based on the multislice computed tomography (MSCT) angiographic phase. The evaluation of the reduced amount of ionizing radiation dose was performed because of this estimation. The study included 51 consecutive patients who qualified for transcatheter aortic valve implantation (TAVI) (78.59 ± 5.72 years). All subjects underwent MSCT: in the native phase dedicated to AVCS as well as angiographic phases aimed to morphologically assess the aortic ostium and arterial accesses for TAVI. Based on the native phase, an AVCS assessment was performed for axial reconstructions at 3.0 mm and 2.0 mm slice thickness (AVCS_{native3.0} and AVCS_{native2.0}). Based on the angiographic phase AVCS was estimated for axial reconstruction at 0.6 mm slice thickness with increased values of lesion density in aortic valve cusps/aortic valve annulus, which is considered a calcification, from a typical value of 130 HU to 500 HU and 600 HU (AVCS_{CTA0.6 500 HU} and AVCS_{CTA0.6 600 HU}). Mathematical formulations were developed, allowing for AVCS native calculation based on AVCS values estimated based on the angiographic phase: AVCS_{native3.0} = 813.920 + 1.510 AVCS_{CTA0.6 500 HU}; AVCS_{native3.0} = 1235.863 + 1.817 AVCS_{CTA0.6 600 HU}; AVCS_{native2.0} = 797.471 + 1.393 AVCS_{CTA0.6 500 HU}; AVCS_{native2.0} = 1228.310 + 1.650 AVCS_{CTA0.6 600 HU}. The amount of a potential reduction in dose length product (DLP) in the case of AVCS estimation was 4.45 ± 1.54%. In summary, relying solely on the angiographic phase of MSCT examination before TAVI, it is possible to conclusively estimate AVCS. This estimation results in a marked reduction in radiation dose in MSCT.

Keywords: aortic valve calcium score; TAVI; radiation dose

1. Introduction

Aortic valve stenosis is the most common primary defect of heart valves [1]. The incidence of aortic stenosis increases with age and in people between 50 and 59 years of age it affects 0.2% of the population; in persons older than 75, as many as 2.8% of the population; in people older than 80 as many as 9.8% of the population [2]. Symptomatic aortic valve stenosis is associated with 50% mortality rate in the period of 2 years [3].

The pathomechanism of aortic valve stenosis development basically involves the damage of the endothelium-covering valve cusps, the migration of lipoproteins to endothelial space, the development of inflammatory reaction, resulting in aortic valve calcification [4,5]. The calcification of the aortic valve is the underlying pathomechanism of aortic stenosis development. Single calcification foci are regarded as the mild calcification of aortic valve,

multiple calcification foci indicate moderate calcification and the complete calcification of cusps, and their thickening is referred to as the severe calcification of the aortic valve [6].

Aortic valve stenosis is a progressive disease process. Generally, the treatment of severe aortic valve stenosis involves a cardiac surgical procedure, i.e., the replacement of aortic valve [7]. An alternative treatment, particularly in elderly patients and/or patients with comorbidities, is transcatheter aortic valve implantation (TAVI) [8,9].

The basic diagnostic method in the qualification procedure for TAVI is the multi-slice computed tomography (MSCT) of the heart and large vessels [10]. It allows for the evaluation of sizes and the geometry of aortic valve, anatomy of aortic ostium as well as the evaluation of vascular accesses for TAVI. The MSCT also allows for the evaluation of aortic valve calcium score (AVCS) [11]. AVCS is a mathematically estimated, quantitative, non-unitary parameter which characterizes the total amount of calcification within the aortic valve region [12]. Based on the guidelines of scientific associations, AVCS is used to differentiate the degrees of aortic stenosis with an aortic ostium surface area below 1.0 cm², a low gradient (<40 mmHg) and maintained left ventricular ejection fraction [13].

The basic reservation regarding MSCT examination for TAVI qualification is the inherent necessity to use ionizing radiation. In the recent years, the doses of radiation have been significantly reduced in MSCT examinations; however, in accordance with the ALARA (As Low as Reasonably Achievable) rule, the methods aimed at a further reduction in the ionizing radiation dose during the procedures utilizing ionizing radiation should be always sought for, while optimizing the adequate quality of the obtained diagnostic images and sometimes sacrificing negligible quality reduction in such images [14,15].

The AVCS assessment, useful during qualification for TAVI in the above-mentioned clinical situations, requires an additional native phase of the MSCT study [11]. The hypothesis of technically feasible, reliable estimation of AVCS value based on the angiographic phase of MSCT examination with the simultaneous omission of the native phase of the examination appears to be of certain importance. In case of a positive verification of the assumed hypothesis it seems reasonable to evaluate the amount of the potential reduction in radiation dose related to application of this estimation.

The aim of the study was to evaluate the estimation efficacy of AVCS based on the angiographic phase of the MSCT examination of the heart and large vessels.

Moreover, the potential reduction in the ionizing radiation dose was evaluated due to the estimation of the value of AVCS based on the angiographic phase instead of performing the native phase of the MSCT.

2. Materials and Methods

2.1. Study Group

The study group included 51 consecutive patients who underwent MSCT examination of the heart and large vessels with AVCS assessment at CT Lab to qualify for TAVI in 2019.

Group size was determined using a sample size calculator. The selection conditions were as follows: population size 38 million, fraction size 0.1, maximum error 10%, confidence level 95%. The required minimum size of the study group was 35. During the analyzed period, 51 patients at the CT Lab were examined, hence the final size of the study group.

2.2. Study Methodology

The current study was performed as part of the project entitled: "Possibility to optimize ionizing radiation procedure in MSCT examination in the qualification procedure for TAVI."

Medical history was obtained from all the included patients, their basic anthropometric parameters were measured and assessment of the MSCT of the heart and large vessels with AVCS was performed.

2.2.1. Basic Anthropometric Measurements

The study group underwent basic anthropometric measurements: their age, gender and body weight were defined. Based on the formula: body weight (kg)/height (m)²,

body mass index (BMI) was calculated. Since the measured anthropometric parameters, subgroups of men and women were selected and included the patients with normal body weight, overweight and obesity, as well as elderly and senile patients. Typical criteria of overweight and obesity, based on BMI, were assumed: BMI between 20 and 24.99 kg/m² as normal body mass, BMI between 25 and 29.99 kg/m² was classed as overweight and a BMI over 30 kg/m² as obesity. In accordance with the guidelines of the World Health Organization, elderly patients were considered persons aged 60–74 and senile patients in the age range 75–90 [16].

2.2.2. MSCT of the Heart and Large Vessels

In all study patients, the MSCT of the heart and large vessels with AVCS assessment was performed. MSCT examination was performed on a 128-slice CT (Somatom Definition AS+, Siemens Healthcare, Erlangen, Germany) following the standard protocol. According to the protocol, the following procedures were performed: topogram, native phase dedicated to the evaluation of AVCS, pre-monitoring and monitoring at trachea bifurcation with image acquisition triggered by post-contrast saturation ROI placed at ascending aorta at 100 HU, ECG-gated angiographic phase dedicated to the morphological evaluation of aortic ostium and angiographic phase dedicated to the imaging of potential arterial accesses for TAVI. Native phase and angiographic phase acquisitions dedicated to the morphological evaluation of aortic ostium also involved tracheal bifurcation at the level of costophrenic angles, and angiographic phase dedicated to imaging of potential arterial accesses for TAVI procedure involved the area ranging from shoulders to the lesser trochanter of the femur. Exposure at 120 kV X-ray lamp was used and mAs values were variable. The volume of the contrast agent administered intravenously was adjusted depending on the examination stage. Using an automated syringe, 70–100 mL of iodinated, non-ionic contrast agent (joheksol, 350 mg iodine/mL; Omnipaque 350, GE Healthcare Oslo, Norway) was administered into the cubital fossa vein at the injection speed of 4.0 mL/s. In the native phase of the examination axial section, reconstructions of 3.0 mm and 2.0 mm slice thicknesses were performed; in the angiographic phase dedicated to morphological evaluation of aortic ostium axial section reconstructions of 3.0 mm and 0.6 mm slice thicknesses were performed; in the angiographic phase dedicated to the imaging of potential arterial access for TAVI procedure, axial section reconstructions of 3.0 mm and 1.0 mm slice thicknesses were obtained. Moreover, angiographic phases of MSCT examination included secondary multiplanar reconstructions (MPR) in frontal and sagittal sections, as well as maximum intensity projection (MIP) and volume rendering technique (VRT).

2.2.3. Evaluation of Aortic Valve Calcium Score

The evaluation of AVCS was performed retrospectively using the syngo.CT CaScoring application (Siemens Healthcare, Erlangen, Germany).

Based on the native phase of MSCT examination, the semi-automatic evaluation of AVCS was performed for axial reconstructions of 3.0 mm and 2.0 mm slice thicknesses (AVCS_{native3.0} and AVCS_{native2.0}, respectively). The lesions were considered calcified, in accordance with Agatston algorithm, if their density exceeded 130 HU. The lesions suggested by the application as calcified were categorized as the lesions in aortic valve cusps/aortic valve annulus or as the lesions outside these structures. The aortic valve calcification categorization for each patient was verified by the consensus of the same two evaluating radiologists. Based on the above categorization the application performed calculations of AVCS values (Figure 1A,B).

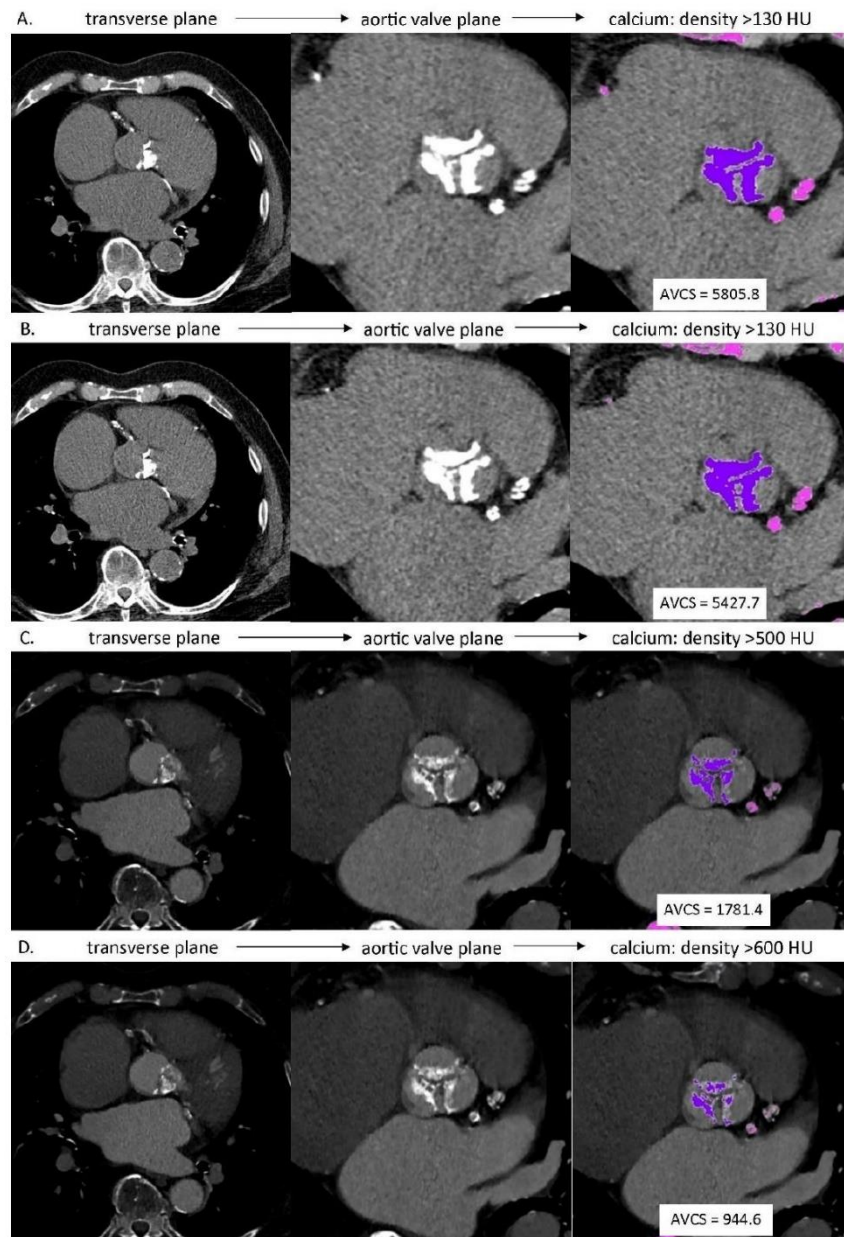


Figure 1. AVCS assessment in MSCT: (A) native phase, axial reconstruction, slice thickness: 3.0 mm, calcium detection threshold: density >130 HU; (B) native phase, axial reconstruction, slice thickness: 2.0 mm, calcium detection threshold: density >130 HU; (C) angiographic phase, axial reconstruction, slice thickness: 0.6 mm, calcium detection threshold: density >500 HU; (D) angiographic phase, axial reconstruction, slice thickness: 0.6 mm, calcium detection threshold: density >600 HU.

Based on the angiographic, ECG-gated, best diastolic phase of MSCT examination dedicated to the morphological evaluation of the aortic valve, AVCS was estimated for axial reconstructions of 0.6 mm slice thickness, with increased values of lesion density in

aortic valve cusps/aortic valve annulus considered to be calcified from a typical value of 130 HU to 500 HU and 600 HU ($AVCS_{CTA0.6\ 500\ HU}$ and $AVCS_{CTA0.6\ 600\ HU}$, respectively). The 500 HU and 600 HU values were subjectively selected to differentiate the calcified lesions in aortic valve cusps/aortic valve annulus from the contrasted lumen of left ventricular outflow tract and/or aortic root. Apart from that, calculations of estimated value of AVCS were performed analogically to the above-described method regarding determination of native AVCS value (Figure 1C,D).

Assessment of AVCS in the native phase and assessment of AVCS in the angiographic phase were separated in time. At the time of the AVCS assessment in the angiographic phase, the investigators had no information about the value of the AVCS in the native phase.

2.2.4. Severity Criteria of Aortic Valve Stenosis

$AVCS_{native3.0}$ values were used to estimate the probability of severe aortic valve stenosis. $AVCS_{native3.0}$ values over 3000 in men and 1600 in women were assumed as indicators of a highly probable severe aortic stenosis. $AVCS_{native3.0}$ values over 2000 in men and 1200 in women were considered as indicators of a probable severe aortic stenosis. The patients whose $AVCS_{native3.0}$ values were lower than 1600 in men and 800 in women were classified as improbable to have a severe aortic stenosis [13].

2.2.5. Ionizing Radiation Dose

Ionizing radiation dose in the analyzed MSCT examinations was characterized by the automated reading of the measurements performed during image acquisition by CT device. The radiation dose was formulated by computed tomography dose index (CTDIvol) and dose length product (DLP) for the native phase dedicated to AVCS evaluation and the angiographic phase used to morphologically evaluate the aortic ostium. Moreover, the total DLP dose was determined for MSCT examination of the heart and large vessels with the AVCS assessment.

2.2.6. Statistical Analysis

Statistical analysis was performed using “Dell Statistica 13” tool (Dell Inc., Round Rock, TX, USA). Mean arithmetic values (X), medians (Me), minimum (Min) and maximum (Max) values as well as standard deviations (SD) were calculated for quantitative variables of the designated parameters. The results for qualitative (nominal) variables were expressed as absolute figures (n) and percentage configurations (%). Distribution of variables was checked using the Shapiro–Wilk test. To determine relationships between the studied variables correlation analysis as well as regression analyses were performed. In the case of quantitative variables of normal distribution, the Pearson correlation coefficient was used. The mathematical formulas for computing the native AVCS from the known AVCS values measured during the angiographic phase of the MSCT were determined by univariate and multivariate regression analysis. The parameters of the obtained formulas in regression analysis were estimated using the least square method. Evaluations of predictive accuracy of the tests were performed using ROC analysis. In the comparative analysis of the selected subgroups, in the case of independent quantitative variables of normal distribution for further statistical analysis, the t -test for independent variables or analysis of variance—ANOVA (parametric univariate)—was used. The results at the level of $p < 0.05$ were considered statistically significant.

3. Results

3.1. Study Group Characteristics

The women constituted 49.02% and the men constituted 50.98% of the study population. The mean age of the included patients was 78.59 ± 5.72 years of age. The basic anthropometric parameters of the study group are presented in Table 1.

Table 1. Clinical characteristics of the study group of patients ($n = 51$).

	X	Me	Min	Max	SD
age [years]	78.59	81.00	62.00	89.00	5.72
BMI [kg/m ²]	27.68	28.26	22.20	33.33	3.03
total cholesterol [mg/dL]	210.36	206.00	117.00	445.00	57.43
LDL cholesterol [mg/dL]	130.84	125.00	46.00	218.00	47.00
HDL cholesterol [mg/dL]	47.52	47.00	33.00	69.00	9.04
triglycerides [mg/dL]	218.28	178.50	66.00	875.00	104.23
glucose [mg/dL]	130.31	114.00	75.00	312.00	50.83
systolic BP [mmHg]	137.50	135.00	105.00	166.00	19.38
diastolic BP [mmHg]	84.85	84.00	62.00	115.00	15.25
creatinine [mg/dL]	1.24	1.23	0.82	1.54	0.23
eGFR [mL/(min × 1.73 m ²)]	63.59	63.50	45.00	101.00	9.95
	<i>n</i>		%		
age					
elderly	9				17.65
senile	42				82.35
gender					
male	26				50.98
female	25				49.02
body mass					
normal	11				21.57
overweight	31				60.78
obesity	9				17.65
CVD					
diabetes	15				29.41
dyslipidemia	28				54.90
arterial hypertension	46				90.20

BMI—body mass index; BP—blood pressure; CVD—cardiovascular diseases; eGFR—estimated glomerular filtration rate; HDL—high-density lipoprotein; LDL—low-density lipoprotein; Max—maximum value; Min—minimum value; *n*—number of patients; SD—standard deviation; X—arithmetic average.

3.2. Aortic Valve Evaluation in a MSCT before TAVI

96.08% of patients were found to have a tricuspid aortic valve, whereas 3.92% of patients had a bicuspid aortic valve. Average sizes of aortic valve annulus and aortic root were 26.64 ± 3.21 mm and 32.16 ± 4.28 mm, respectively, and the height of the aortic root was 19.88 ± 3.79 mm. Standard parameters of aortic valve evaluation in MSCT examination performed before TAVI in the study group are presented in Table 2.

Table 2. Standard parameters of aortic valve evaluation in a MSCT procedure qualifying for TAVI in the study group ($n = 51$).

	<i>n</i>	%			
number of aortic valve cusps					
2	2	3.92			
3	49	96.08			
	X	Me	Min	Max	SD
aortic valve annulus					
maximum measurement [mm]	26.64	26.00	23.00	37.00	3.21
minimum measurement [mm]	20.36	20.00	17.00	27.00	2.33
mean measurement [mm]	23.50	22.50	20.50	32.00	2.62
aortic root					
maximum measurement [mm]	33.52	33.00	28.00	43.00	4.58
minimum measurement [mm]	30.80	30.00	26.00	40.00	4.13
mean measurement [mm]	32.16	31.50	27.50	41.50	4.28
height [mm]	19.88	18.00	14.00	28.00	3.79
distance from coronary ostia to aortic valve annulus					
left coronary artery [mm]	13.16	13.00	10.00	18.00	2.08
right coronary artery [mm]	14.08	14.00	12.00	18.00	1.89

Max—maximum value; Me—median; Min—minimum value; *n*—number of patients; SD—standard deviation; X—arithmetic average.

3.3. AVCS in a MSCT before TAVI

AVCS, depending on the thickness of native image reconstructions, in the study group of patients was 3690.54 ± 2378.82 in the case of 3.0 mm ($AVCS_{\text{native}3.0}$) slice thickness and 3457.03 ± 2190.81 in the case of 2.0 mm ($AVCS_{\text{native}2.0}$) slice thickness. Based on $AVCS_{\text{native}3.0}$ the estimated probability of severe aortic stenosis in 58.82% of the study group was highly probable, in 88.23% it was probable, and in 3.92% it was improbable. The mean value of the blood pool density in the lumen of the left ventricle and the aortic bulb was 380.84 ± 113.33 HU and 392.21 ± 129.12 HU. AVCS estimated based on CT angiographic phase, depending on the increased threshold of calcification detection, was 2068.62 ± 1422.23 with the calcification detection threshold increased up to 500 HU ($AVCS_{\text{CTA}0.6\ 500\ \text{HU}}$) and 1372.39 ± 1044.53 with the calcification detection threshold increased to 600 HU ($AVCS_{\text{CTA}0.6\ 600\ \text{HU}}$). With both the abovementioned calcification detection thresholds, AVCS value estimation was possible in 76.47% and 98.04% of examinations, respectively. In the remaining cases, the indicated density thresholds were insufficient to differentiate between calcium and contrasted blood pool; consequently, syngo.CT CaScoring failed to generate AVCS results. AVCS values in MSCT examinations before TAVI in the tested group of patients are presented in Table 3.

Table 3. AVCS and the parameters characterizing ionizing radiation dose in a MSCT procedure qualifying for TAVI in the study group ($n = 51$).

	X	Me	Min	Max	SD
native aortic valve calcium score (AVCS _{native})					
3.0 mm slice thickness evaluation	3690.54	3022.40	1052.90	9453.40	2378.82
2.0 mm slice thickness evaluation	3457.03	2858.10	1035.40	9148.80	2190.81
	<i>n</i>			%	
probability of severe aortic stenosis (estimated in accordance with AVCS _{native3.0})					
highly probable ($M \geq 3000, F \geq 1600$)	30			58.82	
probable ($M \geq 2000, F \geq 1200$)	45			88.23	
improbable ($M \geq 1600, F \geq 800$)	3			5.88	
	X	Me	Min	Max	SD
estimated on the basis of angiographic phase aortic valve calcium score (AVCS _{CTA0.6})					
500 HU calcification detection threshold	2068.62	1608.00	276.50	5620.00	1422.23
600 HU calcification detection threshold	1372.39	1239.40	119.70	3634.50	1044.53
radiation dose in a native phase dedicated to AVCS evaluation					
CTDIvol [mGy]	2.35	1.87	0.13	13.17	2.55
DLP [mGycm]	30.50	23.30	11.00	143.60	26.85
radiation dose in angiographic phase dedicated to morphological evaluation of aortic ostium					
CTDIvol [mGy]	29.58	16.29	4.72	245.00	45.63
DLP [mGycm]	324.18	220.00	46.30	2058.00	328.41
total radiation dose of MSCT examination of heart and large vessels					
DLP [mGycm]	697.94	554.00	190.00	2380.00	472.17

Max—maximum value; Me—median; Min—minimum value; *n*—number of patients; SD—standard deviation; X—arithmetic average.

3.4. Ionizing Radiation Dose in a MSCT before TAVI

Table 3 also shows the parameters characterizing the ionizing radiation dose in the analyzed MSCT examinations. The mean values of CTDIvol and DLP of native phase dedicated to AVCS evaluation were 2.35 ± 2.55 mGy and 30.50 ± 26.85 mGycm, respectively. Analogous parameters for the angiographic phase, dedicated to morphological evaluation of aortic ostium were 29.58 ± 45.63 mGy and 324.18 ± 328.41 mGycm. Regarding the phase of the examination dedicated to the evaluation of vascular access in the TAVI procedure, the total radiation dose in the analyzed MSCT examinations was, on average, 697.94 ± 472.17 mGycm.

3.5. Correlation Analysis

The correlation analysis indicated statistically significant positive linear relationships between AVCS values, evaluated based on the native phase and AVCS values estimated based on angiographic phase of MSCT examination: r AVCS_{native3.0} vs. AVCS_{CTA0.6 500 HU}—0.85, r AVCS_{native3.0} vs. AVCS_{CTA0.6 600 HU}—0.80, r AVCS_{native2.0} vs. AVCS_{CTA0.6 500 HU}—0.85, r AVCS_{native2.0} vs. AVCS_{CTA0.6 600 HU}—0.78.

3.6. Regression Analysis

Based on the univariate regression analysis, mathematical formulations were determined, allowing for AVCS native calculation based on known AVCS values, estimated based on MSCT angiographic phase:

$$AVCS_{\text{native}3.0} = 813.920 + 1.510 \cdot AVCS_{\text{CTA}0.6 \text{ 500 HU}}$$

$$AVCS_{\text{native}3.0} = 1235.863 + 1.817 \cdot AVCS_{\text{CTA}0.6 \text{ 600 HU}}$$

$$AVCS_{\text{native}2.0} = 797.471 + 1.393 \cdot AVCS_{\text{CTA}0.6 \text{ 500 HU}}$$

$$AVCS_{\text{native}2.0} = 1228.310 + 1.650 \cdot AVCS_{\text{CTA}0.6 \text{ 600 HU}}$$

The highest fit index in the case of the above equations, which was $R^2 = 0.710$, characterized $AVCS_{\text{native}3.0}$ value prediction based on $AVCS_{\text{CTA}0.6 \text{ 500 HU}}$ estimated values. A slightly lower fit index in the case of the above equations, which was $R^2 = 0.708$, characterized $AVCS_{\text{native}3.0}$ value prediction based on $AVCS_{\text{CTA}0.6 \text{ 600 HU}}$ estimated values.

Based on multifactorial regression analysis, the models were developed, allowing for the more precise prediction of actual AVCS, since a known estimated AVCS considers anthropometric parameters (age, gender, and BMI). Statistically significant models obtained in regression analysis are presented in Table 4.

Table 4. Mathematical formulae allowing for the calculation of a native AVCS based on AVCS values estimated based on angiographic phase of a MSCT procedure qualifying for TAVI in the study group ($n = 51$) obtained in a regression analysis. (A) AVCSnative evaluated at 3.0 slice thickness. (B) AVCSnative evaluated at 2.0 slice thickness.

A. AVCS _{native} evaluated at 3.0 slice thickness.		
Parameters Considered in the Model	Mathematical Equation	Parameters of Model Fitting
dependent variable: AVCS _{native3.0} independent variables: AVCS _{CTA0.6 500 HU} , intercept	$AVCS_{\text{native}3.0} = 813.920 + 1.510 \cdot AVCS_{\text{CTA}0.6 \text{ 500 HU}}$	model $p < 0.000$ p AVCS _{CTA0.6 500 HU} : 0.000 intercept p 0.043 model R^2 : 0.710
dependent variable: AVCS _{native3.0} independent variables: AVCS _{CTA0.6 600 HU} , intercept	$AVCS_{\text{native}3.0} = 1.235.863 + 1.817 \cdot AVCS_{\text{CTA}0.6 \text{ 600 HU}}$	model $p < 0.000$ p AVCS _{CTA0.6 500 HU} : 0.000 intercept p 0.001 model R^2 : 0.625
dependent variable: AVCS _{native3.0} independent variables: AVCS _{CTA0.6 500 HU} , gender, intercept	$AVCS_{\text{native}3.0} = 1359.693 + 1.435 \cdot AVCS_{\text{CTA}0.6 \text{ 500 HU}} - 952.227 \text{ female}$	model $p < 0.000$ p AVCS _{CTA0.6 500 HU} : 0.000 gender p : 0.035 intercept p 0.043 model R^2 : 0.737
dependent variable: AVCS _{native3.0} independent variables: AVCS _{CTA0.6 600 HU} , gender, intercept	$AVCS_{\text{native}3.0} = 1527.117 + 1.750 \cdot AVCS_{\text{CTA}0.6 \text{ 600 HU}} - 415.270 \text{ female}$	model $p < 0.000$ p AVCS _{CTA0.6 500 HU} : 0.000 gender p 0.034 intercept p 0.001 model R^2 : 0.624
dependent variable: AVCS _{native3.0} independent variables: AVCS _{CTA0.6 500 HU} , gender, BMI, intercept	$AVCS_{\text{native}3.0} = 2333.771 + 1.474 \cdot AVCS_{\text{CTA}0.6 \text{ 500 HU}} - 974.063 \text{ female} - 37.563 \text{ BMI}$	model $p < 0.000$ p AVCS _{CTA0.6 500 HU} : 0.000 gender p 0.033 BMI p 0.635 intercept p 0.270 model R^2 : 0.731
dependent variable: AVCS _{native3.0} independent variables: AVCS _{CTA0.6 600 HU} , gender, BMI, intercept	$AVCS_{\text{native}3.0} = 3386.066 + 1.876 \cdot AVCS_{\text{CTA}0.6 \text{ 600 HU}} - 428.299 \text{ female} - 73.450 \text{ BMI}$	model $p < 0.000$ p AVCS _{CTA0.6 500 HU} : 0.000 gender p 0.033 BMI p 0.416 intercept p 0.149 model R^2 : 0.621

Table 4. Cont.

B. AVCS _{native} evaluated at 2.0 slice thickness.		
Parameters Considered in the Model	Mathematical Equation	Parameters of Model Fitting
dependent variable: AVCS _{native2.0} independent variables: AVCS _{CTA0.6 500 HU} , intercept	$AVCS_{native2.0} = 797.471 + 1.393 AVCS_{CTA0.6 500 HU}$	model $p < 0.000$ p AVCS _{CTA0.6 500 HU} : 0.000 intercept p 0.033 model R2: 0.708
dependent variable: AVCS _{native2.0} independent variables: AVCS _{CTA0.6 600 HU} , intercept	$AVCS_{native2.0} = 1.228.310 + 1.650 AVCS_{CTA0.6 600 HU}$	model $p < 0.000$ p AVCS _{CTA0.6 500 HU} : 0.000 intercept p 0.000 model R2: 0.607
dependent variable: AVCS _{native2.0} independent variables: AVCS _{CTA0.6 500 HU} , gender, intercept	$AVCS_{native2.0} = 1305.326 + 1.324 AVCS_{CTA0.6 500 HU} - 886.069 \text{ female}$	model $p < 0.000$ p AVCS _{CTA0.6 500 HU} : 0.000 gender p 0.034 intercept p 0.003 model R2: 0.736
dependent variable: AVCS _{native2.0} independent variables: AVCS _{CTA0.6 600 HU} , gender, intercept	$AVCS_{native2.0} = 1484.181 + 1.591 AVCS_{CTA0.6 600 HU} - 364.820 \text{ female}$	model $p < 0.000$ p AVCS _{CTA0.6 500 HU} : 0.000 gender p 0.038 intercept p 0.001 model R2: 0.605
dependent variable: AVCS _{native2.0} independent variables: AVCS _{CTA0.6 500 HU} , gender, BMI, intercept	$AVCS_{native2.0} = 2206.638 + 1.360 AVCS_{CTA0.6 500 HU} - 906.274 \text{ female} - 34.757 \text{ BMI}$	model $p < 0.000$ p AVCS _{CTA0.6 500 HU} : 0.000 gender p 0.033 BMI p 0.635 intercept p 0.260 model R2: 0.730
dependent variable: AVCS _{native2.0} independent variables: AVCS _{CTA0.6 600 HU} , gender, BMI, intercept	$AVCS_{native2.0} = 3323.035 + 1.716 AVCS_{CTA0.6 600 HU} - 377.709 \text{ female} - 72.656 \text{ BMI}$	model p : <0.000 p AVCS _{CTA0.6 500 HU} : 0.000 gender p : 0.037 BMI p : 0.393 intercept p 0.134 model R2: 0.603

The highest fit index in case of the analyzed models, indicating the best prediction, was found in the following models:

$$AVCS_{native3.0} = 1359.693 + 1.435 AVCS_{CTA0.6 500 HU} - 952.227 \text{ female} (R2 = 0.737);$$

$$AVCS_{native2.0} = 1305.326 + 1.324 AVCS_{CTA0.6 500 HU} - 886.069 \text{ female} (R2 = 0.736).$$

Both the above models indicate an independent, statistically significant decrease in actual AVCS value in the case of the estimation of its value in women in comparison with estimation in men.

3.7. Predictive Accuracy Analysis

Using sensitivity and specificity analysis, the accuracy of AVCS values was evaluated. These values were estimated based on the angiographic phase of MSCT examination as a predictive index of severe aortic stenosis probability, based on actual AVCS values (in accordance with AVCS_{native3.0}). The complete results of sensitivity and specificity analysis of the AVCS criteria, determined based on ROC, are presented in Table 5.

Table 5. Prediction of severe aortic stenosis, based on AVCS values, estimated based on angiographic phase of a MSCT procedure qualifying for TAVI in the study group ($n = 51$).

Probability of Severe Aortic Stenosis (in Accordance with AVCS _{native3.0})	Cut-off Point of Estimated AVCS based on ROC Analysis	Test Evaluation Parameters		
		Sensitivity	Specificity	Accuracy
highly probable ($M \geq 3000$)	AVCS _{CTA0.6 500 HU} ≥ 1577.20 .	1.000	0.882	0.913
	AVCS _{CTA0.6 600 HU} ≥ 1234.00 .	1.000	0.889	0.923
highly probable ($K \geq 1600$)	AVCS _{CTA0.6 500 HU} ≥ 1569.00 .	1.000	1.000	1.000
	AVCS _{CTA0.6 600 HU} ≥ 746.40 .	1.000	0.700	0.813
probable ($M \geq 2000$)	AVCS _{CTA0.6 500 HU} ≥ 1183.50 .	0.500	1.000	0.913
	AVCS _{CTA0.6 600 HU} ≥ 899.10 .	0.500	1.000	0.923
probable ($K \geq 1200$)	AVCS _{CTA0.6 500 HU} ≥ 746.40 .	0.167	0.900	0.625
	AVCS _{CTA0.6 600 HU} ≥ 746.40 .	0.308	1.000	0.625
improbable ($M < 1600$)	AVCS _{CTA0.6 500 HU} < 706.00	0.950	0.333	0.870
	AVCS _{CTA0.6 600 HU} < 502.00	0.957	0.333	0.885
improbable ($K < 800$)	uncertain evaluation due to lack of women with AVCS < 800 in the study group			

In the group of women, the highest prediction accuracy was obtained when assuming AVCS_{CTA0.6 500 HU} ≥ 1569.00 value as the predictor of highly probable severe aortic stenosis. The accuracy of such an assumed criterion was 100%. However, in the group of men, the highest prediction accuracy was obtained when assuming the AVCS_{CTA0.6 600 HU} ≥ 1234.00 value as the predictor of highly probable severe aortic stenosis and AVCS_{CTA0.6 600 HU} ≥ 899.10 as the predictor of probable severe aortic stenosis. The accuracy of both these criteria was 92.3%. The remaining assumed criteria showed over 60% accuracy.

3.8. Potential Reduction of Ionizing Dose Analysis

The amount of a potential reduction in DLP ionizing dose in case of AVCS value estimation based on angiographic phase regarding possible omission of the native phase of examination was, on average, 30.50 ± 26.85 mGy. The above reduction amounts to $4.45 \pm 1.54\%$ of the total dose used in the MSCT examination of the heart and large vessels before TAVI. When limiting the study to the aortic valve only (examination involving the native phase dedicated to AVCS evaluation and angiographic phase dedicated to morphological evaluation of aortic ostia, excluding the angiographic phase, dedicated to the evaluation of all potential arterial accesses to TAVI procedure) the above dose reduction constitutes $11.03 \pm 7.96\%$ of the dose of this MSCT examination. No statistically significant differences were found regarding the size of a potential reduction in DLP ionizing radiation dose in the case of AVCS-estimated values based on the angiographic phase, due to the possible omission of a native phase between subgroups of the patients divided in accordance with their gender, body mass and age. The discussed dose reduction was statistically insignificantly higher in women than in men, in overweight and obese patients than in the patients with normal body weight and in senile patients rather than in the elderly. The potential reduction in ionizing radiation dose because of AVCS estimation in the study group and selected study subgroups is presented in Table 6.

Table 6. Potential reduction in ionizing radiation dose because of AVCS estimation, based on the angiographic phase of an MSCT procedures qualifying for TAVI in the study group ($n = 51$).

group	Radiation Dose—DLP [mGycm]			Potential Reduction of Radiation Dose [%]	
	native phase dedicated to AVCS evaluation	angiographic phase dedicated to morphological evaluation of aortic ostium	total MSCT examination of heart and large vessels	regarding examination limited to angiographic phase dedicated to morphological evaluation of aortic ostium	regarding total MSCT examination of heart and large vessels
total study group	30.50 ± 26.85	324.18 ± 328.41	697.94 ± 472.17	11.03 ± 7.96	4.45 ± 1.54
male	36.10 ± 34.43	411.45 ± 417.16	846.42 ± 574.69	10.46 ± 9.94	4.04 ± 1.21
female	24.68 ± 14.06	233.43 ± 163.08	543.52 ± 267.80	11.64 ± 5.33	4.88 ± 1.75
normal body weight	31.59 ± 12.50	497.04 ± 286.49	915.27 ± 394.26	7.01 ± 2.97	3.70 ± 1.22
overweight	34.23 ± 32.65	320.07 ± 358.19	717.10 ± 509.76	11.53 ± 9.03	4.51 ± 1.47
obesity	16.32 ± 5.68	127.08 ± 74.24	366.33 ± 185.92	14.28 ± 6.63	5.16 ± 1.88
elderly age	34.14 ± 22.15	569.00 ± 619.81	758.11 ± 388.54	8.29 ± 5.01	4.39 ± 1.75
senile age	29.72 ± 27.93	271.72 ± 201.48	685.05 ± 491.39	11.63 ± 8.39	4.46 ± 1.52

4. Discussion

The performed examinations indicate that relying solely on the angiographic phase of MSCT examination of the heart and large vessels, it is possible to conclusively estimate the aortic valve calcium score. The increase in the calcification detection threshold from a standard level of 130 HU by the Agatston algorithm, used for actual AVCS calculation based on a native phase of MSCT examination to 500 HU or 600 HU value in angiographic phase of the MSCT examination, allows for the differentiation of some calcifications from the contrasted lumen of left ventricular outflow tract and/or aortic root. The estimated AVCS value is lower than the actual value due to the lost, in this method, calcifications of density between 130 and 500 or 600 HU. However, this study has proved that the obtained values of estimated AVCS strongly correlate with actual AVCS values (r between 0.78 and 0.85) and, using regression equations, recalculation of the estimated values into actual values can be performed with 70% fitting and, having considered the gender of the patients, with 73% fitting. Analogically, the applied method of AVCS estimation allows for evaluation of probability of severe aortic stenosis development and is typically performed based on AVCS actual value measured in a native phase of MSCT examination in axial reconstruction of 3.0 mm slice thickness. The performed ROC analysis has indicated cut-off points of estimated AVCS reflecting the classification criteria of the probability of severe aortic stenosis based on AVCS measured in the native phase. The performed sensitivity/specificity analysis determined the predicted accuracy of the resulting cut-off points of the estimated AVCS within the range of 62.5% and 100.0%.

Here, it appears necessary to comment on the increased calcification detection threshold in the angiographic phase of MSCT examination in the proposed method of AVCS estimation. A slightly higher compatibility between estimated and actual values of AVCS was obtained using the calcification detection threshold set at 500 HU. The increase in detection threshold from 500 HU to 600 HU, in turn, allowed for estimation to be performed in 98.04% of the examinations in comparison with the initial figure which was 76.47%. From a practical point of view, it seems that, while performing AVCS estimation, based on angiographic phase of MSCT examination, the lowest detection threshold, allowing for its performance, should be aimed for.

The applied AVCS estimation method may be of significant clinical importance. Thanks to its application, it has become possible to retrospectively analyze qualification examinations for the TAVI procedure that were performed before the popularization of the native phase, dedicated to AVCS evaluation in these types of examinations. Moreover, this method can be used to reliably estimate AVCS after any thoracic aorta CTA examination or even chest CT scan.

Furthermore, as this study shows, the value estimation of AVCS based on the angiographic phase of MSCT examination, due to the omission of its native phase, is associated with a markedly lower ionizing radiation dose in MSCT examinations, corresponding with ALARA, the main radioprotection principle (As Low as Reasonably Achievable). The amount of a potential reduction in ionizing radiation dose expressed by DLP in the case of the discussed method of AVCS value estimation in the study group was, on average, 30.50 ± 26.85 mGy, which accounts for $4.45 \pm 1.54\%$ of the total dose in the MSCT examination of the heart and large vessels before TAVI and a $11.03 \pm 7.96\%$ dose concerning the heart region. The radiation dose reduction amount was independent of age, gender, and BMI.

The notion of AVCS evaluation based on angiographic phase of the examination has not been widely discussed in the currently available studies. Alqahtani et al., in their studies, assessed the possibility to estimate AVCS based on the MSCT examination of coronary arteries, assuming the calcification detection threshold based on ROI density measurement parameters placed at the ascending aorta, i.e., based on the mean and standard deviation of the abovementioned density. The calcification detection threshold was calculated based on a mathematical formula: mean + 2x standard deviation [17]. Similar to our study, it has been concluded that AVCS estimation, based on the angiographic phase of MSCT examination is possible and its results are reliable. The method used by Alqahtani et al. to estimate the AVCS is a method that requires repeatable and precise localization of ROI in the ascending aorta. This may result in greater variability of the obtained estimation results of this method in comparison to our method." Bettenger et al., in their study, used AVCS estimated based on angiographic phase of MSCT examination, whose aim was to find the most precise prediction threshold for paravalvular leak after TAVI. In the cited above study AVCS was estimated using as many as 6 various thresholds of increased calcification predictions associated with aortic valve in the angiographic phase of MSCT examination: 650 HU, 850 HU, $1.25 \times LA$, $1.5 \times LA$, $LA + 50$ and $LA + 100$. LA was the density in the lumen of aortic valve annulus in the angiographic phase of the examination. In these studies, it was indicated that the applied $LA + 100$ calcification detection threshold is characterized by the highest predictive value for paravalvular leak after TAVI [18]. However, in relatively older studies, Mühlenbruch et al. denied the feasibility of reliable AVCS estimation using the angiographic phase of MSCT examination. The calcium detection threshold in the angiographic phase of MSCT in this study was set at a markedly lower level, 350 HU [19].

However, the authors stress that analogous studies should also be mentioned, as they concern the attempts to estimate the coronary artery calcification score (CACS), solely based on the angiographic phase of MSCT examination. These types of studies were performed, among the others, by Mylonas et al., proving that CACS evaluation, based only on the MSCT angiography scan, is possible and correlates well with CACS evaluated routinely based on non-contrast enhanced examination. In their studies, the same calcification detection threshold was suggested, as in the presented studies by Alqahtani et al. [17,20].

Studies on various methodological aspects of AVCS evaluation appear crucial when considering the growing clinical importance of AVCS, especially in patients with aortic valve stenosis [12,21]. As mentioned before, based on the guidelines of the European Society of Cardiology, AVCS has been considered as the parameter that can be used to differentiate the degrees of aortic stenosis with the aortic ostium surface area below 1.0 cm^2 , a low gradient ($<40 \text{ mmHg}$) and maintained left ventricular ejection fraction. $AVCS_{\text{native}3.0}$ values over 2000 in men and 1200 in women [13] were criteria of highly probable severe aortic stenosis. Recently published multicenter studies by Pawade et al. confirmed the above criteria, obtaining, in the analysis of probable severe aortic stenosis, the thresholds of 2062 Agatston units in men and 1377 Agatston units in women [22]. Ren et al. proved that AVCS evaluation is a reliable marker in the evaluation of AS severity, also in patients with bicuspid aortic valve stenosis [21]. Scientific literature also discusses the significance of the AVCS onset value as a prognostic factor in patients who underwent the TAVI procedure [22,23].

However, the research carried out in recent years also stresses the role of AVCS evaluation in clinical conditions other than aortic stenosis. It has been suggested that, in

patients without aortic valve stenosis, AVCS may be treated as the marker of atherosclerosis development process [24]. Higher values of AVCS are associated with higher risk of cardiovascular events in the future both in patients with cardiovascular diseases as well as in patients without clinical symptoms of cardiovascular disease [25]. Gałąska et al., in their studies, showed that AVCS may even serve as a marker of genetic predisposition to hypercholesterolemia [26].

This study exemplifies the attempt at the optimization of the AVCS methodology evaluation using computed tomography. Another possible direction that scientific studies may follow concerning the AVCS methodology evaluation is its evaluation by other means of diagnostic imaging. Gillis et al. suggested an ultrasound evaluation of AVCS. The AVCS value, evaluated by echocardiography, correlated with the AVCS value, typically evaluated using non-contrast enhanced MSCT [27]. d'Humières T. et al. developed ultrasound AVCS evaluation equally well, correlating with the actual level of aortic valve calcification using less commonly applied three-dimensional echocardiography [28]. However, Le Ven et al. showed that the tissue characteristics of aortic ostium, including a quantitative participation of mineralized, fibrous, and lipid-rich elements may be successfully measured using a multiparametric imaging method of magnetic resonance with good-to-perfect precision, comparable with a histopathological examination [29].

Apart from the issues closely related to the aim of this study the obtained results also indirectly indicate the differences in AVCS between the genders. The performed regression analysis stresses the improvement of fit indices of the obtained mathematical formula, allowing for actual AVCS evaluation based on AVCS estimated values based on angiographic phase of MSCT examination when considering the gender of a studied patient. Female gender enforces correction of the calculated value by a few hundred units of HU, depending on the selected phase and estimation method. The obtained results appear to be in line with the documented fact of lower AVCS values in women. Simard et al. documented that, in patients with tricuspid aortic valve, when the severity of stenosis is similar, women, in comparison with men, exhibit a lower course of valve calcification advancement, but with a higher degree of its fibrosis [30]. Thaden et al. indicated, however, that, for the same degree of aortic stenosis severity, women show lower AVCS and lower mass of aortic valve in comparison with men, and this relationship is independent of valve morphological features. Moreover, AVCS correlates with aortic valve mass [31]. Lower AVCS in women was also observed in the general population. Koshkelashvili et al. documented higher AVCS in men than in women in the general population aged ≥ 65 , but only in the case of Caucasian race [32]. Galas et al. showed higher values of AVCS in men in comparison with women in the group of patients aged ≥ 60 diagnosed due to thoracic pain using MSCT examination of coronary arteries [33].

The basic limitation of the methodology is the constant threshold of calcium density in the angiographic phase (500 or 600 HU). A variable density threshold "mean of blood pool density + standard deviation of blood pool density" would probably be better. However, different approaches are used in the literature. The choice of a specific, fixed threshold of calcium density in the angiographic phase was conditioned by the intention to test the simplest methodological approach. The calcium density threshold in the angiographic phase, based on the measurement of the mean and standard deviation of the blood pool density is a value whose measurement depends on many factors, including longitudinal measurement location (different value when measured in LA, LV, LVOT, aortic bulb, STJ point, ascending aorta or descending aorta), transverse location of measurement (median, eccentric, from the entire outline of the anatomical structure filled with blood), the size and shape of the ROI used for measurement, as well as dependent on the researcher making the measurement (intra-observer and inter-observer variability).

Another important limitation of the study is the small number of studies included in the project. Increasing the size of the study group would be valuable. However, it should be noted that the size of the group was considered in the algorithms of the performed statistical analyses.

Other limitations of the study include: performing the study only in Caucasian individuals; the single-center nature of the study limited the analysis to exams performed on one device in a given MSCT laboratory; the small size of the group of people with a bicuspid aortic valve (only 2 patients); failure to include in the analysis the MSCT exams performed with using lower kilo-voltages of the X-ray tube (100 kV, 80 kV); limited radiation dose characteristics in the analyzed studies using acquisition parameters provided by the CT instead of taking into account the size-specific dose estimation (SSDE); subjective selection of the MSCT phases, on the basis of which the AVCS was assessed. Moreover, the characteristics of the studied group lack information on the age of the menopause of the studied women, information on the medications used, and the results of the control echocardiographic examination. In the opinion of the authors, the above limitations do not significantly reduce the potential usefulness of the conducted research. The results should, therefore, be used as indicators for further research.

5. Conclusions

1. Relying solely on the angiographic phase of MSCT examination of the heart and large vessels, it is possible to conclusively estimate the aortic valve calcium score.
2. The AVCS estimation based on the angiographic phase of the MSCT study, due to the omission of the native phase of the study, results in a lower dose of ionizing radiation.

Author Contributions: Conceptualization, P.G., B.K. and R.P.; methodology, P.G. and B.K.; software, P.G. and R.P.; investigation, P.G., B.K. and P.M.; writing—original draft preparation, P.G. and B.K.; writing—review and editing, R.P.; visualization, P.G.; supervision, K.P. and R.P.; project administration, P.G.; funding acquisition, P.G. All authors have read and agreed to the published version of the manuscript.

Funding: This research did not receive any specific grant from funding agencies in the public, commercial, or not-for-profit sectors. APC was financed by the Wrocław Medical University.

Institutional Review Board Statement: The study was conducted according to the guidelines of the Declaration of Helsinki and approved by the Ethics Committee of Wrocław Medical University (protocol code KB-198/2018).

Informed Consent Statement: Written informed consent has been obtained from the patient(s) to publish this paper.

Data Availability Statement: Study data can be made available upon documented request.

Conflicts of Interest: The authors declare no conflict of interest.

References

1. Boudoulas, K.D.; Triposkiadis, F.; Boudoulas, H. The Aortic Stenosis Complex. *Cardiology* **2018**, *140*, 194–198. [[CrossRef](#)]
2. Thaden, J.J.; Nkomo, V.T.; Enriquez-Sarano, M. The Global Burden of Aortic Stenosis. *Prog. Cardiovasc. Dis.* **2014**, *56*, 565–571. [[CrossRef](#)]
3. Lindman, B.R.; Patel, J.N. Multimorbidity in Older Adults with Aortic Stenosis. *Clin. Geriatr. Med.* **2016**, *32*, 305–314. [[CrossRef](#)]
4. Joseph, J.; Naqvi, S.Y.; Giri, J.; Goldberg, S. Aortic Stenosis: Pathophysiology, Diagnosis, and Therapy. *Am. J. Med.* **2017**, *130*, 253–263. [[CrossRef](#)]
5. Dimitrow, P.P. Aortic stenosis: New pathophysiological mechanisms and their therapeutic implications. *Pol. Arch. Intern. Med.* **2014**, *124*, 723–730. [[CrossRef](#)]
6. Lindman, B.; Clavel, M.-A.; Mathieu, P.; Jung, B.; Lancellotti, P.; Otto, C.M.; Pibarot, P. Calcific aortic stenosis. *Nat. Rev. Dis. Prim.* **2016**, *2*, 1–28. [[CrossRef](#)] [[PubMed](#)]
7. Ramlawi, B.; Bedeir, K.; Lamelas, J. Aortic Valve Surgery: Minimally Invasive Options. *Methodist DeBakey Cardiovasc. J.* **2016**, *12*, 27–32. [[CrossRef](#)]
8. Arora, S.; Misenheimer, J.A.; Ramaraj, R. Transcatheter Aortic Valve Replacement: Comprehensive Review and Present Status. *Tex. Hear. Inst. J.* **2017**, *44*, 29–38. [[CrossRef](#)] [[PubMed](#)]
9. Van Kesteren, F.; Piek, J. Trends in TAVI. *Neth. Hear. J.* **2018**, *26*, 415–416. [[CrossRef](#)] [[PubMed](#)]
10. Achenbach, S.; Delgado, V.; Hausleiter, J.; Schoenhagen, P.; Min, J.K.; Leipsic, J.A. SCCT expert consensus document on computed tomography imaging before transcatheter aortic valve implantation (TAVI)/transcatheter aortic valve replacement (TAVR). *J. Cardiovasc. Comput. Tomogr.* **2012**, *6*, 366–380. [[CrossRef](#)] [[PubMed](#)]

11. Blanke, P.; Weir-McCall, J.R.; Achenbach, S.; Delgado, V.; Hausleiter, J.; Jilaihawi, H.; Marwan, M.; Nørgaard, B.; Piazza, N.; Schoenhagen, P.; et al. Computed tomography imaging in the context of transcatheter aortic valve implantation (TAVI)/transcatheter aortic valve replacement (TAVR): An expert consensus document of the Society of Cardiovascular Computed Tomography. *J. Cardiovasc. Comput. Tomogr.* **2019**, *13*, 1–20. [[CrossRef](#)]
12. Pawade, T.; Sheth, T.; Guzzetti, E.; Dweck, M.R.; Clavel, M.-A. Why and How to Measure Aortic Valve Calcification in Patients with Aortic Stenosis. *JACC: Cardiovasc. Imaging* **2019**, *12*, 1835–1848. [[CrossRef](#)]
13. Baumgartner, H.; Falk, V.; Bax, J.J.; De Bonis, M.; Hamm, C.; Holm, P.J.; Jung, B.; Lancellotti, P.; Lansac, E.; Muñoz, D.R.; et al. 2017 ESC/EACTS Guidelines for the management of valvular heart disease. *Eur. Heart J.* **2017**, *38*, 2739–2791. [[CrossRef](#)]
14. Shnayien, S.; Bressemer, K.K.; Beetz, N.L.; Asbach, P.; Hamm, B.; Niehues, S.M. Radiation Dose Reduction in Preprocedural CT Imaging for TAVI/TAVR Using a Novel 3-Phase Protocol: A Single Institution's Experience. *RöFo* **2020**, *192*, 1174–1182. [[CrossRef](#)]
15. Musolino, S.V.; DeFranco, J.; Schlueck, R. The alara principle in the context of A radiological or nuclear emergency. *Health Phys.* **2008**, *94*, 109–111. [[CrossRef](#)]
16. Alter, M.J. *Science of Flexibility*, 3rd ed.; Human Kinetics: Champaign, IL, USA, 2004.
17. Alqahtani, A.M.; Boczar, K.E.; Kansal, V.; Chan, K.; Dwivedi, G.; Chow, B.J. Quantifying Aortic Valve Calcification using Coronary Computed Tomography Angiography. *J. Cardiovasc. Comput. Tomogr.* **2017**, *11*, 99–104. [[CrossRef](#)]
18. Bettinger, N.; Khalique, O.K.; Krepp, J.M.; Hamid, N.B.; Bae, D.J.; Pulerwitz, T.C.; Liao, M.; Hahn, R.T.; Vahl, T.P.; Nazif, T.; et al. Practical determination of aortic valve calcium volume score on contrast-enhanced computed tomography prior to transcatheter aortic valve replacement and impact on paravalvular regurgitation: Elucidating optimal threshold cutoffs. *J. Cardiovasc. Comput. Tomogr.* **2017**, *11*, 302–308. [[CrossRef](#)]
19. Mühlenbruch, G.; Wildberger, J.; Koos, R.; Das, M.; Thomas, C.; Ruhl, K.; Niethammer, M.; Floh, T.G.; Stanzel, S.; Günther, R.W.; et al. Calcium scoring of aortic valve calcification in aortic valve stenosis with a multislice computed tomography scanner: Non-enhanced versus contrast-enhanced studies. *Acta Radiol.* **2005**, *46*, 561–566. [[CrossRef](#)]
20. Mylonas, I.; Alam, M.; Amily, N.; Small, G.; Chen, L.; Yam, Y.; Hibbert, B.; Chow, B.J. Quantifying coronary artery calcification from a contrast-enhanced cardiac computed tomography angiography study. *Eur. Heart J. Cardiovasc. Imaging* **2013**, *15*, 210–215. [[CrossRef](#)]
21. Dzaye, O.; Whelton, S.P.; Blaha, M.J. Aortic valve calcium scoring on cardiac computed tomography: Ready for clinical use? *J. Cardiovasc. Comput. Tomogr.* **2019**, *13*, 297–298. [[CrossRef](#)]
22. Pawade, T.; Clavel, M.-A.; Tribouilloy, C.; Dreyfus, J.; Mathieu, T.; Tastet, L.; Renard, C.; Gun, M.; Jenkins, W.S.A.; Macron, L.; et al. Computed Tomography Aortic Valve Calcium Scoring in Patients with Aortic Stenosis. *Circ. Cardiovasc. Imaging* **2018**, *11*, e007146. [[CrossRef](#)] [[PubMed](#)]
23. Akodad, M.; Lattuca, B.; Agullo, A.; Macia, J.-C.; Gandet, T.; Marin, G.; Iemmi, A.; Vernhet, H.; Schmutz, L.; Nagot, N.; et al. Prognostic Impact of Calcium Score after Transcatheter Aortic Valve Implantation Performed with New Generation Prosthesis. *Am. J. Cardiol.* **2018**, *121*, 1225–1230. [[CrossRef](#)] [[PubMed](#)]
24. Ann, S.H.; Jung, J.I.; Jung, H.-O.; Youn, H.-J. Aortic Valve Calcium Score Is Associated With Coronary Calcified Plaque Burden. *Int. Heart J.* **2013**, *54*, 355–361. [[CrossRef](#)] [[PubMed](#)]
25. Shekar, C.; Budoff, M. Calcification of the heart: Mechanisms and therapeutic avenues. *Expert Rev. Cardiovasc. Ther.* **2018**, *16*, 527–536. [[CrossRef](#)]
26. Gałąska, R.; Kulawiak-Gałąska, D.; Chmara, M.; Chlebus, K.; Studniarek, M.; Fijałkowski, M.; Wasąg, B.; Rynkiewicz, A.; Gruchala, M. Aortic valve calcium score in hypercholesterolemic patients with and without low-density lipoprotein receptor gene mutation. *PLoS ONE* **2018**, *13*, e0209229. [[CrossRef](#)]
27. Gillis, K.; Bala, G.; Roosens, B.; Hernot, S.; Remory, I.; Scheirlyncq, E.; Geers, J.; Droogmans, S.; Cosyns, B. Clinical validation of an ultrasound quantification score for aortic valve calcifications. *Int. J. Cardiol.* **2018**, *252*, 68–71. [[CrossRef](#)]
28. D'Humières, T.; Faivre, L.; Chamrous, E.; Deux, J.-F.; Bergoënd, E.; Fiore, A.; Radu, C.; Couetil, J.-P.; Benhaïem, N.; Derumeaux, G.; et al. A New Three-Dimensional Echocardiography Method to Quantify Aortic Valve Calcification. *J. Am. Soc. Echocardiogr.* **2018**, *31*, 1073–1079. [[CrossRef](#)]
29. Le Ven, F.; Tizon-Marcos, H.; Fuchs, C.; Mathieu, P.; Pibarot, P.; LaRose, E. Valve Tissue Characterization by Magnetic Resonance Imaging in Calcific Aortic Valve Disease. *Can. J. Cardiol.* **2014**, *30*, 1676–1683. [[CrossRef](#)]
30. Simard, L.; Côté, N.; Dagenais, F.; Mathieu, P.; Couture, C.; Trahan, S.; Bossé, Y.; Mohammadi, S.; Pagé, S.; Joubert, P.; et al. Sex-Related Discordance Between Aortic Valve Calcification and Hemodynamic Severity of Aortic Stenosis. *Circ. Res.* **2017**, *120*, 681–691. [[CrossRef](#)]
31. Thaden, J.J.; Nkomo, V.T.; Suri, R.M.; Maleszewski, J.J.; Soderberg, D.J.; Clavel, M.A.; Pislaru, S.V.; Malouf, J.F.; Foley, T.A.; Oh, J.K.; et al. Sex-related differences in calcific aortic stenosis: Correlating clinical and echocardiographic characteristics and computed tomography aortic valve calcium score to excised aortic valve weight. *Eur. Heart J.* **2016**, *37*, 693–699. [[CrossRef](#)]
32. Koshkelashvili, N.; Codolosa, J.N.; Goykhman, I.; Romero-Corral, A.; Pressman, G.S. Distribution of Mitral Annular and Aortic Valve Calcium as Assessed by Unenhanced Multidetector Computed Tomography. *Am. J. Cardiol.* **2015**, *116*, 1923–1927. [[CrossRef](#)]
33. Galas, A.; Hryniewiecki, T.; Michałowska, I.; Kepka, C.; Abramczuk, E.; Orłowska-Baranowska, E.; Rużyłło, W. Aortic valve calcification in 499 consecutive patients referred for computed tomography. *Arch. Med. Sci.* **2015**, *11*, 952–957. [[CrossRef](#)]

OŚWIADCZENIA WSPÓLAUTORÓW

lek. Bartłomiej Kędzierski
Dział Radiologii i Diagnostyki Obrazowej
Dolnośląski Szpital Specjalistyczny im. T. Marciniaka
- Centrum Medycyny Ratunkowej
ul. Gen. Fiedorfa 2
54-049 Wrocław

Wrocław, 17. kwietnia 2023

OŚWIADCZENIE O WSPÓLAUTORSTWIE

Oświadczam, że w pracy:

1. Bartłomiej Kędzierski; Piotr Macek; Barbara Dziadkowiec-Macek; Krystian Truskiewicz; Rafał Poręba; Paweł Gać. **Radiation Doses in Cardiovascular Computed Tomography.** Life 2023, 13, 990.

Mój udział polegał na: opracowaniu założeń i koncepcji pracy, gromadzeniu i opracowaniu danych naukowych, przygotowaniu i współredagowaniu merytorycznym publikacji oraz opracowaniu ilustracji.

2. Bartłomiej Kędzierski, Paweł Gać, Martyna Głośna, Rafał Poręba, Krystyna Pawlas. **Radiation dose and repeatability of aortic valve measurement by multidetector row computed tomography to assess eligibility for transcatheter aortic valve implantation.** Adv Clin Exp Med. 2020 Aug;29(8):983-992. doi: 10.17219/acem/123624. PMID: 32853487.

Mój udział polegał na: opracowaniu założeń i koncepcji pracy, gromadzeniu i opracowaniu danych naukowych, analizie i interpretacji wyników badań naukowych, współredagowaniu artykułu oraz ostatecznym przygotowaniu publikacji.

3. Paweł Gać, Bartłomiej Kędzierski, Piotr Macek, Krystyna Pawlas, Rafał Poręba. **Estimation of Aortic Valve Calcium Score Based on Angiographic Phase Versus Reduction of Ionizing Radiation Dose in Computed Tomography.** Life (Basel). 2021 Jun 23;11(7):604. doi: 10.3390/life11070604. PMID: 34201824; PMCID: PMC8305341.

Mój udział polegał na: opracowaniu założeń i koncepcji pracy, opracowaniu metodologii badań, analizie i interpretacji wyników badań naukowych oraz współredagowaniu artykułu.



dr hab. n. med. Paweł Gać, prof. UMW
Katedra Zdrowia Populacyjnego
Zakład Zdrowia Środowiskowego i Medycyny Pracy
Uniwersytetu Medycznego we Wrocławiu
ul. Mikulicza-Radeckiego 7
50-345 Wrocław

Wrocław, 17. kwietnia 2023

OŚWIADCZENIE O WSPÓLAUTORSTWIE

Oświadczam, że w pracy:

1. Bartłomiej Kędzierski; Piotr Macek; Barbara Dziadkowiec-Macek; Krystian Truskiewicz; Rafał Poręba; Paweł Gać. **Radiation Doses in Cardiovascular Computed Tomography**. Life 2023, 13, 990.

Mój udział polegał na: opracowaniu założeń i koncepcji pracy, prowadzeniu merytorycznego nadzoru nad przygotowaniem publikacji oraz pozyskiwaniu funduszy niezbędnych do przeprowadzenia projektu.


2. Bartłomiej Kędzierski, Paweł Gać, Martyna Głośna, Rafał Poręba, Krystyna Pawlas. **Radiation dose and repeatability of aortic valve measurement by multidetector row computed tomography to assess eligibility for transcatheter aortic valve implantation**. Adv Clin Exp Med. 2020 Aug;29(8):983-992. doi: 10.17219/acem/123624. PMID: 32853487.

Mój udział polegał na: opracowaniu założeń i koncepcji pracy, gromadzeniu i opracowaniu danych naukowych, analizie i interpretacji wyników badań naukowych, współredagowaniu artykułu oraz ostatecznym przygotowaniu publikacji.

3. Paweł Gać, Bartłomiej Kędzierski, Piotr Macek, Krystyna Pawlas, Rafał Poręba. **Estimation of Aortic Valve Calcium Score Based on Angiographic Phase Versus Reduction of Ionizing Radiation Dose in Computed Tomography**. Life (Basel). 2021 Jun 23;11(7):604. doi: 10.3390/life11070604. PMID: 34201824; PMCID: PMC8305341.

Mój udział polegał na: opracowaniu założeń i koncepcji pracy, opracowaniu metodologii badań, przygotowaniu i opracowaniu wyników badań, analizie i interpretacji wyników badań naukowych, współredagowaniu artykułu, przygotowaniu ilustracji, zarządzaniu projektem oraz pozyskiwaniu funduszy niezbędnych do przeprowadzenia projektu.

Dr hab. n. med. Paweł Gać
Profesor UMW
lekarz specjalista
radiologii i diagnostyki obrazowej
Europejskie Dyploma w Radiologii
EACVI Cardiac Computed Tomography Exam
EACVI Cardiovascular Magnetic Resonance Exam
PZC 238049



prof. dr hab. n. med. Krystyna Pawlas
Katedra Zdrowia Populacyjnego
Zakład Zdrowia Środowiskowego i Medycyny Pracy
Uniwersytetu Medycznego we Wrocławiu
ul. Mikulicza-Radeckiego 7
50-345 Wrocław

Wrocław, 17. kwietnia 2023

OŚWIADCZENIE O WSPÓLAUTORSTWIE

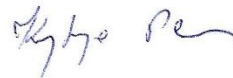
Oświadczam, że w pracy:

1. Bartłomiej Kędzierski, Paweł Gać, Martyna Głońska, Rafał Poręba, Krystyna Pawlas. **Radiation dose and repeatability of aortic valve measurement by multidetector row computed tomography to assess eligibility for transcatheter aortic valve implantation.** Adv Clin Exp Med. 2020 Aug;29(8):983-992. doi: 10.17219/acem/123624. PMID: 32853487.

Mój udział polegał na: przeprowadzeniu krytycznej korekty oraz ostatecznym przygotowaniu publikacji.

2. Paweł Gać, Bartłomiej Kędzierski, Piotr Macek, Krystyna Pawlas, Rafał Poręba. **Estimation of Aortic Valve Calcium Score Based on Angiographic Phase Versus Reduction of Ionizing Radiation Dose in Computed Tomography.** Life (Basel). 2021 Jun 23;11(7):604. doi: 10.3390/life11070604. PMID: 34201824; PMCID: PMC8305341.

Mój udział polegał na prowadzeniu merytorycznego nadzoru nad przygotowaniem publikacji.



prof. dr hab. n. med. Rafał Poręba
Katedra i Klinika Chorób Wewnętrznych Zawodowych
Nadciśnienia Tętniczego i Onkologii Klinicznej
Uniwersytetu Medycznego we Wrocławiu
ul. Borowska 213
50-556 Wrocław

Wrocław, 17. kwietnia 2023

OŚWIADCZENIE O WSPÓLAUTORSTWIE

Oświadczam, że w pracy:

1. Bartłomiej Kędziński; Piotr Macek; Barbara Dziadkowiec-Macek; Krystian Truskiewicz; Rafał Poręba; Paweł Gać. **Radiation Doses in Cardiovascular Computed Tomography**. Life 2023, 13, 990.

Mój udział polegał na: opracowaniu założeń i koncepcji pracy oraz prowadzeniu merytorycznego nadzoru nad przygotowaniem publikacji.

2. Bartłomiej Kędziński, Paweł Gać, Martyna Głośna, Rafał Poręba, Krystyna Pawlas. **Radiation dose and repeatability of aortic valve measurement by multidetector row computed tomography to assess eligibility for transcatheter aortic valve implantation**. Adv Clin Exp Med. 2020 Aug;29(8):983-992. doi: 10.17219/acem/123624. PMID: 32853487.

Mój udział polegał na: opracowaniu założeń i koncepcji pracy, analizie i interpretacji wyników badań naukowych, przeprowadzeniu krytycznej korekty oraz ostatecznym przygotowaniu publikacji.

3. Paweł Gać, Bartłomiej Kędziński, Piotr Macek, Krystyna Pawlas, Rafał Poręba. **Estimation of Aortic Valve Calcium Score Based on Angiographic Phase Versus Reduction of Ionizing Radiation Dose in Computed Tomography**. Life (Basel). 2021 Jun 23;11(7):604. doi: 10.3390/life11070604. PMID: 34201824; PMCID: PMC8305341.

Mój udział polegał na: opracowaniu założeń i koncepcji pracy, przygotowaniu i opracowaniu wyników badań, współredagowaniu artykułu i prowadzeniu merytorycznego nadzoru nad przygotowaniem publikacji.

Prof. dr hab. med. Rafał Poręba
specjalista chorób wewnętrznych
kardiolog, diabetolog, angiolog
4190345



dr n. med. Krystian Truskiewicz
Dział Radiologii i Diagnostyki Obrazowej
Dolnośląski Szpital Specjalistyczny im. T. Marciniaka
Centrum Medycyny Ratunkowej
ul. Fieldorfa 2
50-049 Wrocław

Wrocław, 17. kwietnia 2023

OŚWIADCZENIE O WSPÓLAUTORSTWIE

Oświadczam, że w pracy:

1. Bartłomiej Kędziński; Piotr Macek; Barbara Dziadkowiec-Macek; Krystian Truskiewicz; Rafał Poręba; Paweł Gać. **Radiation Doses in Cardiovascular Computed Tomography**. Life 2023, 13, 990.

Mój udział polegał na: przygotowaniu i współredagowaniu merytorycznym oraz ostatecznym przygotowaniu publikacji.

Krystian
Truskiewicz

2612410 dr n. med. Krystian Truskiewicz
specjalista radiologii
i diagnostyki obrazowej

lek. Barbara Dziadkowiec-Macek
Katedra i Klinika Chorób Wewnętrznych Zawodowych
Nadciśnienia Tętniczego i Onkologii Klinicznej
Uniwersytetu Medycznego we Wrocławiu
ul. Borowska 213
50-556 Wrocław

Wrocław, 17. kwietnia 2023

OŚWIADCZENIE O WSPÓŁAUTORSTWIE

Oświadczam, że w pracy:

1. Bartłomiej Kędziński; Piotr Macek; Barbara Dziadkowiec-Macek; Krystian Truskiewicz; Rafał Poręba; Paweł Gać. **Radiation Doses in Cardiovascular Computed Tomography**. *Life* 2023, 13, 990.

Mój udział polegał na: przygotowaniu i współredagowaniu merytorycznym oraz ostatecznym przygotowaniu publikacji.



lek. Piotr Macek
Katedra i Klinika Chorób Wewnętrznych Zawodowych
Nadciśnienia Tętniczego i Onkologii Klinicznej
Uniwersytetu Medycznego we Wrocławiu
ul. Borowska 213
50-556 Wrocław

Wrocław, 17. kwietnia 2023

OŚWIADCZENIE O WSPÓŁAUTORSTWIE

Oświadczam, że w pracy:

1. Bartłomiej Kędzierski; Piotr Macek; Barbara Dziadkowiec-Macek; Krystian Truskiewicz; Rafał Poręba; Paweł Gać. **Radiation Doses in Cardiovascular Computed Tomography**. Life 2023, 13, 990.

Mój udział polegał na: gromadzeniu danych naukowych, przygotowaniu i współredagowaniu merytorycznym publikacji.

2. Paweł Gać, Bartłomiej Kędzierski, Piotr Macek, Krystyna Pawlas, Rafał Poręba. **Estimation of Aortic Valve Calcium Score Based on Angiographic Phase Versus Reduction of Ionizing Radiation Dose in Computed Tomography**. Life (Basel). 2021 Jun 23;11(7):604. doi: 10.3390/life11070604. PMID: 34201824; PMCID: PMC8305341.

Mój udział polegał na: analizie i interpretacji wyników badań naukowych.



lek. Martyna Hajac z d. Głońska
Ośrodek Diagnostyki Obrazowej
4. Wojskowy Szpital Kliniczny we Wrocławiu
ul. Weigla 5
50-981 Wrocław

Wrocław, 17. kwietnia 2023

OŚWIADCZENIE O WSPÓLAUTORSTWIE

Oświadczam, że w pracy:

1. Bartłomiej Kędziński, Paweł Gać, Martyna Głońska, Rafał Poręba, Krystyna Pawlas.
Radiation dose and repeatability of aortic valve measurement by multidetector row computed tomography to assess eligibility for transcatheter aortic valve implantation.
Adv Clin Exp Med. 2020 Aug;29(8):983-992. doi: 10.17219/acem/123624. PMID: 32853487.

Mój udział polegał na: gromadzeniu i opracowaniu danych naukowych oraz ostatecznym przygotowaniu publikacji.



ZGODA KOMISJI BIOETYCZNEJ

1

KOMISJA BIOETYCZNA
przy
Uniwersytecie Medycznym
we Wrocławiu
ul. Pasteura 1; 50-367 WROCLAW

OPINIA KOMISJI BIOETYCZNEJ Nr KB – 198/2018

Komisja Bioetyczna przy Uniwersytecie Medycznym we Wrocławiu, powołana zarządzeniem Rektora Uniwersytetu Medycznego we Wrocławiu nr 133/XV R/2017 z dnia 21 grudnia 2017 r. oraz działająca w trybie przewidzianym rozporządzeniem Ministra Zdrowia i Opieki Społecznej z dnia 11 maja 1999 r. (Dz.U. nr 47, poz. 480) na podstawie ustawy o zawodzie lekarza z dnia 5 grudnia 1996 r. (Dz.U. nr 28 z 1997 r. poz. 152 z późniejszymi zmianami) w składzie:

dr hab. Jacek Daroszewski (endokrynologia, diabetologia)
prof. dr hab. Krzysztof Grabowski (chirurgia)
dr Henryk Kaczkowski (chirurgia szczękowa, chirurgia stomatologiczna)
mgr Irena Knabel-Krzyszowska (farmacja)
prof. dr hab. Jerzy Liebhart (choroby wewnętrzne, alergologia)
ks. dr hab. Piotr Mrzygłód (duchowny)
mgr prawa Luiza Müller (prawo)
dr hab. Sławomir Sidorowicz (psychiatria)
dr hab. Leszek Szenborn (pediatria, choroby zakaźne)
Danuta Tarkowska (pielęgniarstwo)
prof. dr hab. Anna Wiela-Hojeńska (farmakologia kliniczna)
dr hab. Andrzej Wojnar (histopatologia, dermatologia) przedstawiciel Dolnośląskiej Izby Lekarskiej)
dr hab. Jacek Zieliński (filozofia)

pod przewodnictwem
prof. dr hab. Jana Kornafela (ginekologia i położnictwo, onkologia)

Przestrzegając w działalności zasad Good Clinical Practice oraz zasad Deklaracji Helsińskiej, po zapoznaniu się z projektem badawczym pt.

„Możliwość optymalizacji dawki promieniowania jonizującego w badaniach tomografii komputerowej w procedurze kwalifikacji do zabiegu przezskórnego wszczepienia zastawki aortalnej”

zgłoszonym przez **lek. Bartłomieja Kędzierskiego** zatrudnionego w Zakładzie Radiologii Lekarskiej i Diagnostyki Obrazowej 4 Wojskowego Szpitala Klinicznego we Wrocławiu oraz złożonymi wraz z wnioskiem dokumentami, w tajnym głosowaniu postanowiła **wyrazić zgodę** na przeprowadzenie badania w Zakładzie Radiologii Lekarskiej i Diagnostyki Obrazowej 4 Wojskowego Szpitala Klinicznego we Wrocławiu pod nadzorem prof. dr hab. Krystyny Pawlas **pod warunkiem zachowania anonimowości uzyskanych danych**.

Pouczenie: W ciągu 14 dni od otrzymania decyzji wnioskodawcy przysługuje prawo odwołania do Komisji Odwoławczej za pośrednictwem Komisji Bioetycznej UM we Wrocławiu.

Opinia powyższa dotyczy projektu badawczego będącego podstawą rozprawy doktorskiej.

Wrocław, dnia 24 kwietnia 2018 r.

Uniwersytet Medyczny we Wrocławiu
KOMISJA BIOETYCZNA
przewodniczący
prof. dr hab. Jan Kornafel